5-5-2015

Novel Chemical Tools and Methods for Quantitative Mass Spectrometry-Based Proteomics

Adam Jay McShane
University of Connecticut - Storrs, adam.j.mcshane@gmail.com

Novel Chemical Tools and Methods for Quantitative Mass Spectrometry-Based Proteomics

Adam Jay McShane, Ph.D.

University of Connecticut, 2015

Abstract

Mass spectrometry-based proteomics utilizes a mass spectrometer to study the identity, quantity, localization, modification, interaction, and function of proteins. This technology was applied to quantify cystic fibrosis transmembrane conductance regulator (CFTR) protein, whose mutation is responsible for the lethal disease cystic fibrosis. Mutated CFTR is degraded before it reaches the plasma membrane (PM), where it performs its vital function as a chloride ion channel. The first step of drug modulation is to increase the expression of CFTR in the PM; thus, an accurate measurement of CFTR in the PM is desired. A tandem enrichment strategy of cell-surface biotinylation and gel electrophoretic enrichment, with pulse chase of stable isotopes, was applied to measure the lifetime of CFTR, in the apical PM of BHK-wtCFTR cells. The half-life was determined to be 29.0±2.5h. Quantitation and turnover measurements of CFTR in the apical PM can significantly facilitate the understanding of the cystic fibrosis disease mechanism and thus the development of new disease-modifying drugs.

CFTR and all proteomic quantitation suffers from low sample numbers and replicates due to lengthy analysis time. However, small changes in protein concentration demand increased samples and replicates to ensure statistical and analytical relevance. Towards increasing the throughput of CFTR quantitation, an ultrathroughput multiple reaction monitoring (uMRM) method was designed. CFTR digest samples, containing one common internal standard, were derivatized with unique mass tags. Derivatized, cysteinyl CFTR peptides were then enriched with

an avidin/biotin pull-down strategy before MRM measurements. A 5-plex experiment was designed, and will be compared to traditional MRM measurements of the 5 samples analyzed individually. To evaluate a possible new mass tagging strategy for uMRM, the collisional fragmentation of peptides whose amine groups were derivatized with five linear ω-dimethylamino acids, from 2-(dimethylamino)-acetic acid to 6-(dimethylamino)-hexanoic acid, were investigated. Tandem mass spectra of the derivatized peptides revealed different preferential breakdown pathways. Together with energy resolved mass spectrometry, it was found that shutting down the active participation of the terminal dimethylamino group in fragmentation of derivatized peptides is possible. However, it took a separation of five methylene groups between the terminal dimethylamino group and the amide formed upon peptide derivatization.

Novel Chemical Tools and Methods for Quantitative Mass Spectrometry-Based Proteomics

Adam Jay McShane

B.S., University of Pittsburgh, 2009

A Dissertation

Submitted in Partial Fulfillment of the

Requirements for the Degree of

Doctor of Philosophy

at the

University of Connecticut

2015

Approval Page

Doctor of Philosophy Dissertation

Novel Chemical Tools and Methods for Quantitative Mass Spectrometry-Based Proteomics

Presented by

Adam Jay McShane, B.S.

Major Advisor _____
Xudong Yao, Ph.D.

Associate Advisor _____
Mark W. Peczuh, Ph.D.

Associate Advisor _____
Alfredo Angeles-Boza, Ph.D.

Associate Advisor _____
Christian Brückner, Ph.D.

Associate Advisor _____
Edward J. Neth, Ph.D.

University of Connecticut

2015

Acknowledgements

No man is an island, and nothing can be accomplished without the support of others. I would like to express my appreciation to those who have given their support during graduate school. Utmost Dr. Xudong Yao, my major advisor, for his guidance both in and out of the laboratory. I am forever indebted for his patient mentoring. Next, I would like to thank my associate advisors, Drs. Mark Peczuh, Alfredo Angeles-Boza, Christian Brückner, and Edward Neth, for their counsel.

My former lab mates, Drs. Bekim Bajrami, Pamela Diego-Limpin, and Vahid Farrokhi, for helping during my first steps into graduate school. My current lab mates, Mary Joan Castillo, Song Li, Reza Nemati, Yuanyuan Shen, Lei Wang, and Veronica Cheng for their academic discussions, and generally making graduate school a little more bearable. The faculty and staff in the Department of Chemistry for guiding my graduate experience both educationally and logistically.

Drs. Youngmi Ji and Leon Nesti for welcoming me for two summers into the Clinical and Experimental Orthopaedics group at the NIH. My parents, Lori McShane and Dwayne McShane, for instilling in me the value of education. Lastly, DiAndra Rudzinski for her synthetic chemistry advisement, her sympathetic ear, and her never-tiring support in all aspects of my life.

Table of Contents

Table of Figures and Schemes

Table of Tables and Equations

Chapter 1

An Overview of Quantitative Proteomic Approaches

1.1 Introduction

Proteomics is the study of the protein complement from a particular biological system like a tissue, cell type, or organism. The study includes the protein identity, quantity, localization, modification, interaction, and function. The focus of this chapter is on current quantitative proteomic approaches including immuno-based detection and mass spectrometry-based analysis. With the impact of quantitative proteomics in biological sciences, the goal of the chapter is to take the novice in proteomic quantitation through the fundamentals of the field to current, cutting edge methods, as well as to provide a collection of current literature on the topic for proteomics practitioners. The bulk of the material focuses on mass spectrometry-based detection methods with sections on derivatization-free and derivatization-based quantitation, activity probes, mass spectrometers, sample enrichment techniques, software, and throughput considerations.

1.2 Immuno-based detection methods

1.2.1 Gel-based approaches

In the 1970's, one dimensional gel electrophoresis (1-DE) was introduced as a separation method for the determination of protein molecular weight and for assessing protein purity [1]. The most popular electrophoretic techniques for protein separation are isoelectric focusing (IEF) using immobilized pH gradients (IPGs), and sodium dodecyl sulfate-polyacrylamide gel electrophoresis (SDS-PAGE). Proteins are separated based on their isoelectric point (pI) in IEF, whereas SDS-PAGE separates based on size [2]. In 1975, 2-DE was developed to separate proteins using IEF as the first dimension and SDS-PAGE as the second dimension. Modern 2-DE methods still have similar designs [2,3].

Different methods have been used to visualize proteins after SDS-PAGE separation. Silver staining due to the excellent detectability is among the most routinely used technique; however, it

is not quantitative because it has varying interactions with different proteins and a limited dynamic range. Staining gels using Colloidal Coomassie Blue leads to a better linear dynamic range but relatively compromised limit of detection. Fluorescent labeling has gained popularity due to its sensitivity and wide linear dynamic range [4].

1.2.1.1 Fluorescent two-dimensional difference gel electrophoresis (2-D DIGE)

Despite of the high resolving power, 2-DE has inherent limitations. It suffers from poor sensitivity, low solubilization of membrane proteins, low throughput, and limited gel to gel reproducibility [4-6]. Other reported drawbacks are labor-intensive image analysis and poor representation of extremely acidic or basic proteins as well as small proteins [7,8]. The inherent variability of 2-DE has been addressed by the emergence of fluorescent 2-D DIGE [4-6]. In 2-D DIGE, amine groups of proteins are covalently labeled with 2 spectrally resolvable n-hydroxysuccinimide (NHS) fluorescent dyes, cynine dyes (Cy3 and Cy5), prior to protein separation. To ensure that the same proteins in both samples for comparison have the same relative 2-DE mobility, the dyes have the same mass and charge [4]. Fluorescent labeling also renders 2-D DIGE much more quantitative than colorimetric methods. It has a linear dynamic range of 4 to 5 orders of magnitude, compared to 1 to 3 orders with staining methods [9].

1.2.1.2 Western blots (immunoblotting)

Western blots are a fundamental tool for the measurement of proteins in biomedical labs. The western blot utilizes antibodies that are specific to the protein of interest for detection. From 1979 to 1981, 3 papers were published with the first use of this method [10-12]. Generally, gel electrophoresis is performed first to separate proteins. The proteins are then transferred to a membrane [polyvinylidene fluoride (PVDF) and nitrocellulose membranes are commonly used]. After the transfer, primary and secondary antibodies are added consecutively. Finally, the signal

is produced by adding detection reagents (e.g. chromogenic and colorimetric) to the secondary antibodies. A general procedure is displayed in **Figure 1.1**. Recent technological updates to western blotting include quantum dot (QD) conjugation [13-15], microfluidic engineering [16-20], and imagers (e.g. ChemiDoc™ and G:Box).

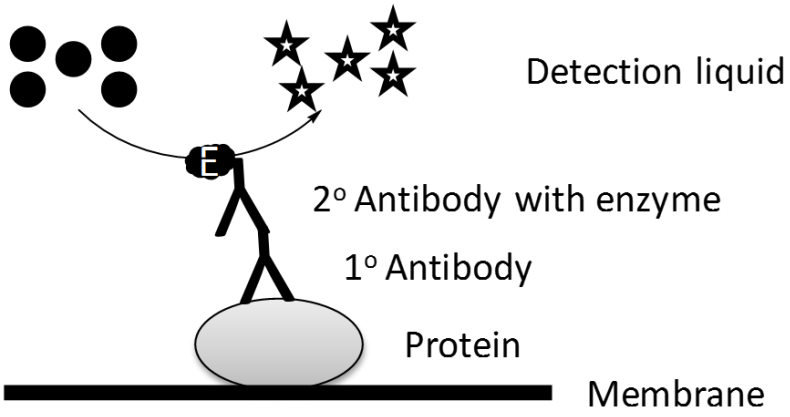

Figure 1.1: Generic western blotting steps.

1.2.2 Non-gel-based approaches

1.2.2.1 Enzyme-linked immunosorbent assays (ELISA) and aptamer-based assays

ELISA uses antibodies and surface binding to accomplish detection. This can be done by indirect antigen binding to the surface or direct antigen binding to antibodies on the surface [21]. Like western blotting the antigen is recognized with an antibody that has an enzyme covalently linked (e.g., horseradish peroxidase). The predecessor to ELISA was described in 1960 [22]. Recent advancements push the detection limit of ELISA to subfemtomolar concentrations [23,24]. The popularity of aptamer-based assays has risen over the last several years in proteomics [25]. Typical aptamers are singly-stranded nucleic acids that can recognize target molecules. The general basis is similar to immuno-based methods. These aptamers are found by screening large libraries of nucleic acid sequences. This technology has been applied to several proteome-level detections [26-29].

1.2.2.2 Surface plasmon resonance (SPR) spectroscopy

SPR spectroscopy is a phenomenon that occurs on an electron rich metal surface (active surface) upon the impact of an incident light with a certain frequency. Techniques based on SPR detect any change of the refractive index on the active surface due to the adsorption of a target analyte [30]. For protein detection, antibodies are extensively used to modify the SPR active surface. As detailed in **Figure 1.2**, the 4 major mechanisms of the antibody-based SPR reported are direct [31], competitive [32], sandwich [33], and inhibition assays [34]. Using antibody arrays leads to an extension of the technique that is referred to as surface plasmon resonance imaging (SPRI). This technique is a high-throughput and multiplexible version of SPR. Biological SPR is categorized as a label-free quantitation method. Thus, there is no need for elaborate sample preparation, which allows for fast, real-time, and reusable sensing [35]. This technique suffers from 2 common antibody-based detection problems: the high cost of immunograde antibodies and non-specific binding of proteins. A vast variety of modifications and alterations have been made to the active surface of SPR to enhance the selectivity and sensitivity of the SPR sensor. The use of nanoparticles together with an immunodetection sandwich compartment is one popular approach [36-38]. This approach has been applied for amplified detection of total prostate-specific antigen (tPSA) [39]. Aptamers are an alternative to protein-based antibodies [40]. Nanostructures (i.e. nanowires, nanoholes and nano-layers) on the active surface have been used to increase antigen binding [41,42]. Using these versatile signal enhancement techniques, achieving an attomolar limit of detection for proteins is possible [43].

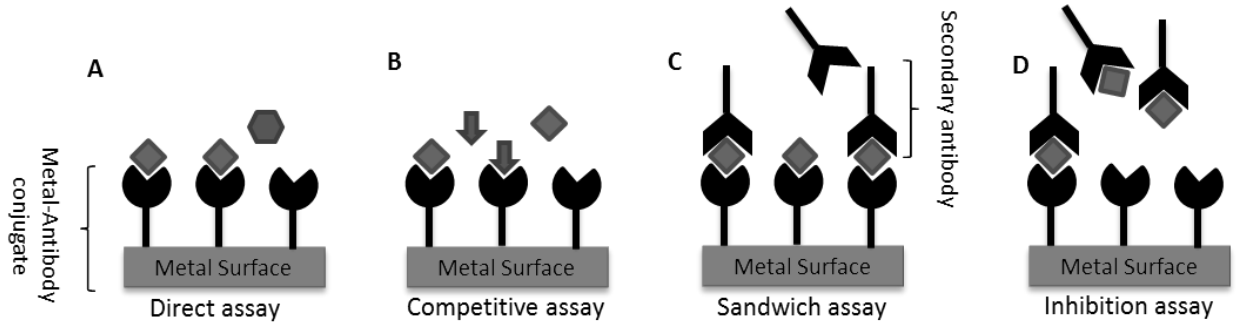

Figure 1.2: Detection mechanisms in SPR-based sensors. A) Direct assay: direct detection of analyte B) Competitive assay: analyte competes with an internal standard C) Sandwich assay: analyte is trapped between 2 antibodies D) Inhibition assay: analyte is pretreated with an antibody.[i]

1.2.2.3 Lab-on-a-chip

The incorporation of microfluidics into small devices that are capable of analysis or experimentation is commonly referred to as "lab-on-a-chip" [44]. These small devices have been used in a variety of ways. Liquid chromatography (LC) on-chip approaches are well represented in the literature [45,46]. These chips have also been used to study the membrane proteome [47] and protein-protein interaction via fluorescence resonance energy transfer (FRET) [48]. Further examples of technology miniaturization can be found in journals dedicated to the on-chip methodology (i.e. Lab-on-a-Chip).

1.3 MS-based detection methods

1.3.1 Introduction

Among various technologies used in quantitative proteomics, MS steps out as the major player in the field. Fast, reproducible, and capable of analyzing highly complex samples are some advantages of MS-based quantitation methods [49]. Two major approaches in MS-based proteomic quantitation are derivatization-based and derivatization-free. Selecting a particular approach for proteomic analysis depends on many factors [50]. In a derivatization-free approach,

[i] Figure by Vahid Farrokhi. McShane, A. J.; Farrokhi, V.; Nemati, R.; Li, S.; Yao, X. An Overview of Quantitative Proteomic Approaches. Comprehensive Analytical Chemistry, Oxford, UK; Elsevier, **2014**; p. 111-135.

there is no concern of the completion and efficiency of chemical reactions or subsequent sample cleanup. Thus this approach delivers a faster and more straightforward solution for a large-scale primary study. Derivatization-based approaches, however, deliver more flexibility and improved sample throughput**. Figure 1.3** categorizes different derivatization-free and derivatization-based quantitation methods. The 2 schools of proteomic research use either direct MS analysis of proteins (top-down proteomics) or analysis of peptides resulted from proteolytic digestion of proteome samples (bottom-up proteomics or shotgun proteomics) [51]. However, the majority of quantitative analysis in proteomics use the bottom-up principle, in which the peptide quantity is representative of protein amount [52]. This chapter will only focus on bottom-up techniques for proteomic quantitation.

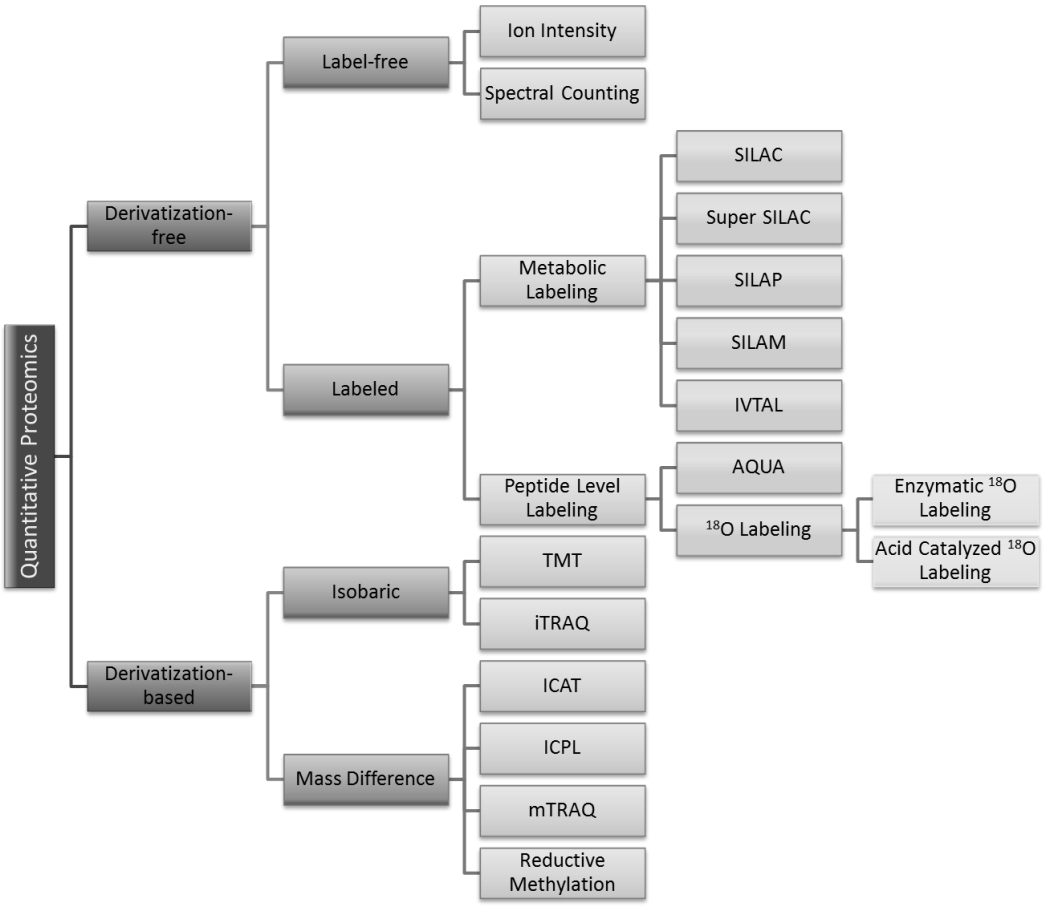

Figure 1.3: Categorization of MS-based proteomics quantitation approaches.

1.3.2 Mass spectrometers

Mass spectrometers are composed of 3 main components: the ionization source, the mass analyzer, and the detector. With the development of different mass analyzers, the choice of mass spectrometer for a specific analysis becomes critical [53]; e.g., if the analysis is to quantitatively profile all proteins in a sample or quantify a pre-selected set of protein targets. One or a combination of mass analyzers, such as time of flight (TOF), quadrupole (Q), ion trap (IT), ion cyclotron resonance (ICR), and Orbitrap™, can be implemented in MS or tandem MS (MS/MS). For non-targeted quantitative proteomics, in which the protein profiling and relative quantitation is performed simultaneously, mass spectrometers with high accuracy and resolution such as Q-TOF, TOF-TOF, or Orbitrap™ are preferred. Mass resolving power and accuracy, which are continuously being improved in new commercial instruments, are the important factors necessary for software-assisted protein identification with high statistical confidence [54]. TOF analyzers are the most traditional analyzer for delivering high mass accuracy and resolution, together with great speed of analysis [55]. An Orbitrap™ analyzer works based on complex electrostatic fields applied between inner and outer electrodes to trap ions. Ions are resolved around the inner electrode depending on the applied electrostatic frequency and the mass-to-charge ratio (*m/z*) of ions [56]. Hybrid versions of the Orbitrap [e.g. linear ion trap-Orbitrap (LTQ-orbitrap™)] have been utilized for protein identification and quantitation [57]. Based on the fundaments of the ion trap, ion movements are controlled by alternating current (AC) and direct current (DC) electric fields that are dynamically trapping, stabilizing, or filtering out the ions depending on the mode of the analysis [58]. Q-TOF instruments are another type of tandem mass spectrometers for global protein profiling and quantitation [59]. The quadrupole is usually used for its ion filtering capability as the first mass analyzer in hybrid instruments. Quadrupole analyzers use AC and DC electric field to

stabilize or destabilize ions with different *m/z* ratios, thus often referred to as mass filters; these analyzers are typically operated at modes with low mass resolution and accuracy [60].

Mass filtering capability of quadrupole analyzers makes triple quadrupole (QqQ) mass spectrometers suitable for targeted proteomic quantitation. These instruments are used in the mode of multiple reaction monitoring (MRM) analysis [61]. Alternative approaches for targeted proteomic quantitation have been reported newly developed hybrid instruments. A quadrupole-orbitrap platform (Q Exactive™) is able to deliver pseudomultiple reaction monitoring (pMRM) analysis. It can also perform the method of parallel reaction monitoring in which a full scan of MS/MS data is achievable from all the precursors and fragments in high resolution and the needed information is extracted after data acquisition [62]. A recent exploration of the Q-TOF instrument performs parallel selection and fragmentation of a range of precursor ions [63-65].

1.3.3 Derivatization-free techniques

1.3.3.1 Label-free quantitation

Label-free quantitation is the simplest, fastest, and cleanest amongst all the MS-based quantitation methods. It has been frequently used in shotgun proteomics in which the protein profiling/quantitation is performed on a large scale and in a non-targeted fashion [66]. The sample goes through the least manipulation before MS analysis. The label-free quantitation can be done based on 1) ion intensity or peak area measurement in the chromatogram for an intact peptide and 2) spectral counting of the fragment ions from all the peptides (originated from a single protein) in a MS/MS-based analysis. Spectral counting is implemented in a data dependent acquisition (DDA) mode. In a DDA tandem mode, selected precursor ions are subjected to fragmentation when their abundances are above a user-set, predefined level. DDA mode-based spectral counting shows good correlation with the protein abundance [67]. However, this method is not

recommended for low abundance proteins due to poor accuracy. Software to assist in label-free quantitation includes an ion intensity chromatogram measurement called MS1 filtering. This increases peak selection accuracy by incorporating the peptide retention time [68]. Another software program takes advantage of simultaneous spectral counting and a total ion chromatogram to enhance the analysis quality [69].

1.3.3.2 Label-assisted quantitation

With the label-free methods in the repertoire of quantitative proteomics practitioners, there is still a need for label-assisted methods to perform quantitation with improved accuracy and precision. Label-assisted methods incorporate stable isotope labels into internal standards (IS) for quantitation; this MS-based quantitation method is termed stable isotope dilution (SID). The incorporation of stable isotope labels can be achieved either without or with chemical derivatization of proteome samples. Use of metabolic labeling, absolute quantitation (AQUA) peptides, and ^{18}O labeling are three common derivatization-free methods.

1.3.3.2.1 Metabolic labeling

Metabolic labeling is capable of labeling the whole proteome in cells or an entire organism. Metabolic labeling of cells is accomplished by the addition of isotopically labeled amino acids into the cell culture media which lacks the same, but non-isotopically labeled amino acids. Each stable isotope label is commonly 1 or 2 Da higher in mass, such as ^{15}N and ^{13}C. Stable isotope labeling with amino acids in cell culture (SILAC) is the most popular method of metabolic labeling [70]. The comprehensiveness and relative simplicity of SILAC makes it commonly used for the relative quantitation of proteome samples [71-73]. Labeling proteins is advantageous because it allows for more accurate quantitation due to the early addition of the IS in sample preparation. This mitigates the sample loss variations from the downstream manipulation, including protein fractionation and

separation, digestion, and peptide separation. A drawback is that it is not applicable to tissue samples or biological fluids, such as plasma and urine. However, an altered approach that uses stable isotope labeled proteome (SILAP) as the IS applies the same metabolic labeling concept to the secretome of a cell line(s) [72]. It was used to make a secretome IS from CAPAN-2 human pancreatic cancer derived cells for relative quantitation of sera proteins from early-stage pancreatic cancer patients. SILAP has also been utilized to investigate different biomarkers for prostate cancer [74]. Stable isotope labeling of mammals (SILAM) is an adapted approach to make the metabolic labeling compatible with tissue analysis [75]. This was accomplished in rats with ^{15}N-enriched spirulina diet. Providing an IS for tissue allows for quantitative pathway analysis [76,77].

Another developed solution for the tissue proteome analysis is super-SILAC [71]. In this approach, labeled proteins are provided from multiple cell lines and used as a combined IS. The cell lines are pooled together to better represent a tissue proteome. Another SILAC derivative is the method of *in vivo* termini amino acid labeling (IVTAL) [78]. This method couples 2 different endoproteases (Arg-C and Lys-N) and 2 different cell culture media (heavy arginine and heavy lysine) to produce isobaric peptides that have varied MS fragment ions [78].

1.3.3.2.2 Absolute quantitation (AQUA) peptides

Absolute quantitation allows for direct comparison of proteomic data obtained on different instruments and in different laboratories. The need to measure the absolute abundance of proteins is achievable using a targeted quantitation approach. A synthetic, isotopically labeled peptide is used as the IS. This peptide is the isotopic counterpart of a signature peptide, which represents a 1:1 ratio with the corresponding protein. There are a number of cautions that need to be considered to choose an endogenous peptide as a signature of the target protein. The signature peptide quantitatively represents the target, therefore should be a stoichiometric equivalence of the protein

[i.e. lacking co/post-translational modifications (PTMs)]. Digestion efficiency, peptide uniqueness, and a number of other peptide selection criteria should be considered in choosing the signature peptide [79]. This type of quantitation is often performed via tandem MS specifically on a MRM platform [80]. Unlike metabolic labeling, AQUA is applicable to quantitation of proteomes of almost every biological source such as tissues, plasma, or cells. Absolute quantitation using synthetic heavy peptides is among the most popular methods for quantitative analysis in system biology and therapeutics and biomarker development [81-84].

1.3.3.2.3 ^{18}O labeling

Isotope labeling of proteome samples can be achieved via enzymatic ^{18}O replacement of ^{16}O on carboxylic groups at C-termini of peptides from proteome digests [85,86]. The source of ^{18}O is $H_2{}^{18}O$ comprised buffer. Enzymatic ^{18}O labeling globally incorporates two ^{18}O atoms at the C-terminus carboxyl group of almost all of the peptides of a proteome digest. Use of enzymes in immobilized formats allows for efficient post-labeling removal and thus eliminating back-exchange of ^{18}O labels [87]. In-gel ^{18}O labeling has been found to facilitate protein identification and quantification [88]. ^{18}O labeling initially developed for relative quantitation has also been adapted for absolute quantitation of proteins [89,90]. Studies of protein PTMs is another application area. ^{18}O labeling has been utilized for quantitation of phosphorylation [91] and deamidation [92,93]. Acid catalysis can also exchange peptidyl carboxylate oxygen atoms, but in a non-selective manner [94,95]. Due to drawbacks like residue and peptide sequence dependence of the labeling and chemical changes of peptides under acidic conditions (e.g. deamidation) the acid labeling should be limited to special applications [90].

1.3.4 Derivatization-based techniques

1.3.4.1 Isobaric tagging

Isobaric mass tagging reagents are the most widely used for derivatizing peptides in quantitative proteomics [96]. While the structure varies, most isobaric mass tagging reagents are comprised of 3 elements: (1) a mass reporter moiety with a unique number of heavy isotope (^{13}C or ^{15}N) substitutions, (2) a mass balancer moiety with complementary labels of heavy isotopes to balance the total mass of the reporter and balancer moieties, and (3) a reactive moiety to tag peptidyl amines. Two sets of amine-reactive isobaric mass tagging reagents, with a common reactive moiety of NHS ester, are commercially available: tandem mass tags (TMT™) [97] and isobaric tags for relative and absolute quantitation (iTRAQ®) [98]. They are designed to label primary amines (N-termini and lysine's side chain amines) in peptides. One example of isobaric tags is shown in **Figure 1.4**.

A set of isobaric tags has identical intact masses and chemical properties which allow for co-elution of differentially derivatized peptides during chromatography. Ions for the derivatized peptides have a common *m/*z and they can be co-selected by the first mass analyzer of tandem MS. The isobaric tags on derivatized peptide ions are then cleaved at a specific site via gas-phase dissociation. A set of reporter ions with unique numbers of heavy isotope labels are then detected. The relative signal intensities of the reporter ions are used to quantify the differentially labeled peptides and thus proteins. Samples that can be analyzed in a single experiment are up to 8 for isobaric derivatization approaches. Recently, thiol-reactive TMT™ reagents coupled with immuno-purification techniques are reported [99]. Reagents that are structurally similar to iTRAQ®/TMT™, but use less expensive deuterium labels, have the potential for further increase in sample throughput [100].

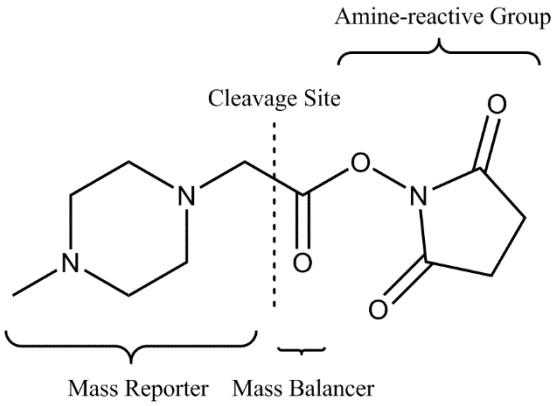

Figure 1.4: The structure of iTRAQ® reagents.

1.3.4.2 Mass-difference reagents

Isotope-coded affinity tag (ICAT®), first invented in 1999, is one of the earliest chemical reagents introduced for quantitative proteomics at the protein level [101]. The original ICAT® reagents include: a thiol-specific reactive group, an isotopically modified linker, and a biotin tag for the enrichment of the tagged peptides. After derivatization, both heavy and light labeled proteins are pooled and enzymatically digested into peptides. The tagged, cysteine-containing peptides are then enriched with avidin affinity chromatography and quantified via MS. Cleavable versions of this reagent was later developed to improve the recovery of the tagged peptides [102]. The heavy version of the so-called cICAT reagents contain 9 ^{13}C instead of 8 ^{2}H and an acid-cleavable biotin moiety. Insertion of an acid-labile linker greatly decreases the elution of non-specifically bound peptides from avidin affinity materials. Isotope-coded protein labels (ICPLs) differentially label all of the free amino groups on proteins for relative quantitation [103]. This method does not require an affinity tag.

The so-called mTRAQ® reagents are developed for introducing differential isotope labels in a mass different manner and are used in MRM-MS quantitation [104]. These reagents have the same chemical structure as those for iTRAQ® reagents, but carry redesigned stable isotope labeling

states. They can also be used for peptide quantitation based on the signal intensity of precursor ions. Reductive methylation of peptidyl amines is another commonly applied technique to introduce differential isotope labels to peptides. Derivatized peptides preferentially produce a_1 ions serving as quantitation reporters [105]. These reporter ions are peptide-specific, thus lessening interference from co-eluting peptides with the same or similar mass. Reductive dimethylation has been applied to analyze low-abundance phosphopeptides [106].

1.3.5 Activity-based probes

Activity-based protein profiling (ABPP) technology utilizes active site-directed chemical probes, combined with a range of analytical methods, for functional proteome analysis. These small molecules are commonly referred to as activity-based probes (ABPs). A typical structure of ABPs is comprised of 3 elements: (1) a reactive group for forming covalent adducts with functional groups at the active site of enzymes, (2) a recognizing moiety for non-covalent interactions with proteins, and (3) a reporting tag for detection and/or separation. Changes in the recognizing structural moiety can vary the reactivity and/or selectivity of the probes [107]. Small "clickable" handles such as an alkyne can also be incorporated as dormant reporting groups for being coupled with quantitation or separation tags after the in vivo reaction of the probes with living cells [108]. One major advantage of ABPP [109,110] over the previous techniques [111,112] is the ability to directly monitor active sites on a multitude of enzyme classes, and the analysis depends on the protein activity not on concentration or abundance. Furthermore, ABPP can be combined with tandem MS analysis for enriched enzyme identification. One approach, termed as activity-based protein profiling by multidimensional protein identification technology (ABPP-MudPIT), was used to profile inhibitor selectivity against hundreds of targets simultaneously via in vitro or in vivo reactions [113]. The integrated design of stable isotopic ABPs allows for easy implementation

of quantitative MS measurements in biological samples [114,115]. Another approach, termed isoTOP-ABPP (isotopic tandem orthogonal proteolysis-activity-based protein profiling), was used to quantitatively profile the intrinsic reactivity of cysteine residues across multiple proteomes by using a heavy isotope labeled valine and a protease-cleavable linker [116].

1.3.6 Sample preparation

Generically, bottom-up proteomics sample preparation involves the solubilzation of proteins from the biological source, with subsequent enzymatic digestion of the proteins to peptides. Each of these preparatory steps allows for unique enrichment techniques. **Figure 1.5** summarizes the workflow and accompanying enrichment techniques.

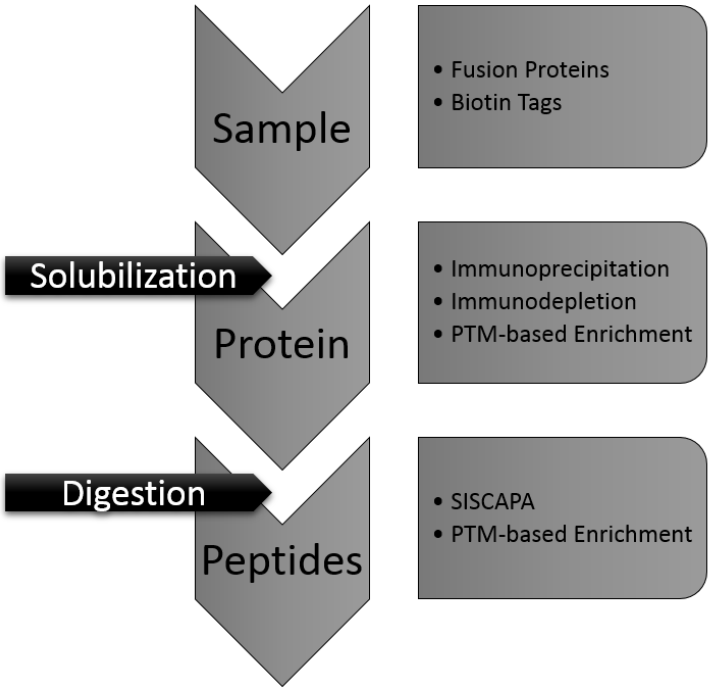

Figure 1.5: Enrichment techniques in proteome analysis.

1.3.6.1 Pre-lysis techniques

1.3.6.1.1 Recombinant fusion proteins

The use of recombinant fusion proteins for protein expression determination and purification is a well-established technique [117]. It uses recombinant DNA technology to fuse a

"tag" to a protein substrate. Commonly used tags are green fluorescent protein (GFP), poly-histidine (His-tag), glutathione s-transferase (GST), and FLAG®. A comprehensive list can be found in the literature [118]. Using these proteins for MS-based quantitation of their tagged-substrates is possible. GFP is a small protein that can produce green fluorescence when illuminated under certain wavelengths. This qualitative measurement has been transcended into a quantitative measurement in MS by introducing SILAC [119] or an amine-specific isotope tag termed iTAG [120]. The inherit fluorescence of GFP was also quantitatively measured and protein binding partners were determined with shotgun proteomics [121]. All of these measurements exploit immunoprecipitation (IP) of the GFP fusion protein. There are commercial products (e.g. GFP-Trap®) that recognize GFP and pull down protein complexes. His-tag can also be used similarly. The original use of recombinant polyhistidine protein with immobilized metal ion affinity chromatography (IMAC) was described in 1988 [122]. This was applied to purify proteins by adding the small tag. It can also be used for the same purpose, but with subsequent MS analysis. There are, however, few quantitative examples of this [123].

1.3.6.1.2 Biotin tagging at specific sites

Chemical derivatization of proteins can be performed at the cellular level. There are many forms of chemical "tagging," but biotin tagging is commonly used. Biotin has a very low dissociation rate ($K_D \approx 10^{-15}$M) from avidin [124]. This kinetic property is the basis for enrichment of biotin-tagged proteins with avidin on a solid support (e.g. agarose beads). The non-bound proteins can then be washed away, and the bound proteins eluted. By functionalizing the biotin moiety with reactive groups, biotin tagging can be performed to specific sites on proteins. Two examples that use functionalized biotin in quantitative proteomics are experiments measuring lysine exposure on a peptide [125] and cell surface protein expression [126].

1.3.6.2 Protein-level enrichment

1.3.6.2.1 Antibody-based enrichment

Co-immunoprecipitation (co-IP) is a common technique to enrich protein interaction complexes. This method uses an antibody to bind a known protein, which in turn has known or unknown binding partners. Shotgun proteomics is then performed to determine the enriched proteins. Quantitative MS is used to validate bound proteins and measure binding stoichiometry for proteins in the complexes prepared via IP [127,128]. Quantitation approaches used include SILAM [129], label-free [130], and AQUA peptides with a normalization step [131].

1.3.6.2.2 Immunodepletion

Proteome samples often have very large ranges in protein concentration. Dominant, high abundance proteins can compromise the analysis of minor protein components. For instance, plasma is composed of a complex mixture of proteins and albumin and immunoglobulin G (IgG) compose over 60% of the total protein amount in plasma [132]. These abundant proteins can make the analysis of medium to low abundance proteins very difficult [133,134]. Depletion of these and several other abundant proteins allow for in-depth analysis of low abundance ones. There are many commercial products for protein immunodepletion. Applications of the products are reported for a Seppro® column in a label-free method [135]. Seppro® column in a SILAP method [136], a Hu-6 Multiple Affinity Removal System (MARS) kit in an iTRAQ® method [137], and a Hu-6 MARS kit in another iTRAQ®-based method [138]. Caution should be observed if a low abundance protein has affinity to a high abundance protein because it can be co-depleted.

1.3.6.2.3 Techniques based on PTMs

PTMs of proteins enable many important functions in organisms [139]. Proteins with PTMs can be enriched in a variety of ways: antibody-based, chemical derivatization, and ionic

interaction-based [89]. Antibodies that are highly specific to a particular PTM site greatly help functional assays. Antibodies that preferably bind a class of PTM, e.g. proteins carrying phosphotyrosine residues, make possible the in-depth quantitative proteomic analysis of these proteins. The sub-stoichiometric nature of PTMs yields a low concentration of modified proteins. Enrichment of these proteins allows for improved analysis.

1.3.6.3 Peptide-level enrichment

1.3.6.3.1 Stable isotope standards and capture by anti-peptide antibodies (SISCAPA)

Immunoenrichment can be applied at the peptide level, particularly in the SISCAPA method [140]. Target peptides together with their stable isotope labeled counterparts (used as quantitation references) are enriched by antibodies that are developed against antigens with almost the same sequences. The antibodies are often covalently attached to magnetic beads for sample cleanup. This technique boasts an improved limit of quantitation and increased inter-laboratory reproducibility [141].

1.3.6.3.2 Techniques based on PTMs

Many of the techniques used to enrich PTMs at the protein level are applicable at the peptide level. A popular method for enrichment of phosphopeptides is to use an immobilized metal affinity column. The molecular basis for the enrichment is the phosphate affinity to transition metal ions, such as, copper, nickel, cobalt, iron, aluminum, gallium, and zinc [142]. A comprehensive source for phosphopetide enrichment strategies can be found in a recent review [143]. Lectin-based chromatography is used to enrich for glycopeptides [144]. Lectins are proteins that have an affinity for carbohydrates. With multiple available enrichment options, choosing a right one for the experiment is important. For determining which proteins have a certain PTM, protein-level enrichment can be performed. However, if a type of PTM is of interest, then peptide-level

enrichment will yield less sample complexity. The use of multiple antibodies to enrich for multiple PTMs simultaneously has led to the development of PTMScan® technology [145]. A monoclonal antibody specific to the diglycine tag on lysine residues has also been used to enrich ubiquitinated tryptic peptides [146].

1.3.7 Liquid chromatography

In shotgun (bottom-up) proteomics workflows, proteins are digested by proteases and the resulting peptides are separated by LC before MS analysis [147]. With the rapid advancement in LC and MS instrumentation, LC-based proteomics overwhelms the 2-DE-based approaches. The shotgun proteomics pipeline can provide improved throughput, sensitive protein profiling, and accurate protein quantitation. When working with complex samples, such as human serum, the bottom-up approach produces thousands of peptides with very different abundances and some of the peptides have similar *m/z* ratios. This requires high resolution separation of peptides prior to MS analysis. LC reduces ion suppression of co-eluting peptides during ionization and increases the likelihood of detecting low abundance peptides [147]. Different LC methods have been developed for proteomic analyses such as reversed phase (RP), ion-exchange (IEX), and hydrophilic interactions chromatography (HILIC). RP separations are the dominant choice due to the very high resolving power and electrospray ionization (ESI) MS-friendly solvents.

1.3.7.1 Common separation modes

1.3.7.1.1 RP chromatography

Introduced in 1976, RP chromatography is the mostly used approach for peptide separation [147,148]. Peptides are separated in a RP column upon partitioning between the hydrophobic stationary phase and the mobile phase. Peptides are loaded onto the column using low organic solvent, allowing for initial desalting and concentration of the sample. Separation and elution of

the peptides occur by increasing the percentage of organic solvent in the mobile phase; commonly used solvents are acetonitrile and methanol due to their appropriate solvent strength, volatility, viscosity, and MS compatibility. Acidic modifiers help improve resolution of RP chromatography of peptides by acting as ion pairing agents for positively charged groups on peptides. RP stationary phases are mostly silica-based C18 resin and acid additives help improve peak resolution by keeping residual silanol groups protonated. From a separation perspective, trifluoroacetic acid (TFA) has a higher hydrophobicity and enables narrower peaks than other acids like acetic acid and formic acid (FA). FA, however, is the common choice for online use with ESI MS to minimize ion suppression.

1.3.7.1.2 IEX chromatography

Peptide separation in IEX chromatography is based on electrostatic interactions between charged groups on the peptides and the charged stationary phase. The mobile phase can be a buffer whose salt strength changes during separation. Separation can also be achieved by changing the pH value of the mobile phase to neutralize the charge of the analytes and/or stationary phase. IEX chromatography is classified into cation exchange (CX) and anion exchange (AX) chromatography [149]. CX is divided into 2 categories: strong cation exchange (SCX) and weak cation exchange (WCX). SCX chromatography utilizes strong acids such as sulfonic acid derivatives and is the second mostly used chromatographic method in LC-based proteomic analysis. WCX, on the other hand, is restricted to a smaller pH range and its application is limited [147,150,151].

1.3.7.1.3 HILIC

HILIC uses a polar stationary phase to separate proteins and peptides. Samples are loaded onto a column using a low aqueous mobile phase and are eluted by increasing the water content of the mobile phase [152]. HILIC is very suitable for separation of polar species such as sialic acid-

containing glycopeptides which have limited retention on most RP materials [153]. A variant of HILIC is electrostatic repulsion-hydrophobic interactions chromatography (ERLIC) and it utilizes ion-exchange stationary phase and a high organic mobile phase [152,154].

1.3.7.2 Multidimensional LC strategies

When working with complex peptide mixtures like a proteome digest, multiple separations help with analysis of minor components in the mixture. Coupling two different modes of LC results in the improved separation of peptides and thus reduced number of co-eluting peptides for MS analysis. To utilize the maximum separation space afforded by multidimensional LC, orthogonality of different chromatography modes which separate peptides based on largely different properties is important [155]. For example, SCX-RP is more orthogonal than a RP-RP combination. Multidimensional LC can be achieved by coupling 2 or more 1-D techniques either online or offline [147]. LC separation of peptides that utilizes different protonation states of peptides at low and high pH in a RP-RP combination is also attractive. This combination avoids the use of MS-unfriendly salts used in SCX-RP separations [156,157]. **Figure 1.6** illustrates the first MudPIT system for the direct analysis of large protein complexes [158,159].

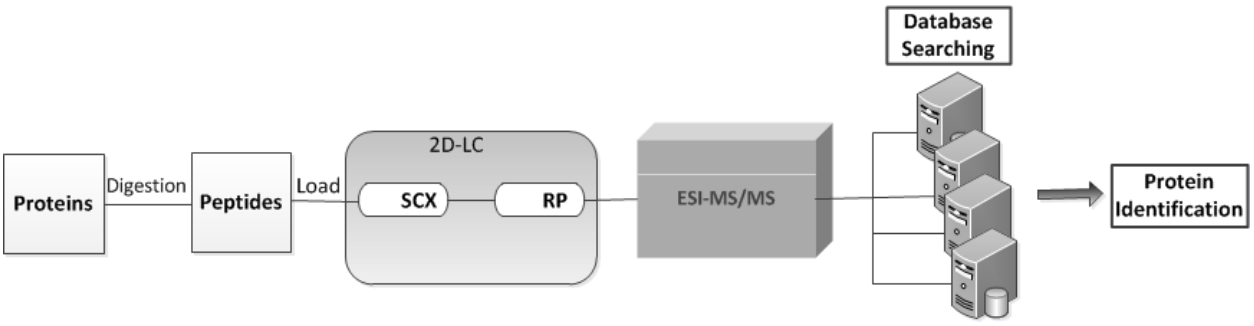

Figure 1.6: Online 2-D chromatography systems coupled with MS/MS.[i]

[i] Figure by Reza Nemati. McShane, A. J.; Farrokhi, V.; Nemati, R.; Li, S.; Yao, X. An Overview of Quantitative Proteomic Approaches. Comprehensive Analytical Chemistry, Oxford, UK; Elsevier, **2014**; p. 111-135.

1.3.7.3 LC using new separation media

Ultra performance liquid chromatography (UPLC) is an important advancement in chromatography due to the significantly improved speed, resolution, and sensitivity [160]. UPLC typically uses separation media with a particle size less than 2.0 μm [161,162]. UPLC systems operate under very high pressure to accommodate the use of small particles. This technology allows for faster flow rates, while maintaining the separation efficiency and thus increasing the sample throughput of analysis [161,163].

As an alternative to wholly porous sub-2 μm particles, 1.7 μm fused-core particles surrounded by a 0.5 μm porous silica layer with 90 Å pores, have emerged. In a comparative study, substantially lower back pressure was reported when the fused core particles were used. This allowed for columns to be coupled in series which increased the peak efficiency up to 92750 plates [164]. Wider-pore fused-core particles have an average pore diameter of 160 Å. The wider-pore particles are particularly useful for increased sample loading and the rapid separation of peptides using volatile mobile phases [165].

1.3.7.4 Nanoscale LC

Nanoscale liquid chromatography (nano-LC) using RP separation materials is the default choice for LC-MS of peptides from proteome digests. Nano-LC has excellent sensitivity using 50-100 μm diameter columns and 200-300 nL/min flow rates [166]. An all-inclusive definition for nano-LC is a LC that separates nanoliter amounts of sample, with nanoliter amounts of mobile phase, and yields detection limits in the range of nanograms per milliliter [167].

1.3.7.5 GeLC method

In this method, proteins in cell lysates or complex mixtures are typically first separated by SDS PAGE. Followed by in-gel enzymatic digestion of the separated proteins, the resulting

peptides are extracted for 1-D or multidimensional LC separation before MS analysis. This approach takes advantage of high resolution SDS-PAGE for proteins under denaturing condition, thus reducing the sample complexity at the protein level. LC separations further reduce sample complexity at the peptide level. Also, with staining gel bands, it's possible to separate gel pieces containing high abundance proteins [158]. This technique can be applied to 2-D gels as well [168].

1.3.8 Software

Software tools are a must for proteome analysis, considering the massive data produced. Data analysis typically starts with peptide identification with a set of tandem mass spectra and database search engines, such as Mascot [169], Sequest [170], and X!Tandem [171]. Extracted ion chromatograms (XIC) can be reconstructed and the ratios of signal intensities estimated from either peak heights or areas for quantitative analysis. Statistical analysis of results is essential, including assignment of significant scores, normalization of peptide abundances, and statistical evaluation of quantitation results, as well as function and location of proteins. Significant development of MS-based proteomic technologies in the past decade encouraged the concurrent advance in data analysis tools [172-174]. Further reading on bioinformatics and other computing concerns for proteomics can be found elsewhere in this book.

1.3.9 Analyte multiplexing and sample throughput

Contemporary proteomics demands high-throughput and multiplexed analytical strategies and platforms. In the early stages of the biomarker discovery pipeline, for instance, multiplexed analysis of peptides from thousands of proteins in a few samples is required. However, further down the pipeline there is a shift towards high-throughput analysis because the number of samples increases dramatically and number of peptides or analytes decreases [175]. MRM MS methods currently dominate MS-based high-throughput quantitative proteomics [176,177]. Efforts in

developing MRM approaches to perform both multiplexed and high throughput analysis via either immuno-enrichment [178] or ultra-throughput multiple reaction monitoring (UMRM) [179] are reported. New MS strategies to improve the sample throughput of proteomic analysis are emerging using recently available mass spectrometers.

1.4 Conclusion

The field of proteomics has evolved significantly thanks to collective efforts from practitioners with eclectic backgrounds. Technological advances in every step of the proteome analysis pipeline, from sample preparation to MS analysis to protein identification and quantitation to protein functional denotation, have significantly reduced the induction period of initial learning and encouraged the widespread adaption of proteomics. Fruitful applications continuously emerge in the study of biomarkers, disease, medicine, food and plants, and the environment, just to name a few. The inherit sample complexity and diversity still present both technical challenges and opportunities for in-depth analysis of the entire proteome.

1.5 References

1. Laemmli, U. K. Cleavage of Structural Proteins during the Assembly of the Head of Bacteriophage T4. *Nature*. **1970**, 227, 680-685.

2. Righetti, P. G.; Candiano, G. Recent Advances in Electrophoretic Techniques for the Characterization of Protein Biomolecules: A Poker of Aces. *J. Chromatogr. A.* **2011**, 1218, 8727-8737.

3. O'Farrell, P. H. High Resolution Two-Dimensional Electrophoresis of Proteins. *J. Biol. Chem.* **1975**, 250, 4007-4021.

4. Monteoliva, L.; Albar, J. P. Differential Proteomics: An Overview of Gel and Non-Gel Based Approaches. *Brief. Funct. Genomics*. **2004**, 3, 220-239.

5. Ünlü, M.; Morgan, M. E.; Minden, J. S. Difference Gel Electrophoresis. A Single Gel Method for Detecting Changes in Protein Extracts. *Electrophoresis*. **1997**, 18, 2071-2077.

6. Minden, J. S.; Dowd, S. R.; Meyer, H. E.; Stühler, K. Difference Gel Electrophoresis. *Electrophoresis*. **2009**, 30, S156-S161.

7. Tannu, N. S.; Hemby, S. E. Two-Dimensional Fluorescence Difference Gel Electrophoresis for Comparative Proteomics Profiling. *Nat. Protoc*. **2006**, 1, 1732-1742.

8. Van den Bergh, G.; Clerens, S.; Vandesande, F.; Arckens, L. Reversed-phase High-performance Liquid Chromatography Prefractionation Prior to Two-dimensional Difference Gel Electrophoresis and Mass Spectrometry Identifies New Differentially Expressed Proteins between Striate Cortex of Kitten and Adult Cat. *Electrophoresis*. **2003**, 24, 1471-1481.

9. Tonge, R.; Shaw, J.; Middleton, B.; Rowlinson, R.; Rayner, S.; Young, J.; Pognan, F.; Hawkins, E.; Currie, I.; Davison, M. Validation and Development of Fluorescence Two-

dimensional Differential Gel Electrophoresis Proteomics Technology. *Proteomics*. **2001**, 1, 377-396.

10. Burnette, W. "Western Blotting": Electrophoretic Tranfer of Proteins from Sodium Dodecyl Sulfate-Polyacrylamide Gels to Unmodified Nitrocellulose and Radiographic Detection with Antibody and Radioiodinated Protein A. *Anal. Biochem*. **1981**, 112, 195-203.

11. Renart, J.; Reiser, J.; Stark, G. R. Transfer of Proteins from Gels to Diazobenzyloxymethyl-Paper and Detection with Antisera: A Method for Studying Antibody Specificity and Antigen Structure. *Proc. Natl. Acad. Sci. U. S. A.* **1979**, 76, 3116-3120.

12. Towbin, H.; Staehelin, T.; Gordon, J. Electrophoretic Transfer of Proteins from Polyacrylamide Gels to Nitrocellulose Sheets: Procedure and some Applications. *Proc. Natl. Acad. Sci. U. S. A.* **1979**, 76, 4350-4354.

13. Kale, S.; Kale, A.; Gholap, H.; Rana, A.; Desai, R.; Banpurkar, A.; Ogale, S.; Shastry, P. Quantum Dot Bio-Conjugate: As a Western Blot Probe for Highly Sensitive Detection of Cellular Proteins. *J. Nanopart. Res*. **2012**, 14, 732/1-732/15.

14. Chen, W.; Xu, D.; Liu, L.; Peng, C.; Zhu, Y.; Ma, W.; Bian, A.; Li, Z.; Yuanyuan; Jin, Z.; Zhu, S.; Xu, C.; Wang, L. Ultrasensitive Detection of Trace Protein by Western Blot Based on POLY-Quantum Dot Probes. *Anal. Chem*. **2009**, 81, 9194-9198.

15. Ornberg, R. L.; Harper, T. F.; Liu, H. Western Blot Analysis with Quantum Dot Fluorescence Technology: A Sensitive and Quantitative Method for Multiplexed Proteomics. *Nat. Methods*. **2005**, 2, 79-81.

16. Pan, W.; Chen, W.; Jiang, X. Microfluidic Western Blot. *Anal. Chem*. **2010**, 82, 3974-3976.

17. Hou, C.; Herr, A. E. Microfluidic Integration of Western Blotting is Enabled by Electrotransfer-Assisted Sodium Dodecyl Sulfate Dilution. *Analyst*. 2013, 138, 158-163.

18. Hughes, A. J.; Herr, A. E. Microfluidic Western Blotting. *Proc. Natl. Acad. Sci. U. S. A.* **2012**, 109, 21450-21455.

19. Kim, D.; Karns, K.; Tia, S. Q.; He, M.; Herr, A. E. Electrostatic Protein Immobilization using Charged Polyacrylamide Gels and Cationic Detergent Microfluidic Western Blotting. *Anal. Chem*. **2012**, 84, 2533-2540.

20. Tia, S. Q.; He, M.; Kim, D.; Herr, A. E. Multianalyte on-Chip Native Western Blotting. *Anal. Chem*. **2011**, 83, 3581-3588.

21. Voller, A.; Bartlett, A.; Bidwell, D. E. Enzyme Immunoassays with Special Reference to ELISA Techniques. *J. Clin. Pathol*. **1978**, 31, 507-520.

22. Yalow, R. S.; Berson, S. A. Immunoassay of Endogenous Plasma Insulin in Man. *J. Clin. Invest*. **1960**, 39, 1157-1175.

23. Rissin, D. M.; Kan, C. W.; Campbell, T. G.; Howes, S. C.; Fournier, D. R.; Song, L.; Piech, T.; Patel, P. P.; Chang, L.; Rivnak, A. J.; Ferrell, E. P.; Randall, J. D.; Provuncher, G. K.; Walt, D. R.; Duffy, D. C. Single-Molecule Enzyme-Linked Immunosorbent Assay Detects Serum Proteins at Subfemtomolar Concentrations. *Nat. Biotechnol*. **2010**, 28, 595-599.

24. Rissin, D. M.; Fournier, D. R.; Piech, T.; Kan, C. W.; Campbell, T. G.; Song, L.; Chang, L.; Rivnak, A. J.; Patel, P. P.; Provuncher, G. K.; Ferrell, E. P.; Howes, S. C.; Pink, B. A.; Minnehan, K. A.; Wilson, D. H.; Duffy, D. C. Simultaneous Detection of Single Molecules and Singulated Ensembles of Molecules Enables Immunoassays with Broad Dynamic Range. *Anal. Chem*. **2011**, 83, 2279-2285.

25. Wilson, R. High-Content Aptamer-Based Proteomics. *J. Proteomics*. **2011**, 74, 1852-1854.

26. Bruno, J. G.; Carrillo, M. P.; Phillips, T.; Edge, A. Discrimination of Recombinant from Natural Human Growth Hormone using DNA Aptamers. *J. Biomol. Tech*. **2011**, 22, 27-36.

27. Gold, L.; Ayers, D.; Bertino, J.; Bock, C.; Bock, A.; Brody, E. N.; Carter, J.; Dalby, A. B.; Eaton, B. E.; Fitzwater, T.; Flather, D.; Forbes, A.; Foreman, T.; Fowler, C.; Gawande, B.; Goss, M.; Gunn, M.; Gupta, S.; Halladay, D.; Heil, J.; Heilig, J.; Hicke, B.; Husar, G.; Janjic, N.; Jarvis, T.; Jennings, S.; Katilius, E.; Keeney, T. R.; Kim, N.; Koch, T. H.; Kraemer, S.; Kroiss, L.; Le, N.; Levine, D.; Lindsey, W.; Lollo, B.; Mayfield, W.; Mehan, M.; Mehler, R.; Nelson, S. K.; Nelson, M.; Nieuwlandt, D.; Nikrad, M.; Ochsner, U.; Ostroff, R. M.; Otis, M.; Parker, T.; Pietrasiewicz, S.; Resnicow, D. I.; Rohloff, J.; Sanders, G.; Sattin, S.; Schneider, D.; Singer, B.; Stanton, M.; Sterkel, A.; Stewart, A.; Stratford, S.; Vaught, J. D.; Vrkljan, M.; Walker, J. J.; Watrobka, M.; Waugh, S.; Weiss, A.; Wilcox, S. K.; Wolfson, A.; Wolk, S. K.; Zhang, C.; Zichi, D. Aptamer-Based Multiplexed Proteomic Technology for Biomarker Discovery. *PLoS One*. **2010**, 5, e15004.

28. Janssen, K. P.; Knez, K.; Spasic, D.; Schrooten, J.; Lammertyn, J. Multiplexed Protein Detection using an Affinity Aptamer Amplification Assay. *Anal. Bioanal Chem*. **2012**, 404, 2073-2081.

29. Srinivas, R. L.; Chapin, S. C.; Doyle, P. S. Aptamer-Functionalized Microgel Particles for Protein Detection. *Anal. Chem*. **2011**, 83, 9138-9145.

30. Abdulhalim, I.; Zourob, M.; Lakhtakia, A. Surface Plasmon Resonance for Biosensing: A Mini-Review. *Electromagnetics*. **2008**, 28, 214-242.

31. Retra, K.; Geitmann, M.; Kool, J.; Smit, A. B.; de Esch, I. J.; Danielson, U. H.; Irth, H. Development of Surface Plasmon Resonance Biosensor Assays for Primary and Secondary Screening of Acetylcholine Binding Protein Ligands. *Anal. Biochem*. **2010**, 407, 58-64.

32. Estevez, M.; Belenguer, J.; Gomez-Montes, S.; Miralles, J.; Escuela, A. M.; Montoya, A.; Lechuga, L. M. Indirect Competitive Immunoassay for the Detection of Fungicide

Thiabendazole in Whole Orange Samples by Surface Plasmon Resonance. *Analyst*. **2012**, 137, 5659-5665.

33. Gnedenko, O. V.; Mezentsev, Y. V.; Molnar, A. A.; Lisitsa, A. V.; Ivanov, A. S.; Archakov, A. I. Highly Sensitive Detection of Human Cardiac Myoglobin using a Reverse Sandwich Immunoassay with a Gold Nanoparticle-Enhanced SPR Biosensor. *Anal. Chim. Acta*. **2013**, 759, 105-109.

34. Alterman, M.; Sjöbom, H.; Säfsten, P.; Markgren, P.; Danielson, U. H.; Hämäläinen, M.; Löfås, S.; Hultén, J.; Classon, B.; Samuelsson, B. P1/P1' Modified HIV Protease Inhibitors as Tools in Two New Sensitive Surface Plasmon Resonance Biosensor Screening Assays. *Eur. J. Pharm. Sci*. **2001**, 13, 203-212.

35. Lausted, C.; Hu, Z.; Hood, L. Quantitative Serum Proteomics from Surface Plasmon Resonance Imaging. *Mol. Cell. Proteomics*. **2008**, 7, 2464-2474.

36. Law, W. C.; Yong, K. T.; Baev, A.; Prasad, P. N. Sensitivity Improved Surface Plasmon Resonance Biosensor for Cancer Biomarker Detection Based on Plasmonic Enhancement. *ACS Nano*. **2011**, 5, 4858-4864.

37. Hong, X.; Hall, E. A. Contribution of Gold Nanoparticles to the Signal Amplification in Surface Plasmon Resonance. *Analyst*. **2012**, 137, 4712-4719.

38. Yang, C.; Brooks, E.; Li, Y.; Denny, P.; Ho, C.; Qi, F.; Shi, W.; Wolinsky, L.; Wu, B.; Wong, D. T. Detection of Picomolar Levels of Interleukin-8 in Human Saliva by SPR. *Lab Chip*. **2005**, 5, 1017-1023.

39. Uludag, Y.; Tothill, I. E. Cancer Biomarker Detection in Serum Samples using Surface Plasmon Resonance and Quartz Crystal Microbalance Sensors with Nanoparticle Signal Amplification. *Anal. Chem*. **2012**, 84, 5898-5904.

40. Li, Y.; Lee, H. J.; Corn, R. M. Detection of Protein Biomarkers using RNA Aptamer Microarrays and Enzymatically Amplified Surface Plasmon Resonance Imaging. *Anal. Chem.* **2007**, 79, 1082-1088.

41. Byun, K. M.; Yoon, S. J.; Kim, D.; Kim, S. J. Experimental Study of Sensitivity Enhancement in Surface Plasmon Resonance Biosensors by use of Periodic Metallic Nanowires. *Opt. Lett*. **2007**, 32, 1902-1904.

42. Ferreira, J.; Santos, M. J.; Rahman, M. M.; Brolo, A. G.; Gordon, R.; Sinton, D.; Girotto, E. M. Attomolar Protein Detection using in-Hole Surface Plasmon Resonance. *J. Am. Chem. Soc*. **2008**, 131, 436-437.

43. Sim, H. R.; Wark, A. W.; Lee, H. J. Attomolar Detection of Protein Biomarkers using Biofunctionalized Gold Nanorods with Surface Plasmon Resonance. *Analyst*. **2010**, 135, 2528-2532.

44. Becker, H.; Gartner, C. Microfluidics and the Life Sciences. *Sci. Prog*. **2012**, 95, 175-198.

45. Gama, M. R.; Collins, C. H.; Bottoli, C. B. Nano-Liquid Chromatography in Pharmaceutical and Biomedical Research. *J. Chromatogr. Sci*. **2013**, 51, 694-703.

46. Li, Y,; Zhang, Y.; Qiu, F.; Qiu, Z. Proteomic identification of exosomal LRG1: a potential urinary biomarker for detecting NSCLC. *Electrophoresis*. **2011,** 32, 1976-1983.

47. Ohlsson, G.; Tabaei, S. R.; Beech, J.; Kvassman, J.; Johanson, U.; Kjellbom, P.; Tegenfeldt, J. O.; Hook, F. Solute Transport on the Sub 100 Ms Scale Across the Lipid Bilayer Membrane of Individual Proteoliposomes. *Lab. Chip*. **2012**, 12, 4635-4643.

48. Benz, C. B.; Retzbach, H.; Nagl, S.; Belder, D. Protein-Protein Interaction Analysis in Single Microfluidic Droplets using FRET and Fluorescence Lifetime Detection. *Lab Chip*, **2013**, 13, 2808-2814.

49. Pailleux, F.; Beaudry, F. Internal Standard Strategies for Relative and Absolute Quantitation of Peptides in Biological Matrices by Liquid Chromatography Tandem Mass Spectrometry. *Biomed. Chromatogr*. **2012**, 26, 881-891.

50. Yao, X. Derivatization or Not: A Choice in Quantitative Proteomics. *Anal. Chem*. **2011**, 83, 4427-4439.

51. McLafferty, F. W.; Breuker, K.; Jin, M.; Han, X.; Infusini, G.; Jiang, H.; Kong, X.; Begley, T. P. Top-Down MS, a Powerful Complement to the High Capabilities of Proteolysis Proteomics. *Febs Journal*. **2007**, 274, 6256-6268.

52. Yates, J. R.; Ruse, C. I.; Nakorchevsky, A. Proteomics by Mass Spectrometry: Approaches, Advances, and Applications. *Annu. Rev. Biomed. Eng*. **2009**, 11, 49-79.

53. Domon, B.; Aebersold, R. Mass Spectrometry and Protein Analysis. *Sci. Signal*. **2006**, 312, 212.

54. Thompson, J. D.;Schaeffer-Reiss, C.; Ueffing, M. A Brief Summary of the Different Types of Mass Spectrometers used in Proteomics. Functional Proteomics, Totowa, NJ; Springer, **2008**; p. 3.

55. Standing, K. Timing the Flight of Biomolecules: A Personal Perspective. *Int. J. Mass Spectrom*. **2000**, 200, 597-610.

56. Yates, J. R.; Cociorva, D.; Liao, L.; Zabrouskov, V. Performance of a Linear Ion Trap-Orbitrap Hybrid for Peptide Analysis. *Anal. Chem*. **2006**, 78, 493-500.

57. Lu, B.; Motoyama, A.; Ruse, C.; Venable, J.; Yates, J. R. Improving Protein Identification Sensitivity by Combining MS and MS/MS Information for Shotgun Proteomics using LTQ-Orbitrap High Mass Accuracy Data. *Anal. Chem*. **2008**, 80, 2018-2025.

58. March, R. E. An Introduction to Quadrupole Ion Trap Mass Spectrometry. *J. Mass Spectrom*. **1997**, 32, 351-369.

59. Chernushevich, I. V.; Loboda, A. V.; Thomson, B. A. An Introduction to Quadrupole–time-of-Flight Mass Spectrometry. *J. Mass Spectrom*. **2001**, 36, 849-865.

60. Miller, P. E.; Denton, M. B. The Quadrupole Mass Filter: Basic Operating Concepts. *J. Chem. Educ*. **1986,** 63, 617.

61. Kuzyk, M. A.; Smith, D.; Yang, J.; Cross, T. J.; Jackson, A. M.; Hardie, D. B.; Anderson, N. L.; Borchers, C. H. Multiple Reaction Monitoring-Based, Multiplexed, Absolute Quantitation of 45 Proteins in Human Plasma. *Mol. Cell. Proteomics*. **2009**, 8, 1860-1877.

62. Michalski, A.; Damoc, E.; Hauschild, J.; Lange, O.; Wieghaus, A.; Makarov, A.; Nagaraj, N.; Cox, J.; Mann, M.; Horning, S. Mass Spectrometry-Based Proteomics using Q Exactive, a High-Performance Benchtop Quadrupole Orbitrap Mass Spectrometer. *Mol. Cell. Proteomics*. **2011**, 10, M111.011015.

63. Liu, Y.; Hüttenhain, R.; Surinova, S.; Gillet, L. C.; Mouritsen, J.; Brunner, R.; Navarro, P.; Aebersold, R. Quantitative Measurements of N-Linked Glycoproteins in Human Plasma by SWATH-MS. *Proteomics*. **2013**, 13, 1247-1256.

64. Gillet, L. C.; Navarro, P.; Tate, S.; Röst, H.; Selevsek, N.; Reiter, L.; Bonner, R.; Aebersold, R. Targeted Data Extraction of the MS/MS Spectra Generated by Data-Independent Acquisition: A New Concept for Consistent and Accurate Proteome Analysis. *Mol. Cell. Proteomics*. **2012**, 11, O111.016717.

65. Held, J. M.; Schilling, B.; D'Souza, A. K.; Srinivasan, T.; Behring, J. B.; Sorensen, D. J.; Benz, C. C.; Gibson, B. W. Label-Free Quantitation and Mapping of the ErbB2 Tumor Receptor

by Multiple Protease Digestion with Data-Dependent (MS1) and Data-Independent (MS2) Acquisitions. *Int. J. Proteomics*. **2013**, 10.1155/2013/791985.

66. Zhu, W.; Smith, J. W.; Huang, C. M. Mass Spectrometry-Based Label-Free Quantitative Proteomics. *J. Biomed. Biotechnol*. **2010**, 10.1155/2010/840518.

67. Liu, H.; Sadygov, R. G.; Yates, J. R., 3rd. A Model for Random Sampling and Estimation of Relative Protein Abundance in Shotgun Proteomics. *Anal. Chem*. **2004**, 76, 4193-4201.

68. Schilling, B.; Rardin, M. J.; MacLean, B. X.; Zawadzka, A. M.; Frewen, B. E.; Cusack, M. P.; Sorensen, D. J.; Bereman, M. S.; Jing, E.; Wu, C. C.; Verdin, E.; Kahn, C. R.; Maccoss, M. J.; Gibson, B. W. Platform-Independent and Label-Free Quantitation of Proteomic Data using MS1 Extracted Ion Chromatograms in Skyline: Application to Protein Acetylation and Phosphorylation. *Mol. Cell. Proteomics*. **2012**, 11, 202-214.

69. Freund, D. M.; Prenni, J. E. Improved Detection of Quantitative Differences using a Combination of Spectral Counting and MS/MS Total Ion Current. *J. Proteome Res*. **2013**, 12, 1996-2004.

70. Oda, Y.; Huang, K.; Cross, F. R.; Cowburn, D.; Chait, B. T. (SILAC)Accurate Quantitation of Protein Expression and Site-Specific Phosphorylation. *Proc. Natl. Acad. Sci. U. S. A*. **1999**, 96, 6591-6596.

71. Geiger, T.; Madden, S. F.; Gallagher, W. M.; Cox, J.; Mann, M. Proteomic Portrait of Human Breast Cancer Progression Identifies Novel Prognostic Markers. *Cancer Res*. **2012**, 72, 2428-2439.

72. Yu, K. H.; Barry, C. G.; Austin, D.; Busch, C. M.; Sangar, V.; Rustgi, A. K.; Blair, I. A. Stable Isotope Dilution Multidimensional Liquid Chromatography-Tandem Mass Spectrometry for Pancreatic Cancer Serum Biomarker Discovery. *J. Proteome Res*. **2009**, 8, 1565-1576.

73. Wang, C. I.; Chien, K. Y.; Wang, C. L.; Liu, H. P.; Cheng, C. C.; Chang, Y. S.; Yu, J. S.; Yu, C. J. Quantitative Proteomics Reveals Regulation of Karyopherin Subunit Alpha-2 (KPNA2) and its Potential Novel Cargo Proteins in Nonsmall Cell Lung Cancer. *Mol. Cell. Proteomics*. **2012**, 11, 1105-1122.

74. Zhao, T.; Zeng, X.; Bateman, N. W.; Sun, M.; Teng, P. N.; Bigbee, W. L.; Dhir, R.; Nelson, J. B.; Conrads, T. P.; Hood, B. L. Relative Quantitation of Proteins in Expressed Prostatic Secretion with a Stable Isotope Labeled Secretome Standard. *J. Proteome Res*. **2012**, 11, 1089-1099.

75. McClatchy, D. B.; Yates, J. R., 3rd. Stable Isotope Labeling of Mammals (SILAM). *CSH Protoc*. **2008**, pdb.prot4940.

76. Rauniyar, N.; McClatchy, D. B.; Yates, J. R., 3rd. Stable Isotope Labeling of Mammals (SILAM) for in Vivo Quantitative Proteomic Analysis. *Methods*. **2013**, 61, 260-268.

77. Rayavarapu, S.; Coley, W.; Cakir, E.; Jahnke, V.; Takeda, S.; Aoki, Y.; Gordish-Dressman, H.; Jaiswal, J. K.; Hoffman, E. P.; Brown, K. J.; Hathout, Y.; Nagaraju, K. Identification of Disease Specific Pathways using in Vivo SILAC Proteomics in Dystrophin Deficient Mdx Mouse. *Mol. Cell. Proteomics*. **2013**, 12, 1061-1073.

78. Nie, A. Y.; Zhang, L.; Yan, G. Q.; Yao, J.; Zhang, Y.; Lu, H. J.; Yang, P. Y.; He, F. C. In Vivo Termini Amino Acid Labeling for Quantitative Proteomics. *Anal. Chem*. **2011**, 83, 6026-6033.

79. Kamiie, J.; Ohtsuki, S.; Iwase, R.; Ohmine, K.; Katsukura, Y.; Yanai, K.; Sekine, Y.; Uchida, Y.; Ito, S.; Terasaki, T. Quantitative Atlas of Membrane Transporter Proteins: Development and Application of a Highly Sensitive Simultaneous LC/MS/MS Method Combined with Novel in-Silico Peptide Selection Criteria. *Pharm. Res*. **2008**, 25, 1469-1483.

80. Schmidt, C.; Urlaub, H. Absolute Quantification of Proteins using Standard Peptides and Multiple Reaction Monitoring. In Quantitative Methods in Proteomics, *Methods Mol. Biol*. **2012,** 893, 249-265.

81. Gerber, S. A.; Rush, J.; Stemman, O.; Kirschner, M. W.; Gygi, S. P. (AQUA)Absolute Quantification of Proteins and Phosphoproteins from Cell Lysates by Tandem MS. *Proc. Natl. Acad. Sci. U. S. A.* **2003**, 100, 6940-6945.

82. Percy, A. J.; Chambers, A. G.; Parker, C. E.; Borchers, C. H. Absolute Quantitation of Proteins in Human Blood by Multiplexed Multiple Reaction Monitoring Mass Spectrometry. *Methods Mol. Biol*. **2013**, 1000, 167-189.

83. Percy, A. J.; Chambers, A. G.; Yang, J.; Borchers, C. H. Multiplexed MRM-Based Quantitation of Candidate Cancer Biomarker Proteins in Undepleted and Non-Enriched Human Plasma. *Proteomics*. **2013**, 13, 2202-2215.

84. Guingab-Cagmat, J. D.; Newsom, K.; Vakulenko, A.; Cagmat, E. B.; Kobeissy, F. H.; Zoltewicz, S.; Wang, K. K.; Anagli, J. In Vitro MS-based Proteomic Analysis and Absolute Quantification of Neuronal-glial Injury Biomarkers in Cell Culture System. *Electrophoresis*. **2012**, 33, 3786-3797.

85. Yao, X.; Freas, A.; Ramirez, J.; Demirev, P. A.; Fenselau, C. Proteolytic 18O Labeling for Comparative Proteomics: Model Studies with Two Serotypes of Adenovirus. *Anal. Chem*. **2001**, 73, 2836-2842.

86. Fenselau, C.; Yao, X. Proteolytic Labeling with 18O for Comparative Proteomics Studies: Preparation of 18O-Labeled Peptides and the 18O/16O Peptide Mixture. *Methods Mol. Biol*. **2007**, 359, 135-142.

87. Chen, X.; Cushman, S. W.; Pannell, L. K.; Hess, S. Quantitative Proteomic Analysis of the Secretory Proteins from Rat Adipose Cells using a 2D Liquid Chromatography-MS/MS Approach. *J. Proteome Res*. **2005**, 4, 570-577.

88. Broedel, O.; Krause, E.; Stephanowitz, H.; Schuemann, M.; Eravci, M.; Weist, S.; Brunkau, C.; Wittke, J.; Eravci, S.; Baumgartner, A. In-Gel 18O Labeling for Improved Identification of Proteins from 2-DE Gel Spots in Comparative Proteomic Experiments. *J. Proteome Res*. **2009**, 8, 3771-3777.

89. Zhao, Y.; Jensen, O. N. Modification-Specific Proteomics: Strategies for Characterization of Post-Translational Modifications using Enrichment Techniques. *Proteomics*. **2009**, 9, 4632-4641.

90. Jiang, H.; Ramos, A. A.; Yao, X. Targeted Quantitation of Overexpressed and Endogenous Cystic Fibrosis Transmembrane Conductance Regulator using Multiple Reaction Monitoring Tandem Mass Spectrometry and Oxygen Stable Isotope Dilution. *Anal. Chem*. **2010**, 82, 336-342.

91. Alghamdi, W. M.; Gaskell, S. J.; Barber, J. Detection of Low-Abundance Protein Phosphorylation by Selective 18O Labeling and Mass Spectrometry. *Anal. Chem*. **2012**, 84, 7384-7392.

92. Liu, H.; Wang, F.; Xu, W.; May, K.; Richardson, D. Quantitation of Asparagine Deamidation by Isotope Labeling and Liquid Chromatography Coupled with Mass Spectrometry Analysis. *Anal. Biochem*. **2013**, 432, 16-22.

93. Fukuda, M.; Takao, T. Quantitative Analysis of Deamidation and Isomerization in Beta2-Microglobulin by 18O Labeling. *Anal. Chem*. **2012**, 84, 10388-10394.

94. Niles, R.; Witkowska, H. E.; Allen, S.; Hall, S. C.; Fisher, S. J.; Hardt, M. Acid-Catalyzed Oxygen-18 Labeling of Peptides. *Anal. Chem*. **2009**, 81, 2804-2809.

95. Haaf, E.; Schlosser, A. Peptide and Protein Quantitation by Acid-Catalyzed 18O-Labeling of Carboxyl Groups. *Anal. Chem*. **2012**, 84, 304-311.

96. Dayon, L.; Hainard, A.; Licker, V.; Turck, N.; Kuhn, K.; Hochstrasser, D. F.; Burkhard, P. R.; Sanchez, J. Relative Quantification of Proteins in Human Cerebrospinal Fluids by MS/MS using 6-Plex Isobaric Tags. *Anal. Chem*. 2008, 80, 2921-2931.

97. Thompson, A.; Schäfer, J.; Kuhn, K.; Kienle, S.; Schwarz, J.; Schmidt, G.; Neumann, T.; Hamon, C. Tandem Mass Tags: A Novel Quantification Strategy for Comparative Analysis of Complex Protein Mixtures by MS/MS. *Anal. Chem*. **2003**, 75, 1895-1904.

98. Ross, P. L.; Huang, Y. N.; Marchese, J. N.; Williamson, B.; Parker, K.; Hattan, S.; Khainovski, N.; Pillai, S.; Dey, S.; Daniels, S. Multiplexed Protein Quantitation in Saccharomyces Cerevisiae using Amine-Reactive Isobaric Tagging Reagents. *Mol. Cell. Proteomics*. **2004**, 3, 1154-1169.

99. Murray, C. I.; Uhrigshardt, H.; O'Meally, R. N.; Cole, R. N.; Van Eyk, J. E. Identification and Quantification of S-Nitrosylation by Cysteine Reactive Tandem Mass Tag Switch Assay. *Mol. Cell. Proteomics*. **2012**, 11, M111.013441.

100. Sohn, C. H.; Lee, J. E.; Sweredoski, M. J.; Graham, R. L.; Smith, G. T.; Hess, S.; Czerwieniec, G.; Loo, J. A.; Deshaies, R. J.; Beauchamp, J. Click Chemistry Facilitates Formation of Reporter Ions and Simplified Synthesis of Amine-Reactive Multiplexed Isobaric Tags for Protein Quantification. *J. Am. Chem. Soc*. **2012**, 134, 2672-2680.

101. Gygi, S. P.; Rist, B.; Gerber, S. A.; Turecek, F.; Gelb, M. H.; Aebersold, R. Quantitative Analysis of Complex Protein Mixtures using Isotope-Coded Affinity Tags. *Nat. Biotechnol*. **1999**, 17, 994-999.

102. Hansen, K. C.; Schmitt-Ulms, G.; Chalkley, R. J.; Hirsch, J.; Baldwin, M. A.; Burlingame, A. Mass Spectrometric Analysis of Protein Mixtures at Low Levels using Cleavable 13C-Isotope-Coded Affinity Tag and Multidimensional Chromatography. *Mol. Cell. Proteomics*. **2003**, 2, 299-314.

103. Schmidt, A.; Kellermann, J.; Lottspeich, F. A Novel Strategy for Quantitative Proteomics using Isotope-coded Protein Labels. *Proteomics*. **2005**, 5, 4-15.

104. DeSouza, L. V.; Krakovska, O.; Darfler, M. M.; Krizman, D. B.; Romaschin, A. D.; Colgan, T. J.; Siu, K. mTRAQ-based Quantification of Potential Endometrial Carcinoma Biomarkers from Archived Formalin-fixed Paraffin-embedded Tissues. *Proteomics*. **2010**, 10, 3108-3116.

105. Hsu, J.; Huang, S.; Shiea, J.; Huang, W.; Chen, S. Beyond Quantitative Proteomics: Signal Enhancement of the A1 Ion as a Mass Tag for Peptide Sequencing using Dimethyl Labeling. *J. Proteome Res*. **2005**, 4, 101-108.

106. Boersema, P. J.; Foong, L. Y.; Ding, V. M.; Lemeer, S.; van Breukelen, B.; Philp, R.; Boekhorst, J.; Snel, B.; den Hertog, J.; Choo, A. B. In-Depth Qualitative and Quantitative Profiling of Tyrosine Phosphorylation using a Combination of Phosphopeptide Immunoaffinity Purification and Stable Isotope Dimethyl Labeling. *Mol. Cell. Proteomics*. **2010**, 9, 84-99.

107. Wang, Z.; Gu, C.; Colby, T.; Shindo, T.; Balamurugan, R.; Waldmann, H.; Kaiser, M.; van der Hoorn, R. A. B-Lactone Probes Identify a Papain-Like Peptide Ligase in Arabidopsis Thaliana. *Nat. Chem. Biol*. **2008**, 4, 557-563.

108. Kolb, H. C.; Finn, M.; Sharpless, K. B. Click Chemistry: Diverse Chemical Function from a Few Good Reactions. *Angew. Chem. Int. Ed*. **2001**, 40, 2004-2021.

109. Cutter, J. L.; Cohen, N. T.; Wang, J.; Sloan, A. E.; Cohen, A. R.; Panneerselvam, A.; Schluchter, M.; Blum, G.; Bogyo, M.; Basilion, J. P. Topical Application of Activity-Based Probes for Visualization of Brain Tumor Tissue. *PLoS One*. **2012**, 7, e33060.

110. Adibekian, A.; Martin, B. R.; Chang, J. W.; Hsu, K.; Tsuboi, K.; Bachovchin, D. A.; Speers, A. E.; Brown, S. J.; Spicer, T.; Fernandez-Vega, V. Confirming Target Engagement for Reversible Inhibitors in Vivo by Kinetically Tuned Activity-Based Probes. *J. Am. Chem. Soc*. **2012**, 134, 10345-10348.

111. Kam, C. M.; Abuelyaman, A. S.; Li, Z.; Hudig, D.; Powers, J. C. Biotinylated Isocoumarins, New Inhibitors and Reagents for Detection, Localization, and Isolation of Serine Proteases. *Bioconjug. Chem*. **1993**, 4, 560-567.

112. Abuelyaman, A. S.; Hudig, D.; Woodard, S. L.; Powers, J. C. Fluorescent Derivatives of Diphenyl [1-(N-Peptidylamino) Alkyl] Phosphonate Esters: Synthesis and use in the Inhibition and Cellular Localization of Serine Proteases. *Bioconjug. Chem*. **1994**, 5, 400-405.

113. Jessani, N.; Niessen, S.; Wei, B. Q.; Nicolau, M.; Humphrey, M.; Ji, Y.; Han, W.; Noh, D.; Yates, J. R.; Jeffrey, S. S. A Streamlined Platform for High-Content Functional Proteomics of Primary Human Specimens. *Nat. Methods*. **2005**, 2, 691-697.

114. Hekmat, O.; He, S.; Warren, R. A. J.; Withers, S. G. A Mechanism-Based ICAT Strategy for Comparing Relative Expression and Activity Levels of Glycosidases in Biological Systems. *J. Proteome Res*. **2008**, 7, 3282-3292.

115. Altun, M.; Kramer, H. B.; Willems, L. I.; McDermott, J. L.; Leach, C. A.; Goldenberg, S. J.; Kumar, K.; Konietzny, R.; Fischer, R.; Kogan, E. Activity-Based Chemical Proteomics

Accelerates Inhibitor Development for Deubiquitylating Enzymes. *Chem. Biol*. **2011**, 18, 1401-1412.

116. Weerapana, E.; Wang, C.; Simon, G. M.; Richter, F.; Khare, S.; Dillon, M. B.; Bachovchin, D. A.; Mowen, K.; Baker, D.; Cravatt, B. F. Quantitative Reactivity Profiling Predicts Functional Cysteines in Proteomes. *Nature*. **2010**, 468, 790-795.

117. Young, C. L.; Britton, Z. T.; Robinson, A. S. Recombinant Protein Expression and Purification: A Comprehensive Review of Affinity Tags and Microbial Applications. *Biotechnol. J*. **2012**, 7, 620-34.

118. Terpe, K. Overview of Tag Protein Fusions: From Molecular and Biochemical Fundamentals to Commercial Systems. *Appl. Microbiol. Biotechnol*. **2003**, 60, 523-33.

119. Trinkle-Mulcahy, L.; Boulon, S.; Lam, Y. W.; Urcia, R.; Boisvert, F.; Vandermoere, F.; Morrice, N. A.; Swift, S.; Rothbauer, U.; Leonhardt, H.; Lamond, A. Identifying Specific Protein Interaction Partners using Quantitative Mass Spectrometry and Bead Proteomes. *J. Cell Biol*. **2008**, 183, 223-239.

120. Galan, J. A.; Paris, L. L.; Zhang, H.; Adler, J.; Geahlen, R. L.; Tao, W. A. Proteomic Studies of Syk-Interacting Proteins using a Novel Amine-Specific Isotope Tag and GFP Nanotrap. *J. Am. Soc. Mass Spectrom*. **2011**, 22, 319-328.

121. Neumuller, R. A.; Wirtz-Peitz, F.; Lee, S.; Kwon, Y.; Buckner, M.; Hoskins, R. A.; Venken Koen, J. T.; Bellen, H. J.; Mohr, S. E.; Perrimon, N. Stringent Analysis of Gene Function and Protein-Protein Interactions using Fluorescently Tagged Genes. *Genetics*. **2012**, 190, 931-940.

122. Hochuli, E.; Bannwarth, W.; Dobeli, H.; Gentz, R.; Stuber, D. Genetic Approach to Facilitate Purification of Recombinant Proteins with a Novel Metal Chelate Adsorbent. *Nat. Biotechnol*. **1988**, 6, 1321-1325.

123. Song, M. N.; Moon, P. G.; Lee, J. E.; Na, M.; Kang, W.; Chae, Y. S.; Park, J. Y.; Park, H.; Baek, M. C. Proteomic Analysis of Breast Cancer Tissues to Identify Biomarker Candidates by Gel-Assisted Digestion and Label-Free Quantification Methods using LC-MS/MS. *Arch. Pharm. Res*. **2012**, 35, 1839-1847.

124. Green, N. M. Avidin. 1. The use of (14-C)Biotin for Kinetic Studies and for Assay. *Biochem. J.* **1963**, 89, 585-591.

125. Ovod, V.; Scott, E. A.; Flake, M. M.; Parker, S. R.; Bateman, R. J.; Elbert, D. L. Exposure of the Lysine in the Gamma Chain Dodecapeptide of Human Fibrinogen is Not Enhanced by Adsorption to Poly(Ethylene Terephthalate) as Measured by Biotinylation and Mass Spectrometry. *J. Biomed. Mater. Res. A.* **2012**, 100, 622-631.

126. Karhemo, P. R.; Ravela, S.; Laakso, M.; Ritamo, I.; Tatti, O.; Makinen, S.; Goodison, S.; Stenman, U. H.; Holtta, E.; Hautaniemi, S.; Valmu, L.; Lehti, K.; Laakkonen, P. An Optimized Isolation of Biotinylated Cell Surface Proteins Reveals Novel Players in Cancer Metastasis. *J. Proteomics*. **2012**, 77, 87-100.

127. Vermeulen, M.; Hubner, N. C.; Mann, M. High Confidence Determination of Specific Protein-Protein Interactions using Quantitative Mass Spectrometry. *Curr. Opin. Biotechnol*. **2008**, 19, 331-337.

128. Gingras, A. C.; Gstaiger, M.; Raught, B.; Aebersold, R. Analysis of Protein Complexes using Mass Spectrometry. *Nat. Rev. Mol. Cell Biol*. **2007**, 8, 645-654.

129. Lu, X. M.; Tompkins, R. G.; Fischman, A. J. SILAM for Quantitative Proteomics of Liver Akt1/PKBalpha After Burn Injury. *Int. J. Mol. Med*. **2012**, 29, 461-471.

130. Smaczniak, C.; Li, N.; Boeren, S.; America, T.; van Dongen, W.; Goerdayal, S. S.; de Vries, S.; Angenent, G. C.; Kaufmann, K. Proteomics-Based Identification of Low-Abundance

Signaling and Regulatory Protein Complexes in Native Plant Tissues. *Nat. Protoc*. **2012**, 7, 2144-2158.

131. Rogstad, S. M.; Sorkina, T.; Sorkin, A.; Wu, C. C. Improved Precision of Proteomic Measurements in Immunoprecipitation Based Purifications using Relative Quantitation. *Anal. Chem*. **2013**, 85, 4301-4306.

132. Tirumalai, R. S.; Chan, K. C.; Prieto, D. A.; Issaq, H. J.; Conrads, T. P.; Veenstra, T. D. Characterization of the Low Molecular Weight Human Serum Proteome. *Mol. Cell. Proteomics*. **2003**, 2, 1096-1103.

133. Faulkner, S.; Elia, G.; Hillard, M.; O'Boyle, P.; Dunn, M.; Morris, D. Immunodepletion of Albumin and Immunoglobulin G from Bovine Plasma. *Proteomics*. **2011**, 11, 2329-2335.

134. Shi, T.; Su, D.; Liu, T.; Tang, K.; Camp, D. G.,2nd; Qian, W. J.; Smith, R. D. Advancing the Sensitivity of Selected Reaction Monitoring-Based Targeted Quantitative Proteomics. *Proteomics*. **2012**, 12, 1074-1092.

135. Hao, P.; Ren, Y.; Xie, Y. Label-Free Relative Quantification Method for Low-Abundance Glycoproteins in Human Serum by micrOTOF-Q. *J. Chromatogr. B. Analyt Technol. Biomed. Life. Sci*. **2009**, 877, 1657-1666.

136. Wehr, A. Y.; Hwang, W. T.; Blair, I. A.; Yu, K. H. Relative Quantification of Serum Proteins from Pancreatic Ductal Adenocarcinoma Patients by Stable Isotope Dilution Liquid Chromatography-Mass Spectrometry. *J. Proteome Res*. **2012**, 11, 1749-1758.

137. Ortea, I.; Roschitzki, B.; Ovalles, J. G.; Longo, J. L.; de la Torre, I.; Gonzalez, I.; Gomez-Reino, J. J.; Gonzalez, A. Discovery of Serum Proteomic Biomarkers for Prediction of Response to Infliximab (a Monoclonal Anti-TNF Antibody) Treatment in Rheumatoid Arthritis: An Exploratory Analysis. *J. Proteomics*. **2012**, 77, 372-382.

138. Cao, Z.; Yende, S.; Kellum, J. A.; Robinson, R. A. Additions to the Human Plasma Proteome Via a Tandem MARS Depletion iTRAQ-Based Workflow. *Int. J. Proteomics*. **2013**, 654356.

139. Prabakaran, S.; Lippens, G.; Steen, H.; Gunawardena, J. Post-Translational Modification: Nature's Escape from Genetic Imprisonment and the Basis for Dynamic Information Encoding. *Rev. Syst. Biol. Med*. **2012**, 4, 565-583.

140. Anderson, N. L.; Anderson, N. G.; Haines, L. R.; Hardie, D. B.; Olafson, R. W.; Pearson, T. W. Mass Spectrometric Quantitation of Peptides and Proteins using Stable Isotope Standards and Capture by Anti-Peptide Antibodies (SISCAPA). *J. Proteome Res*. **2004**, 3, 235-244.

141. Kuhn, E.; Whiteaker, J. R.; Mani, D. R.; Jackson, A. M.; Zhao, L.; Pope, M. E.; Smith, D.; Rivera, K. D.; Anderson, N. L.; Skates, S. J.; Pearson, T. W.; Paulovich, A. G.; Carr, S. A. Interlaboratory Evaluation of Automated, Multiplexed Peptide Immunoaffinity Enrichment Coupled to Multiple Reaction Monitoring Mass Spectrometry for Quantifying Proteins in Plasma. *Mol. Cell. Proteomics*. **2012**, 11, M111.013854.

142. Gaberc-Porekar, V.; Menart, V. Perspectives of Immobilized-Metal Affinity Chromatography. *J. Biochem. Biophys. Methods*. **2001**, 49, 335-360.

143. Beltran, L.; Cutillas, P. R. Advances in Phosphopeptide Enrichment Techniques for Phosphoproteomics. *Amino Acids*. **2012**, 43, 1009-1024.

144. Wuhrer, M.; Catalina, M. I.; Deelder, A. M.; Hokke, C. H. Glycoproteomics Based on Tandem Mass Spectrometry of Glycopeptides. *J. Chromatogr. B. Analyt Technol. Biomed. Life. Sci*. **2007**, 849, 115-128.

145. Stokes, M. P.; Farnsworth, C. L.; Moritz, A.; Silva, J. C.; Jia, X.; Lee, K. A.; Guo, A.; Polakiewicz, R. D.; Comb, M. J. PTMScan Direct: Identification and Quantification of Peptides

from Critical Signaling Proteins by Immunoaffinity Enrichment Coupled with LC-MS/MS. *Mol. Cell. Proteomics*. **2012**, 11, 187-201.

146. Na, C. H.; Jones, D. R.; Yang, Y.; Wang, X.; Xu, Y.; Peng, J. Synaptic Protein Ubiquitination in Rat Brain Revealed by Antibody-Based Ubiquitome Analysis. *J. Proteome Res*. **2012**, 11, 4722-4732.

147. Di Palma, S.; Hennrich, M. L.; Heck, A. J.; Mohammed, S. Recent Advances in Peptide Separation by Multidimensional Liquid Chromatography for Proteome Analysis. *J. Proteomics*. **2012**, 75, 3791-3813.

148. Gruber, K. A.; Stein, S.; Brink, L.; Radhakrishnan, A.; Udenfriend, S. Fluorometric Assay of Vasopressin and Oxytocin: A General Approach to the Assay of Peptides in Tissues. *Proc. Natl. Acad. Sci. U. S. A.* **1976**, 73, 1314-1318.

149. Donato, P.; Cacciola, F.; Mondello, L.; Dugo, P. Comprehensive Chromatographic Separations in Proteomics. *J. Chromatogr. A*. **2011**, 1218, 8777-8790.

150. Motoyama, A.; Yates III, J. R. Multidimensional LC Separations in Shotgun Proteomics. *Anal. Chem*. **2008**, 80, 7187-7193.

151. Nie, S.; Dai, J.; Ning, Z.; Cao, X.; Sheng, Q.; Zeng, R. Comprehensive Profiling of Phosphopeptides Based on Anion Exchange Followed by Flow-through Enrichment with Titanium Dioxide (AFET*). J. Proteome Res*. **2010**, 9, 4585-4594.

152. Alpert, A. J. Hydrophilic-Interaction Chromatography for the Separation of Peptides, Nucleic Acids and Other Polar Compounds. *J. Chromatogr. A*. **1990**, 499, 177-196.

153. Palmisano, G.; Lendal, S. E.; Engholm-Keller, K.; Leth-Larsen, R.; Parker, B. L.; Larsen, M. R. Selective Enrichment of Sialic Acid-Containing Glycopeptides using Titanium Dioxide

Chromatography with Analysis by HILIC and Mass Spectrometry. *Nat. Protoc.* **2010**, 5, 1974-1982.

154. Zhang, H.; Guo, T.; Li, X.; Datta, A.; Park, J. E.; Yang, J.; Lim, S. K.; Tam, J. P.; Sze, S. K. Simultaneous Characterization of Glyco-and Phosphoproteomes of Mouse Brain Membrane Proteome with Electrostatic Repulsion Hydrophilic Interaction Chromatography. *Mol. Cell. Proteomics*. **2010**, 9, 635-647.

155. Gilar, M.; Olivova, P.; Daly, A. E.; Gebler, J. C. Orthogonality of Separation in Two-Dimensional Liquid Chromatography. *Anal. Chem*. **2005**, 77, 6426-6434.

156. Kong, R. P. W.; Siu, S. O.; Lee, S. S. M.; Lo, C.; Chu, I. K. Development of Online High-/Low-pH Reversed-Phase-Reversed-Phase Two-Dimensional Liquid Chromatography for Shotgun Proteomics: A Reversed-Phase-Strong Cation Exchange-Reversed-Phase Approach. *J. Chromatogr. A*. **2011**, 1218, 3681-3688.

157. Lau, E.; Lam, M. P. Y.; Siu, S. O.; Kong, R. P. W.; Chan, W. L.; Zhou, Z.; Huang, J.; Lo, C.; Chu, I. K. Combinatorial use of Offline SCX and Online RP-RP Liquid Chromatography for iTRAQ-Based Quantitative Proteomics Applications. *Mol. BioSyst*. **2011**, 7, 1399-1408.

158. Stasyk, T.; Huber, L. A. Zooming in: Fractionation Strategies in Proteomics. *Proteomics*. **2004**, 4, 3704-3716.

159. Link, A. J.; Eng, J.; Schieltz, D. M.; Carmack, E.; Mize, G. J.; Morris, D. R.; Garvik, B. M.; Yates, J. R. Direct Analysis of Protein Complexes using Mass Spectrometry. *Nat. Biotechnol*. **1999**, 17, 676-682.

160. Pratima, N. A.; Shraddha, B.; Zibran, S. Review of Ultra Performance Liquid Chromatography and its Applications. *Int. J. Res. Pharm. Sci*. (Jaipur, India). **2013**, 3, 19-40.

161. Swartz, M. E. UPLC™: An Introduction and Review. *J. Liq. Chromatogr. Rel. Technol.* **2005**, 28, 1253-1263.

162. Sherathia, B.; Prajapati, G.; Singh, R.; Jat, R. Ultra Performance Liquid Chromatography: Comparative Study Over HPLC. *Int. J. Pharm. Sci. Rev. Res.* **2012**, 15, 54-57.

163. Roumeliotis, T. I.; Halabalaki, M.; Alexi, X.; Ankrett, D.; Giannopoulou, E.; Skaltsounis, A.; Sayan, B. S.; Alexis, M. N.; Townsend, P. A.; Garbis, S. D. Pharmacoproteomic Study of the Natural Product Ebenfuran III in DU-145 Prostate Cancer Cells: The Quantitative and Temporal Interrogation of Chemically Induced Cell Death at the Protein Level. *J. Proteome Res.* **2013**, 12, 1591-1603.

164. Cunliffe, J. M.; Maloney, T. D. Fused-Core Particle Technology as an Alternative to Sub-2-Mm Particles to Achieve High Separation Efficiency with Low Backpressure. *J. Sep. Sci.* **2007**, 30, 3104-3109.

165. Schuster, S.; Wagner, B.; Boyes, B.; Kirkland, J. Wider Pore Superficially Porous Particles for Peptide Separations by HPLC. *J. Chromatogr. Sci.* **2010**, 48, 566-571.

166. Metodiev, M. V. Applications of Nanoscale Liquid Chromatography Coupled to Tandem Mass Spectrometry in Quantitative Studies of Protein Expression, Protein–Protein Interaction, and Protein Phosphorylation. Nanoproteomics, Toms, S. A; Weil, R. J. Springer, **2011**; p. 99.

167. Ali, I.; Aboul-Enein, H. Y.; Cazes, J. A Journey from Mikhail Tswett to Nano Chromatography. *J. Liq. Chromatogr. Rel. Technol.* **2010**, 33, 645-653.

168. Fröhlich, T.; Helmstetter, D.; Zobawa, M.; Crecelius, A. C.; Arzberger, T.; Kretzschmar, H. A.; Arnold, G. J. Analysis of the HUPO Brain Proteome Reference Samples using 2-D DIGE and 2-D LC-MS/MS. *Proteomics*. **2006**, 6, 4950-4966.

169. Eng, J. K.; McCormack, A. L.; Yates Iii, J. R. An Approach to Correlate Tandem Mass Spectral Data of Peptides with Amino Acid Sequences in a Protein Database. *J. Am. Soc. Mass Spectrom*. **1994**, 5, 976-989.

170. Cottrell, J.; London, U. Probability-Based Protein Identification by Searching Sequence Databases using Mass Spectrometry Data. *Electrophoresis*. **1999**, 20, 3551-3567.

171. Craig, R.; Beavis, R. C. TANDEM: Matching Proteins with Tandem Mass Spectra. *Bioinformatics*. **2004**, 20, 1466-1467.

172. Ong, S.; Mann, M. Mass Spectrometry–based Proteomics Turns Quantitative. *Nat. Chem. Biol*. **2005**, 1, 252-262.

173. Cox, J.; Mann, M. Quantitative, High-Resolution Proteomics for Data-Driven Systems Biology. *Annu. Rev. Biochem*. **2011**, 80, 273-299.

174. Escher, C.; Reiter, L.; MacLean, B.; Ossola, R.; Herzog, F.; Chilton, J.; MacCoss, M. J.; Rinner, O. Using iRT, a Normalized Retention Time for More Targeted Measurement of Peptides. *Proteomics*. **2012**, 12, 1111-1121.

175. Rifai, N.; Gillette, M. A.; Carr, S. A. Protein Biomarker Discovery and Validation: The Long and Uncertain Path to Clinical Utility. *Nat. Biotechnol*. **2006**, 24, 971-983.

176. Cho, C. J.; Drabovich, A. P.; Batruch, I.; Diamandis, E. P. Verification of a Biomarker Discovery Approach for Detection of Down Syndrome in Amniotic Fluid Via Multiplex Selected Reaction Monitoring (SRM) Assay. *J. Proteomics*. **2011**, 74, 2052-2059.

177. Gallien, S.; Duriez, E.; Domon, B. Selected Reaction Monitoring Applied to Proteomics. *J. Mass Spectrom*. **2011**, 46, 298-312.

178. Whiteaker, J. R.; Zhao, L.; Anderson, L.; Paulovich, A. G. An Automated and Multiplexed Method for High Throughput Peptide Immunoaffinity Enrichment and Multiple Reaction

Monitoring Mass Spectrometry-Based Quantification of Protein Biomarkers. *Mol. Cell. Proteomics*. **2010**, 9, 184-196.

179. Yao, X.; Bajrami, B.; Shi, Y. Ultrathroughput Multiple Reaction Monitoring Mass Spectrometry. *Anal. Chem*. **2010**, 82, 794-797.

Chapter 2

Targeted Proteomic Quantitation of the Absolute Expression and Turnover of Cystic Fibrosis Transmembrane Conductance Regulator in the Apical Plasma Membrane

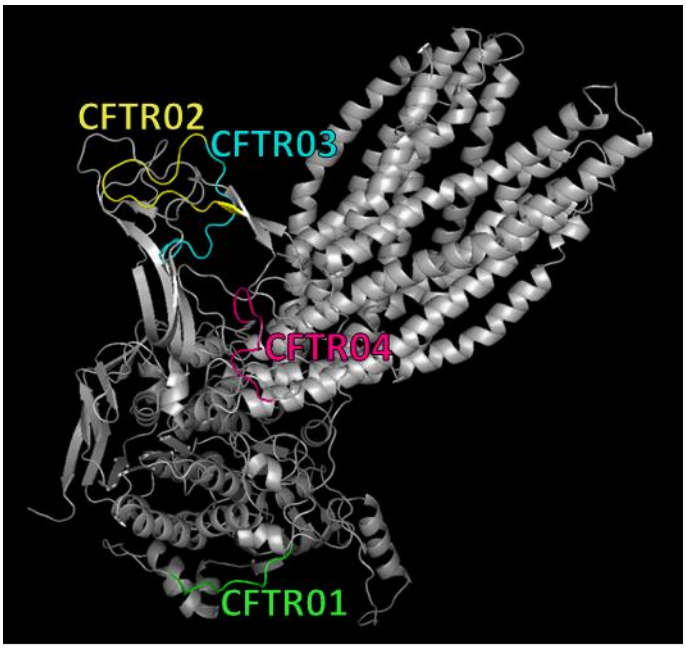

2.1 Introduction

For cystic fibrosis (CF), the most common autosomal recessive genetic disease, there is a recent paradigm shift from treating disease symptoms toward developing drugs that repair fundamental defects in the anion channel of cystic fibrosis transmembrane conductance regulator (CFTR) [1-3]. CFTR is a member of the ATP-binding cassette (ABC) transporter superfamily and functions as a cAMP-dependent, protein kinase-activated Cl^- channel in the plasma membrane (PM). It has five structural domains: two transmembrane domains (TMD1 and TMD2), two nucleotide-binding domains (NBD1 and NBD2), and a unique regulatory domain (RD). Deletion of a phenylalanine at position 508 (F508del) is the most frequent mutation, accounting for ~90% of the CF population. The F508del mutation is located in NBD1, putatively interfacing with TMDs, and impairs coupled domain folding, PM expression, ion channel function, and protein stability [4,5]. The misfolded mutant is retained inside cells at the endoplasmic reticulum (ER), and is degraded by the proteasome [6]. Evidence suggests that, during biosynthesis and trafficking of CFTR, different domains of the protein interact with various chaperone systems, facilitating the maturation of wild-type CFTR (wtCFTR) and the recognition of F508del mutant. Thus, F508del expression in the apical PM is minimal; consequently, F508del CF patients do not have sufficient CFTR channel activity in epithelial cells in their airways, intestine, pancreas, sweat ducts, testes, and other fluid-transporting tissues [7,8].

Two major categories of new CFTR modulator drugs are currently under extensive clinical and research investigations [9]; *corrector drugs* repair the biogenesis, trafficking, and ultimately the apical PM expression of the protein and *potentiator drugs* enable the channel function of mutant CFTR proteins in the PM. Corrector drugs like VX-809 (Lumacaftor) repair folding and trafficking of CFTR mutants and enhance the apical PM expression of F508del [2,10,11]. The

rescue of PM expression of mutant CFTR, like F508del, by corrector drugs is the first step into restoring Cl^- channel activity. However, VX-809 has limited clinical benefit for F508del CF patients, and its mechanism of action has yet to be fully understood [2,12]. In addition, it is generally agreed that the first generation of CF drugs has reached an apparent therapeutic ceiling [2,3,13-16]. In-depth analysis of how current investigational drugs work will gain mechanistic insights for developing future CF medicines. These studies would be greatly enhanced by accurate measurements of CFTR and its mutants in cells, especially in the PM where the protein performs its vital ion channel function.

Difficulties in the analysis of CFTR are among the major challenges for molecular investigations of CF drug action. CFTR is a large, glycosylated, multi-domain, and low abundance integral membrane protein. In order to evaluate the efficacy of drug compounds, efficient methods are needed to detect and quantify changes in the PM CFTR expression. Historically, western blot analysis of CFTR has been the central CFTR quantitation method in CF research [17]; newly-developed antibodies have greatly improved the sensitivity of the method [18]. However, the reproducibility, precision, accuracy, and robustness of the method are less than ideal, only providing semi-quantitative measurements, with a relatively large coefficient of variance and a narrow dynamic range. Furthermore, CFTR aggregates and degrades during sample preparations, leading to large measurement variations. These critical problems with membrane proteins present major, intrinsic challenges for quantitative analysis [19-21]. Other methods for quantifying surface expression of CFTR require engineered cells [e.g. green fluorescent (GFP) fusion proteins] and are not directly applicable to primary cells, which are better systems for testing new experimental drugs.

Technology innovations, from genomics [22] to proteomics [23,24], have played important roles in advancing CF research and therapy. We have developed the first quantitative method to mitigate the intrinsic analytical problems with full-length CFTR and use CFTR signature peptides as measurement surrogates [25]. CFTR is digested into peptides that are relatively easy to prepare for mass spectrometry (MS) quantitation. CFTR quantified in this work ranges from a few tens of picograms to low nanograms per million baby hamster kidney cells overexpressing wtCFTR (BHK-wtCFTR) or human colorectal adenocarcinoma cells (HT-29) [25]. A signature peptide is selected for quantitation by a method of liquid chromatography—stable isotope dilution—multiple reaction monitoring MS (LC-SID-MRM MS). It is the method of choice for quantifying target proteins in complex biomatrices [26-28], which is regarded as the MS version of western blot analysis, and has comparable sensitivity but superior specificity. MRM MS monitors gas-phase dissociation reactions of target analytes, which requires sequential detection of an analyte precursor ion as the reactant followed by one or several analyte fragment ions as the products; therefore, it is highly specific and can be applied to complex samples with minimal component separation. The sensitivity and specificity afforded by MRM MS method lifts the dependence on high-quality antibodies for conventional immunoassays of protein targets like CFTR [18].

However, later addition of peptide quantitation reference standards cannot be used to normalize (1) differential sample loss during CFTR enrichment—CFTR has low concentration in the PM and it is essential to enrich the protein to obtain the needed quantitation limit and (2) variations in proteolytic digestion of CFTR—membrane proteins are difficult to digest completely [29]. Thus peptide-level quantitation reference standards are less than ideal for the absolute quantitation of CFTR. More reliable absolute quantitation of PM CFTR will enable accurate and precise sample-to-sample, day-to-day, analyst-to-analyst, and lab-to-lab comparison of results,

similar to that shown for LC-SID-MRM MS quantitation of plasma proteins [26], and greatly facilitating the development of new CF drugs. Herein we report a general workflow (**Scheme 2.1**) for the enrichment and *absolute* quantitation of large, low-abundance CFTR (and other membrane proteins) in the apical PM (broadly referred to as the fraction of PM that is not in contact with culture support and thus is accessible to cell surface biotinylation) of BHK-wtCFTR and CFBE cells. With a variation of this method, CFTR turnover in the apical PM of BHK-wtCFTR cells is measured for the first time without using radioisotopes.

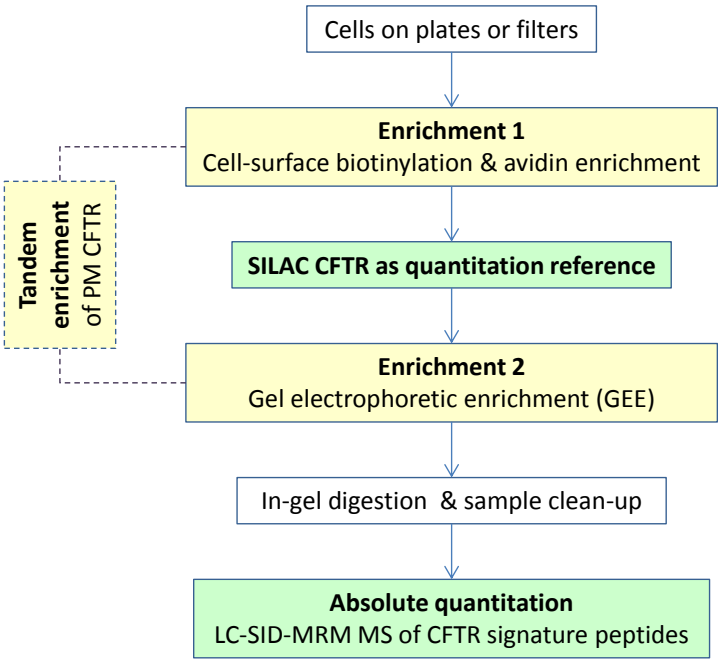

Scheme 2.1: Tandem enrichment of CFTR in the PM and workflow for targeted proteomic quantitation of the absolute expression**.**

2.2 Experimental

2.2.1 Materials

Urea, Tris base, iodoacetamide, acrylamide/bis-acrylamide solution (40%, 29:1), N,N,N',N'-tetramethylethylenediamine, L-leucine, L-lysine, L-arginine, methotrexate, doxycycline, protease inhibitor cocktail, sodium orthovanadate, 1 M tris-HCl buffer solution, phosphate buffer saline (PBS, 10x pH 7.4), Triton X-100, and the anhydrides were purchased from

Sigma-Aldrich, Inc. (St. Louis, MO). Pierce cell surface protein isolation kit, dithioerythritol (DTE), β-mercaptoethanol (β-ME), iodoacetamide, trifluoroacetic acid (TFA), ammonium bicarbonate, ammonium persulfate, formic acid, and HPLC grade acetonitrile were purchased from Fisher Scientific (Fair Lawn, NJ). The peptide CFTR01 was synthesized by AnaSpec (San Jose, CA) or Peptide 2.0 (Chantilly, VA). Isotopic CFTR01 peptide (NSILTET[L-$^{13}C_6{}^{15}N$]HR was synthesized by Cambridge Research Biochemicals (Cleveland, UK). ^{18}O-Water (>97%) was purchased from Cambridge Isotope Laboratories (Andover, MA) or given as a gift from Olinax (Hamilton, ON, Canada). Water was obtained from a Milli-Q ultrapure water purification system (Millipore, Billerica, MA). Proteomics grade recombinant trypsin was purchased from Roche Applied Science (Indianapolis, IN). Human embryonic kidney cell line (HEK293F) stably transfected with fused cDNA for wtCFTR and GFP (HEK293F-D042-JK)—HEK293F-wtCFTR—was a gift from Dr. John C. Kappes (University of Alabama at Birmingham). A cystic fibrosis bronchial-derived cell line complimented with a 4.7 Kb wild type CFTR cDNA (CFBE 41o-/pCEP–CFTR N 4.7 kb) and a cystic fibrosis bronchial-derived cell line complimented with a 4.7 Kb F508del CFTR cDNA (CFBE 41o-/pCEP –CFTR F508del 4.7 kb) were from Dr. Dieter Gruenert (University of California at San Francisco) [30]. The HT-29 cell line was purchased from American Type Culture Collection (Manassas, VA). Purified full-length CFTR samples were gifts from Dr. L. J. DeLucas (University of Alabama at Birmingham) and Dr. J. He (Accelagen, San Diego, CA). Purification of the later full-length CFTR sample was performed according to a procedure developed by Dr. J. R. Riordan at the University of North Carolina, Chapel Hill. The absolute concentration of this highly-purified CFTR sample was obtained by amino acid analysis and this sample was used as the reference standard to quantify stable isotope labeled CFTR samples prepared in-house (see the following section). Amino acid analysis for the highly-purified,

native CFTR was performed at the Keck Biotechnology Resource Laboratory at Yale University. DMEM, Ham's F-12, DME/Low media deficient in L-arginine, L-leucine and L-lysine, and fetal bovine serum were purchased from Thermo Scientific HyClone (Logan, UT). Dialyzed fetal bovine serum was purchased from Life Technologies (Thermo, Carlsbad, CA).

2.2.2 Cell culture and preparation of protein quantitation standard

BHK-wtCFTR cells were cultured in DMEM/Ham's F-12 with 550 μM methotrexate and 10% of each of the following reagents: fetal bovine serum, pen-strep, non-essential amino acids, and sodium pyruvate. The heavy isotope labeled, full-length CFTR was obtained, by the method of stable isotope labeling by amino acids in cell culture (SILAC) [31], from BHK-wtCFTR cells cultured in DME/Low deficient in L-lysine, L-leucine, and L-arginine supplemented with 550 μM methotrexate, 0.4 mM L-arginine•HCl, 0.8 mM L-lysine•HCl, 0.8 mM L-leucine-1,2-^{13}C (Cambridge Isotopes, Andover, MA), and 10% of dialyzed fetal bovine serum. Cells grown in this labeled media were allowed at least 7-8 doublings prior to harvesting. CFBE 41o-/pCEP–CFTR N 4.7 kb and CFBE 41o-/pCEP–CFTR F508del 4.7 kb were grown in MEM medium with 0.3 g/L L-Glutamine, 1 g/L Glucose, 2.2 g/L $NaHCO_3$, 10% of fetal bovine serum, 20 mM sodium pyruvate, 10,000 mcg/ml streptomycin, and 10,000 units/ml penicillin. The CFBE cells were grown in plates or snapwell filters (Sigma-Aldrich, St. Louis, MO) that were coated with human fibronectin (Fisher Scientific, Fair Lawn, NJ). The HEK293F-wtCFTR cells stably transfected with wtCFTR-GFP fused cDNA were cultured using DMEM with 10% fetal bovine serum and doxycycline added at 0, 0.25, 0.75, or 1.00 μg/mL the night before cell harvesting.

2.2.3 Cell-surface biotinylation and cell lysate fractionation

Surface biotinylation [25,32] was performed on cells using the surface protein isolation kit from Pierce, following the manufacturer's instructions. Briefly, cells were first labeled with a thiol-

cleavable, amine-reactive biotinylation reagent [sulfosuccinimidyl-2-(biotinamido)ethyl-1,3-dithiopropionate (sulfo-NHS-SS-biotin)] and quenched. The biotinylated cells were dislodged by trypsinization or scraping from the plates or filters, and subsequently lysed with buffer. The lysis buffer (800 µL) containing 1% (v/v) Triton X-100, 150 mM NaCl, 20 mM Tris-HCl at pH 7.2, and 1% (v/v) protease inhibitors was used for the lysis of 12-14 million BHK-wtCFTR cells or 6-8 million CFBE cells. The labeled proteins were captured on avidin agarose and released using Triton X-100 buffer containing 50 mM dithiothreitol (DTT).

2.2.4 Gel-based electrophoretic enrichment (GEE)

Gel electrophoresis was performed using a resolving gel consisting of 8% acrylamide and 0.2% bisacrylamide. BioRad glass plates with 1.0 mm spacer plates and 10-well comb were used for analysis of overexpressed CFTR; a single well allowing for 20 µL loading volume was sufficient for analysis of overexpressed CFTR in about 8 µg of total biotinylated protein. For endogenous CFTR, 1.5 mm spacer plates and 2-well comb consisting of 1 preparative well for sample loading (680 µL, 500 µg of total biotinylated proteins) and 1 well for loading the standard molecular weight protein marker or purified CFTR were used. For the turnover study, 1.5 mm spacer plates and a 5-well (120 µL) comb were used. CFTR samples were mixed with Laemmli sample buffer and incubated at 30^{o}C for 30 mins. Gel electrophoresis was carried out at 200 V constant voltage for 45 min or until the dye front reached the bottom of the gel.

2.2.5 Digestion

Gel pieces at the interface between the resolving and the stacking gels (~1 mm^3) were excised for further sample preparation. Gel pieces were washed (25 mM ammonium bicarbonate in H_2O/acetonitrile), reduced (10 mM DTE), and alkylated (20 mM iodoacetamide) before

trypsinization (20 ng/µL). The resulting digestion solution was dried via SpeedVac (Savant, Farmingdale, NY) and overnight lyophilization (Labconco, Kansas City, MO).

2.2.6 LC-SID-MRM MS

The optimization and data analysis of this work was assisted by the Skyline software[33]. The preparation of stable isotope reference $^{18}O(\Delta 4)$-CFTR01 and LC-SID-MRM MS quantitation were performed following previously reported procedures [25]. Some exceptions were those experiments where CFTR protein quantitation was accomplished in CFBE and BHK-wtCFTR cells. In those cases, an Eksigent NanoLC-Ultra $2D^+$ (Redwood City, CA) was used at a flow rate of 400 nL/min with a self-pack Picofrit column (New Objective, Woburn, MA) filled with 2.7 µM diameter, 160Å pore Halo resin (MacMod, Chadds Ford, PA) and the length of resin bed was around 15 cm. Solvent A was composed of 98.8% H_2O, 1.0% acetonitrile, and 0.2% formic acid (v/v) and solvent B's composition was 98.8% acetonitrile, 1.0% water, and 0.2% formic acid (v/v). A typical running gradient was 1%B at 0 min → 3%B at 5 min → 30%B at 50 min → 80%B at 59 min → 90%B at 69 min →1%B at 80 min, with 10 min equilibration. Samples were loaded on the trap column at flow rate of 4 µL/min at 1% solvent B for 10 min. A triple quadrupole mass spectrometer was used, 4000 QTrap from ABSCIEX (Foster City, CA). Transitions for the native and stable isotope labeled peptides are summarized in **Table 2.1**.

2.2.7 Peptide derivatization and ultrathroughput multiple reaction monitoring (uMRM) MS [34]

Following in-gel digestion of the HEK293F-wtCFTR cell lysate the N-termini of the peptide mixtures were derivatized with anhydrides (acetic, propionic, butyric, valeric, or succinic anhydride). To each sample were added 70 µL of acetonitrile, 70 µL of 1M ammonium bicarbonate, and 10 µL of the appropriate anhydride, and samples were incubated on ice for 1 h.

Following the incubation, another addition of 100 µL of acetonitrile, 100 µL of 1M ammonium bicarbonate, and 10 µL of the appropriate anhydrate were added, samples were incubated on ice for an additional 2 h. After the chemical derivatization, the modified peptides were dried and desalted using hydrophilic-lipophilic-balanced sorbent (HLB, Oasis®) and lyophilized. The resulting 5 derivatized digests were combined for a single uMRM MS experiment.

2.2.8 PM CFTR turnover study

In a typical experiment, BHK-wtCFTR cells for each time point were grown in triplicate in non-isotopic media. At time zero, the media was aspirated, the cells were washed twice with PBS, and isotopically labeled media was added as follows: (1) BHK-wtCFTR media minus arginine, leucine, and lysine and supplemented with 0.4 mM L-arginine•HCl, 0.8 mM L-lysine•HCl, 0.8 mM L-leucine-1,2-$^{13}C_{2=}$ or (2) BHK-wtCFTR media minus arginine, leucine, and lysine and supplemented with 0.4 mM L-arginine-$^{13}C_6$•HCl (Cambridge Isotopes, Andover, MA), 0.8 mM L-lysine-$^{13}C_6{}^{15}N_2$•HCl (Cambridge Isotopes, Andover, MA) and 0.8 mM L-leucine. At the appropriate time, the cells were biotinylated, combined, and fractionated as previously detailed. After protein digestion, signature peptides for native and stable isotope labeled CFTR were quantified by LC-SID-MRM MS.

Peptide	**Origin**	**Sequence**	**Transition Type**
CFTR01	Native	NSILTETLHR	$[M+2H]^{2+} \rightarrow y_7, y_6, y_5$
L(Δ4)-CFTR01	SILAC	NSI[L-1,2-$^{13}C_2$]TET[L-1,2-$^{13}C_2$]HR	
R(Δ6)-CFTR01	SILAC	NSILTETLH[R-$^{13}C_6$]	
^{18}O(Δ4)-CFTR01	Synthetic, ^{18}O-Labeling	NSILT[E-$^{18}O_2$]TLH[R-$^{18}O_2$]	
L(Δ7)-CFTR01	Synthetic	NSILTET[L-$^{13}C_6{}^{15}$N]HR	
CFTR02	Native	LSLVPDSEQGEAILPR	$[M+2H]^{2+} \rightarrow y_{12}, y_{10}, y_9$
L(Δ6)-CFTR02	SILAC	[L-1,2-$^{13}C_2$]S[L-1,2-$^{13}C_2$]VPDSEQGEAI[L-1,2-$^{13}C_2$]PR	
R(Δ6)-CFTR02	SILAC	LSLVPDSEQGEAILP[R-$^{13}C_6$]	
CFTR03	Native	ISVISTGPTLQAR	$[M+2H]^{2+} \rightarrow y_8, y_7, y_6$
R(Δ6)-CFTR03	SILAC	ISVISTGPTLQA[R-$^{13}C_6$]	
CFTR04	Native	NSILNPINSIR	$[M+2H]^{2+} \rightarrow y_8, y_7, y_6$
R(Δ6)-CFTR04	SILAC	NSILNPINSI[R-$^{13}C_6$]	

Table 2.1: CFTR signature peptides and isotopic counterparts with respective transitions for LC-SID-MRM MS analysis. "Δx" denotes a mass increase; i.e., Δ4 means a mass increase of 4 Da for the isotope-labeled peptide compared with the native counterpart.

2.3 Results and discussion

2.3.1 A general strategy of cell-surface biotinylation and GEE for the tandem enrichment of large and low-abundance PM proteins

Membrane proteins are critical for cells to communicate with the extra-cellular environment. Receptors and transporters in the PM thus form the most dominant protein class for developing drugs to treat human disease [35]. These membrane proteins are typically large, hydrophobic, and low in abundance. Preparation of membrane proteins and proteome samples is a major analytical bottleneck in analysis [19,20]. We have thus designed a novel, broadly-applicable workflow to enrich low-abundance, large membrane proteins by sequential use of (1) the established method of cell surface biotinylation and (2) a method of gel electrophoretic enrichment (GEE), which is a variant of gel electrophoresis (**Scheme 2.1**).

GEE makes special use of sodium dodecyl sulfate-polyacrylamide gel electrophoresis (SDS-PAGE) for separation of protein mixtures. In the GEE method, non-gradient gels are used for protein fractionation and the gel compositions are formulated in such a way that proteins larger than a minimum molecular weight do not migrate appreciably in the resolving gel. It is a simple but effective approach for enriching high-molecular weight proteins (e.g. >150 kDa) in a complex mixture (**Figure 2.1**). For enriching CFTR, the composition for the resolving gel is 8% acrylamide and 0.2% bisacrylamide. This composition slows the migration of large proteins and limits their location to the interface region of the resolving and stacking gel while allowing for the electrophoretic migration of smaller proteins. With or without gel staining, a protein fraction with a predictable lower cutoff of molecular weight (i.e., proteins that have molecular weights higher than a designed value) can be reproducibly sampled by excising gel slices at a fixed location near the interface (**Figure 2.1**) for subsequent in-gel digestion and MS analysis.

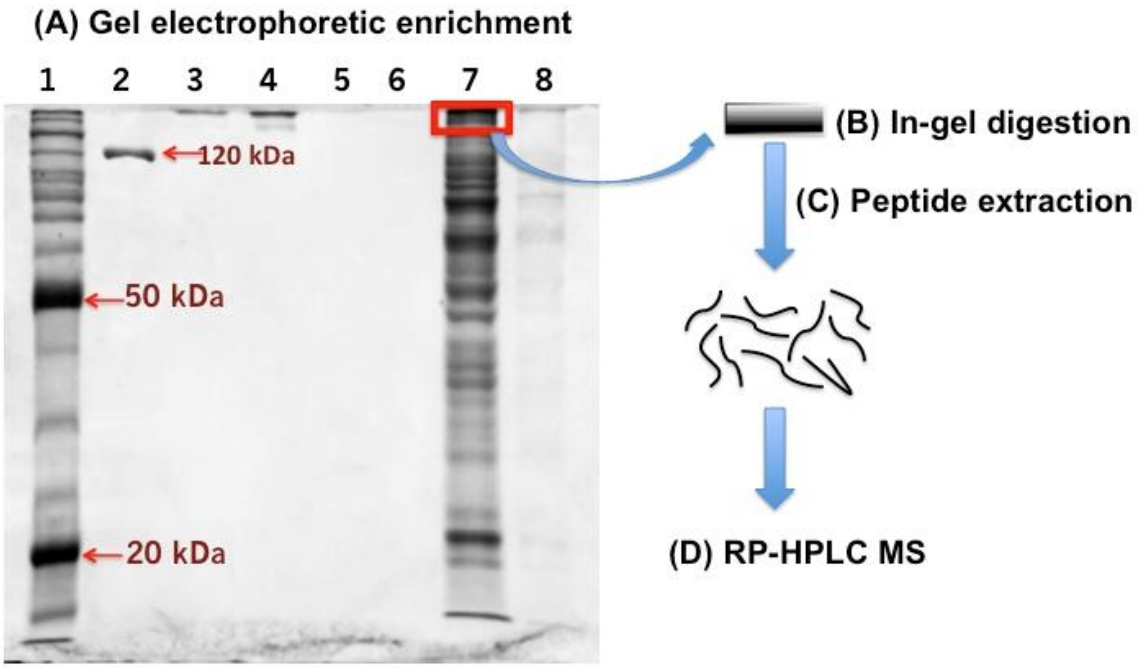

Figure 2.1: Gel electrophoretic enrichment (GEE) of large membrane proteins. The large proteins are sampled by slicing the gel piece at the interface of the stacking gel and the resolving gel (**A**). Samples loaded were: **1,** protein ladder; **2**, β-galactosidase; **3,** 500 ng of CFTR; **4,** 1 μg of CFTR; **5,** 10 μg of BHK-wtCFTR biotinylated fraction; **6,** 1 μg of BHK-wtCFTR biotinylated fraction; **7,** 30 μg of BHK-wtCFTR Triton X-100 extract; and **8,** 3 μg of BHK-wtCFTR Triton X-100 extract. The gel piece (red box) was cut for in-gel digestion (**B**; other bands were low-molecular weight membrane proteins removed by GEE), and the resulting peptides were extracted (**C**) and analyzed by LC-SID-MRM MS (**D**).[i]

Expression of CFTR in the PM is low, and the tandem enrichment strategy made CFTR quantitation possible by LC-SID-MRM MS [36], without using antibody enrichment of the protein [25]; this is due to both the increase in CFTR concentration and the decrease in the sample complexity for MS quantitation. Mutant CFTR proteins, even after therapeutic intervention, exist in even lower amounts in the PM; thus, enrichment of PM CFTR is necessary for quantifying the protein by MS. A study was performed to compare LC-SID-MRM MS quantitation of CFTR signature peptides prepared by the tandem enrichment workflow with those in the direct digestion

[i] Work and figure by Alexis Ramos. McShane, A. J.; Bajrami, B.; Ramos, A. A.; Diego-Limpin, P. A.; Farrokhi, V.; Coutermarsh, B. A.; Stanton, B. A.; Jensen, T.; Riordan, J. R.; Wetmore, D.; Joseloff, E.; Yao, X. Targeted Proteomic Quantitation of the Absolute Expression and Turnover of Cystic Fibrosis Transmembrane Conductance Regulator in the Apical Plasma Membrane. *J. Proteome Res.* **2014**, 13, 4676-4685.

mixture of the PM subproteome prepared by surface biotinylation and avidin pull-down for HT-29 cells. Only the former workflow resulted in confident quantitation, and the measurement gave 40 fmol of apical PM CFTR per million cells, equivalent to 23,000 molecules per cell (**Figures 2.1** and **2.2**). It should be noted that this amount is based on a peptide quantitation reference standard [^{18}O(Δ4)-CFTR01] [25] and thus represents the lower range of PM CFTR in HT-29 cells (see later section for discussion on protein vs. peptide quantitation reference standards). Although the GEE method by itself can be used for preparing CFTR signature peptides from various protein (mixture) samples containing CFTR, it is necessary to have the surface biotinylation enrichment in the workflow. Thus, only matured full-length CFTR (commonly referred to as the "Band C" [37] by the CF research and clinical community) in the PM is sampled for quantitation; the GEE method does not separate the non-glycosylated CFTR (commonly referred to as the "Band B"[37]) from that which is fully matured.

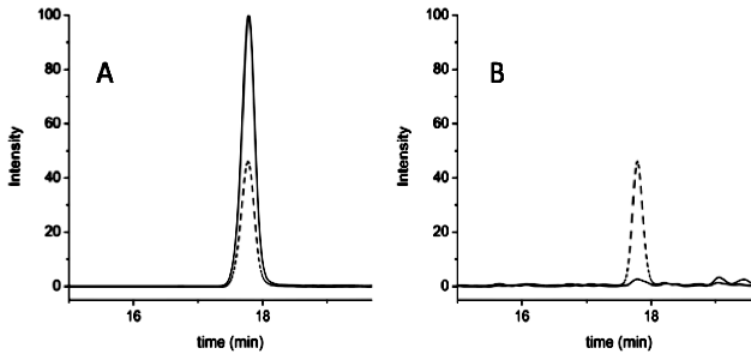

Figure 2.2: It is essential to use a tandem enrichment strategy for preparing PM CFTR samples. MRM ion chromatograms are shown for the native signature peptide (solid line) and the spiked stable isotope reference peptide (dotted line) of digests of HT-29 cell lysate prepared by surface biotinylation and GEE (A) and surface biotinylation only (B).[i]

Another analytical advantage for the GEE method is compatibility with various solubilizing reagents used for preparing samples containing CFTR. To enhance solubilization of

[i] Work and figure by Alexis Ramos. McShane, A. J.; Bajrami, B.; Ramos, A. A.; Diego-Limpin, P. A.; Farrokhi, V.; Coutermarsh, B. A.; Stanton, B. A.; Jensen, T.; Riordan, J. R.; Wetmore, D.; Joseloff, E.; Yao, X. Targeted Proteomic Quantitation of the Absolute Expression and Turnover of Cystic Fibrosis Transmembrane Conductance Regulator in the Apical Plasma Membrane. *J. Proteome Res.* **2014**, 13, 4676-4685.

membrane proteins, SDS and other detergents are used in the extraction and digestion buffers. However, the presence of detergents can interfere with protease activity during protein digestion, and can also affect chromatographic separation and suppress ionization of resulting peptides. Although the detergents can be removed after digestion, cleanup of detergent-containing peptide mixtures can cause significant sample loss and has varying efficiencies. In contrast, during the gel-based sample preparations detergents and other interfering reagents are removed by extensive washing before digestion. It has been reported that protein mixtures can be concentrated to a thin band after a short-running SDS-PAGE; the main purpose of this practice has been the removal of detergents in membrane protein preparations for enhanced MS-based proteomic analysis,[38,39] not to enrich low-abundance proteins based on their size. Compared to the in-solution digestion, the in-gel digestion also increases the digestion efficiency for membrane proteins [40,41]; this is possibly attributed to the decreased protein aggregation during digestion. By immobilizing hydrophobic membrane proteins in the gel matrix, aggregation of membrane proteins and large protein fragments produced at the initial stage of the protein digestion is likely minimized.

2.3.2 SILAC CFTR as quantitation reference standard for absolute quantitation of PM CFTR

The full-length CFTR quantitation reference standard was prepared through metabolic labeling using the SILAC method [31]. Lysates of BHK-wtCFTR cells cultured with media containing leucine-1,2-^{13}C CFTR (seven doublings) were prepared by a buffer containing Triton X-100. The SILAC CFTR amount in the Triton X-100 extract was quantified against a highly-purified, full-length native CFTR standard (this native CFTR could be used as the master reference standard for different laboratories) using the GEE method for sample preparation and LC-SID-MRM MS for CFTR quantitation. Concentration of native CFTR was determined by amino acid

analysis to be 0.175 (±0.025) µg/µL. The quantity of SILAC CFTR was measured in triplicate using two signature peptides (CFTR01 and CFTR02). The protein concentration in the SILAC Triton X-100 extract was determined to be 4.72 (±0.07) ng/µL (**Table 2.2**). It should be noted that the SILAC CFTR reference standard was used as the Triton X-100 extracts directly for quantifying CFTR samples.

Sample #	Area CFTR01		Area CFTR02		Area Ratio CFTR01	Area Ratio CFTR02	SILAC CFTR Amount (ng)
	Native	L(Δ4)	Native	L(Δ6)	Native/L(Δ4)	Native/L(Δ6)	
1	4457	2100	10080	4703	2.12	2.14	140.8
2	8690	3980	18850	9263	2.18	2.03	142.9
3	3890	1810	7879	3717	2.15	2.12	140.8
						Average	141.5

Table 2.2: Preparation of SILAC CFTR quantitation reference standard. The area ratios between the native peptides and heavy isotope labeled peptides were used to calculate the concentration of SILAC CFTR in cell lysate, which was labeled with leucine-1,2-^{13}C. Highly-purified full-length CFTR (300 ng) was used to calibrate the absolute amount of SILAC CFTR. Sample volume was 30 µL.[i]

A quantitative analysis was performed to examine the difference in CFTR between using the SILAC CFTR protein standard and using a stable isotopic synthetic peptide L(Δ7)-CFTR01. HEK293F-wtCFTR cells which overexpress wtCFTR upon induction with doxycycline at different concentrations (0, 0.25, 0.50, 0.75 and 1.0 µg/mL) were used. Apical PM CFTR was prepared by the tandem enrichment workflow (**Scheme 2.1**). One additional quantitation reference, peptide L(Δ7)-CFTR01, was added to the peptide mixtures resulting from in-gel digestion. Furthermore, five different samples were derivatized with different acid anhydrates (acetic, propionic, butyric, valeric, or succinic anhydride), respectively; with this sample-specific coding procedure, all five

[i] Work and table by Bekim Bajrami. McShane, A. J.; Bajrami, B.; Ramos, A. A.; Diego-Limpin, P. A.; Farrokhi, V.; Coutermarsh, B. A.; Stanton, B. A.; Jensen, T.; Riordan, J. R.; Wetmore, D.; Joseloff, E.; Yao, X. Targeted Proteomic Quantitation of the Absolute Expression and Turnover of Cystic Fibrosis Transmembrane Conductance Regulator in the Apical Plasma Membrane. *J. Proteome Res.* **2014**, 13, 4676-4685.

samples were quantified in a single experiment of LC-SID-uMRM MS experiment [34]. The signature peptide CFTR01 was monitored in this study (**Table 2.3**). Expression of native CFTR in these doxycycline-inducible HEK293F-wtCFTR cells was determined according to both L(Δ4)-CFTR01 and L(Δ7)-CFTR01. While both data sets observed the increased expression of CFTR, with the increase in the doxycycline concentration, CFTR amounts measured according to the peptide standard L(Δ7)-CFTR01—added after in-gel-digestion of CFTR—were only 14 to 17% of the corresponding measurements based on L(Δ4)-CFTR01, produced via in-gel digestion of SILAC CFTR (**Table 2.3**). This study shows that for absolute quantitation of membrane proteins like CFTR, it is essential to use protein standards to obtain better quantitation accuracy.

The use of an isotopic protein reference allows for *advantageous* addition of an internal standard at an early step of sample preparation. For the PM CFTR quantitation, SILAC CFTR was added as the reference in the surface biotinylation fraction of membrane proteins before further sample preparations. In comparison, conventional LC-SID-MRM MS uses isotopic reference peptides [25-28,42]. For absolute quantitation of membrane proteins, peptide references are not acceptable. Membrane proteins are hard to digest; in a typical experiment the yield of signature peptide CFTR01 is only 14-17% and this yield varies from one sample preparation to another (**Table 2.3**). Furthermore, CFTR is prone to aggregation and degradation during sample preparation; for instance, preparation of CFTR for SDS-PAGE is performed at 30°C instead of boiling temperature. Addition of SILAC CFTR before GEE and protein digestion largely minimized variations in sample preparation and afforded the absolute quantitation of CFTR in CFBE cells.

Doxycycline (μg/mL)	Relative Area CFTR01			Area Ratio	Native CFTR Absolute Amount (ng)[c]	CFTR Digestion Efficiency (%)[d]
	Native	L(Δ4)[a]	L(Δ7)[b]	Native/L(Δ4)		
0	0	3802	16350	0	0	-
0.25	3654	4229	15640	0.86	130	15
0.75	4405	2110	7337	2.09	313	16
1.00	3279	1103	3723	2.97	446	17
1.25	29880	7560	30190	3.95	593	14

Table 2.3: Absolute amounts of PM CFTR for HEK293F-wtCFTR cells. Area ratios (Native/SILAC) were used to calculate expressed native CFTR. [a]: 150 ng of SILAC CFTR was added to each sample; [b]: 500 fmol of L(Δ7)-CFTR01 was added; [c]: amount of PM CFTR for each 10 cm plate; [d]: Relative areas for L(Δ4) and L(Δ7) peptides, together with the known amounts of SILAC CFTR and L(Δ7)-CFTR01, gave measurements for the digestion efficiency for CFTR. These numbers should represent the lower limits for the digestion efficiency, because sample loss during GEE and peptide preparation could also be attributed to the calculated efficiency.[i]

2.3.3 Absolute quantitation of apical PM expression of CFTR in CFBE 41o- cells

The CFBE cell line is a common model for CF research and drug development. We performed absolute quantitation of apical PM CFTR in CFBE 41o- cells grown on plates and snapwell filters via LC-MRM MS of signature peptides. Three signature peptides, CFTR01, CFTR02, and CFTR04 were monitored by LC-SID-MRM MS (**Figure 2.3**), but only CFTR01 and CFTR02 peptides were consistently able to be quantified for measuring their precursor CFTR protein in the PM, together with CFTR in the cytoplasm (i.e., CFTR in the Triton X-100 extract after removing PM CFTR). Quantitation results based on CFTR01 and CFTR02 were comparable (**Table 2.2**). Each sample was repeated with at least three different biological preparations. Results are summarized in **Table 2.4**. As expected, surface expression of CFTR in CFBE cells (14.1% of CFTR in the whole cell lysate) grown in snapwell filters is higher than that of CFBE cells grown in flasks (10.1%). CFBE cells grown on snapwell filters mimic airway epithelial cells with the air-

[i] Work and table by Bekim Bajrami. McShane, A. J.; Bajrami, B.; Ramos, A. A.; Diego-Limpin, P. A.; Farrokhi, V.; Coutermarsh, B. A.; Stanton, B. A.; Jensen, T.; Riordan, J. R.; Wetmore, D.; Joseloff, E.; Yao, X. Targeted Proteomic Quantitation of the Absolute Expression and Turnover of Cystic Fibrosis Transmembrane Conductance Regulator in the Apical Plasma Membrane. *J. Proteome Res.* **2014**, 13, 4676-4685.

liquid interface creating a polarized cell environment, increasing the PM expression of CFTR. The absolute quantitation method reported in this work will also enable accurate measurements of CFTR in primary cells. Absolute quantitation of PM CFTR will set the basis for the comparison of results and thus, greatly amplify the overall outcome of CF research and therapy. In reference, high reproducibility for LC-SID-MRM MS quantitation of protein targets in complex matrices has recently been shown for sample-to-sample, day-to-day, analyst-to-analyst, and lab-to-lab comparisons [26].

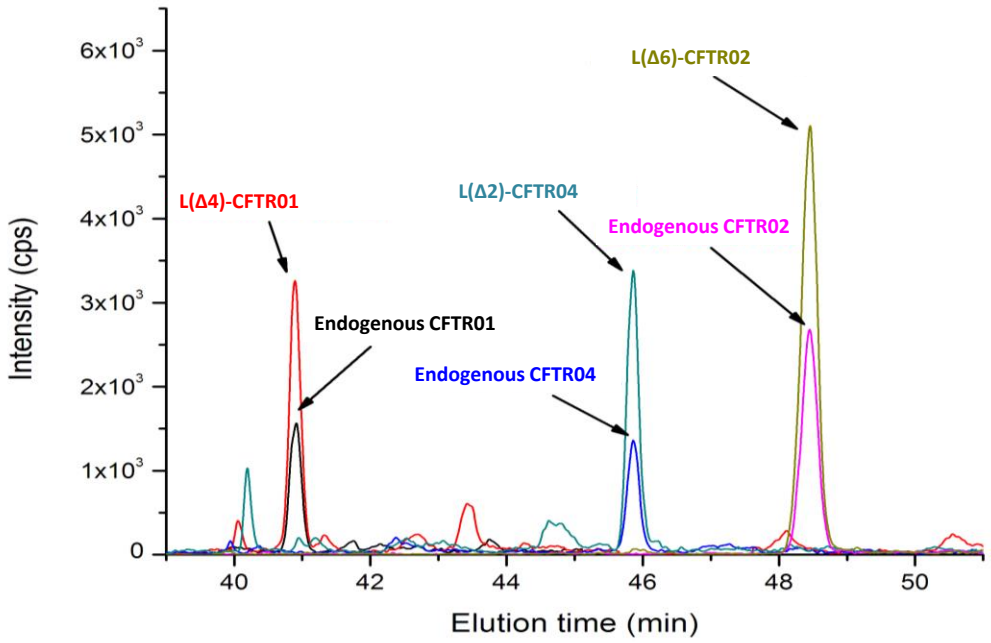

Figure 2.3: LC-SID-MRM MS chromatograms of signature peptides for quantifying CFTR in the apical PM of CFBE cells grown on filters. Peptide denotations in **Table 2.1**.[i]

[i] Work and figure by Bekim Bajrami. McShane, A. J.; Bajrami, B.; Ramos, A. A.; Diego-Limpin, P. A.; Farrokhi, V.; Coutermarsh, B. A.; Stanton, B. A.; Jensen, T.; Riordan, J. R.; Wetmore, D.; Joseloff, E.; Yao, X. Targeted Proteomic Quantitation of the Absolute Expression and Turnover of Cystic Fibrosis Transmembrane Conductance Regulator in the Apical Plasma Membrane. *J. Proteome Res.* **2014**, 13, 4676-4685.

Sample	CFTR Amount (ng/million cells)	PM Expression (%)
Plate, Biotinylated	2.90 ± 0.03	10.3 ± 0.4
Plate, Flow-through	25.0 ± 0.8	
Filter, Biotinylated	6.75 ± 0.18	14.1 ± 2.0
Filter, Flow-through	41.2 ± 4.7	

Table 2.4: Absolute quantitation and surface expression of CFTR protein in CFBE 41o- cells.[i]

2.3.4 Turnover of CFTR in the apical PM

We designed and performed the first quantitative analysis of CFTR turnover in the PM using stable isotopes. BHK-wtCFTR cells were originally cultured in native culture media. At time zero, culture media were switched to SILAC media containing stable isotope labeled lysine and arginine or leucine; thus, native CFTR in the PM started to decrease with time, and SILAC CFTR labeled with the stable isotopes started to appear and increase. At different time intervals, cells were harvested, and the protein fraction containing PM CFTR was processed according to the tandem enrichment workflow (**Scheme 2.1**). Native CFTR in the PM was quantified against the newly-synthesized isotopic CFTR by LC-SID-MRM MS of signature peptides. The time-course for the newly produced CFTR was followed for up to 60 or 84 hrs, through two experiments. The average area ratio of the signature peptides from the newly-incorporated CFTR versus the native CFTR (isotopic/native) was normalized to the maximum, and then the percentage of remaining native CFTR (denoted as R in **Figure 2.4**) was calculated. The natural logarithm of R (for data points up to 48 h; incorporation of isotope labels were saturated beyond 48 h) was plotted against time and fitted according to 1st-order kinetics [11,43] with an adjusted R^2 of 0.9496. The half-life ($t_{1/2}$) of native CFTR in the PM was calculated to be 29.0±2.5 h.

[i] Work and table by Bekim Bajrami. McShane, A. J.; Bajrami, B.; Ramos, A. A.; Diego-Limpin, P. A.; Farrokhi, V.; Coutermarsh, B. A.; Stanton, B. A.; Jensen, T.; Riordan, J. R.; Wetmore, D.; Joseloff, E.; Yao, X. Targeted Proteomic Quantitation of the Absolute Expression and Turnover of Cystic Fibrosis Transmembrane Conductance Regulator in the Apical Plasma Membrane. *J. Proteome Res.* **2014**, 13, 4676-4685.

Rescuing CFTR mutant proteins for expression in the apical PM is only the first step. The rescued mutants have to be stable in the membrane and perform the channel function for Cl^- ions. It has been recently reported that the CF drug VX-809 can fully rescue the PM expression of F508del, but the lifespan of the rescued mutant falls short compared with that of wtCFTR [11]. Conventional western blot analysis of CFTR cannot be applied for turnover studies of PM CFTR. Although metabolic pulse-chase of radioisotopes provides a useful tool for this analysis [11], a more convenient method for accurate measurements of the protein turnover in the PM can be greatly beneficial to CF research and drug development. The combination of metabolic stable isotope labeling and quantitative proteomics is an emerging alternative to radioisotope methods [44,45]. Under this experimental framework, coupling the tandem enrichment of CFTR with highly sensitive MRM MS has made it possible to measure CFTR turnover ($t_{1/2}$ = 29.0±2.5 hrs) in the PM of BHK-wtCFTR cells. In comparison, a shorter half-life ($t_{1/2}$ ~14 hrs) was recently reported for CFTR in the whole cell lysate of the same cell line [11]. These results are in agreement with the observation that PM proteins degrade more slowly than do proteins that do not reach the membrane [43].

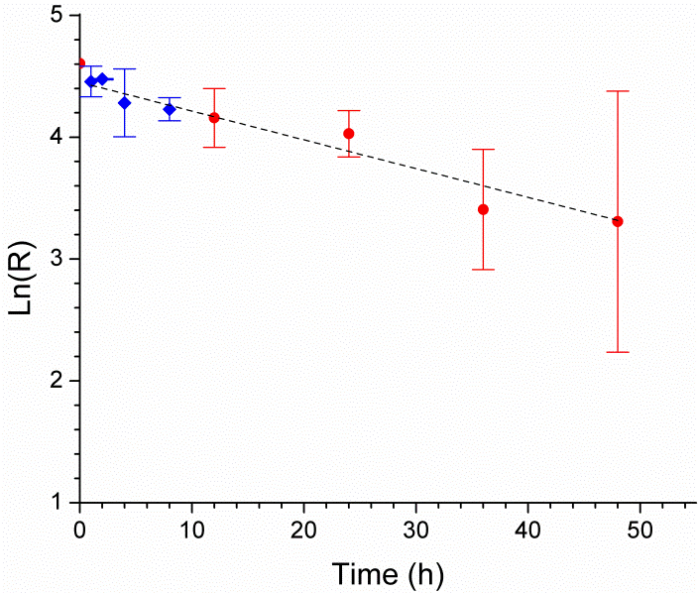

Figure 2.4: Turnover of CFTR in the PM of BHK-wtCFTR cells. R represents normalized percentage degradation of native CFTR (see results and discussion). Blue and red data points were from two separate sets of experiments: isotopic leucine and isotopic arginine/lysine CFTR incorporation, respectively. Peptides CFTR01, 03, and 04 were monitored for the blue data points, and the individual transitions were used for the error calculations. Peptides CFTR01-04 were monitored for the red data points, and analytical triplicate measurements were used for error calculations (slope=-0.0239±0.0021, adjusted R^2=0.9496).

2.4 Conclusion

Membrane receptors and transporters form the most important class of protein targets for understanding intercellular communication and developing new drugs. Recent advances in MS-based quantitative proteomics, in combination with new sample preparation workflows, have made it possible to obtain unprecedented accuracy and precision in membrane protein measurements. Targeted quantitation of apical PM CFTR reported in this work exemplifies an important application of contemporary proteomics technologies and it will help significantly with understanding the disease mechanism of CF and developing future medicine for its treatment.

2.5 References

1. Elborn, J. S.: Fixing cystic fibrosis CFTR with correctors and potentiators. Off to a good start. *Thorax.* **2012**, 67, 4-5.

2. Okiyoneda, T.; Veit, G.; Dekkers, J. F.; Bagdany, M.; Soya, N.; Xu, H. J.; Roldan, A.; Verkman, A. S.; Kurth, M.; Simon, A.; Hegedus, T.; Beekman, J. M.; Lukacs, G. L.: Mechanism-based corrector combination restores Delta F508-CFTR folding and function. *Nat. Chem. Biol.* **2013**, 9, 444-U69.

3. Hanrahan, J. W.; Sampson, H. M.; Thomas, D. Y.: Novel pharmacological strategies to treat cystic fibrosis. *Trends Pharmacol. Sci.* **2013**, 34, 119-125.

4. Riordan, J. R.: CFTR function and prospects for therapy. *Annu. Rev. Biochem.* **2008**, 77, 701-726.

5. Sheppard, D. N.; Welsh, M. J.: Structure and function of the CFTR chloride channel. *Physiol. Rev.* **1999**, 79, S23-45.

6. Amaral, M. D.: CFTR and chaperones - Processing and degradation. *J. Mol. Neurosci.* **2004**, 23, 41-48.

7. Pilewski, J. M.; Frizzell, R. A.: Role of CFTR in airway disease. *Physiol. Rev.* **1999**, 79, S215-55.

8. Kreda, S. M.; Davis, C. W.; Rose, M. C.: CFTR, Mucins, and Mucus Obstruction in Cystic Fibrosis. *Cold Spring Harbor Perspect.Med.* **2012**, 2, a009589.

9. Rowe, S. M.; Verkman, A. S.: Cystic fibrosis transmembrane regulator correctors and potentiators. *Cold Spring Harbor Perspect.Med.* **2013**, 3, a009761.

10. Van Goor, F.; Hadida, S.; Grootenhuis, P. D. J.; Burton, B.; Stack, J. H.; Straley, K. S.; Decker, C. J.; Miller, M.; McCartney, J.; Olson, E. R.; Wine, J. J.; Frizzell, R. A.; Ashlock, M.;

Negulescu, P. A.: Correction of the F508del-CFTR protein processing defect in vitro by the investigational drug VX-809. *Proc. Natl. Acad. Sci. U.S.A.* **2011**, 108, 18843-18848.

11. He, L. H.; Kota, P.; Aleksandrov, A. A.; Cui, L. Y.; Jensen, T.; Dokholyan, N. V.; Riordan, J. R.: Correctors of Delta F508 CFTR restore global conformational maturation without thermally stabilizing the mutant protein. *FASEB J.* **2013**, 27, 536-545.

12. Birault, V.; Solari, R.; Hanrahan, J.; Thomas, D. Y.: Correctors of the basic trafficking defect of the mutant F508del-CFTR that causes cystic fibrosis. *Curr. Opin. Chem. Biol.* **2013**, 17, 353-360.

13. Lukacs, G. L.; Verkman, A. S.: CFTR: folding, misfolding and correcting the DeltaF508 conformational defect. *Trends Mol.Med.* **2012**, 18, 81-91.

14. Phuan, P. W.; Veit, G.; Tan, J.; Roldan, A.; Finkbeiner, W. E.; G, L. L.; Verkman, A. S.: Synergy-Based Small-Molecule Screen Using a Human Lung Epithelial Cell Line Yields DeltaF508-CFTR Correctors That Augment VX-809 Maximal Efficacy. *Mol. Pharmacol.* **2014**, 86, 42-51.

15. Mendoza, J. L.; Schmidt, A.; Li, Q.; Nuvaga, E.; Barrett, T.; Bridges, R. J.; Feranchak, A. P.; Brautigam, C. A.; Thomas, P. J.: Requirements for efficient correction of DeltaF508 CFTR revealed by analyses of evolved sequences. *Cell.* **2012**, 148, 164-74.

16. Okiyoneda, T.; Lukacs, G. L.: Fixing cystic fibrosis by correcting CFTR domain assembly. *J. Cell Biol.* **2012**, 199, 199-204.

17. Farinha, C. M.; Penque, D.; Roxo-Rosa, M.; Lukacs, G.; Dormer, R.; McPherson, M.; Pereira, M.; Bot, A. G.; Jorna, H.; Willemsen, R.; Dejonge, H.; Heda, G. D.; Marino, C. R.; Fanen, P.; Hinzpeter, A.; Lipecka, J.; Fritsch, J.; Gentzsch, M.; Edelman, A.; Amaral, M. D.:

Biochemical methods to assess CFTR expression and membrane localization. *J. Cystic Fibrosis.* **2004**, 3, 73-77.

18. Farinha, C. M.; Mendes, F.; Roxo-Rosa, M.; Penque, D.; Amaral, M. D.: A comparison of 14 antibodies for the biochemical detection of the cystic fibrosis transmembrane conductance regulator protein. *Mol. Cell. Probes* **2004**, 18, 235-42.

19. Wu, C. C.; Yates, J. R.: The application of mass spectrometry to membrane proteomics. *Nat. Biotechnol.* **2003**, 21, 262-267.

20. Speers, A. E.; Wu, C. C.: Proteomics of Integral Membrane Proteins - Theory and Application. *Chem. Rev.* **2007**, 107, 3687-3714.

21. Farrokhi, V.; McShane, A. J.; Nemati, R.; Yao, X. D.: Stable Isotope Dilution Mass Spectrometry for Membrane Transporter Quantitation. *AAPS J.* **2013**, 15, 1222-1231.

22. Riordan, J. R.; Rommens, J. M.; Kerem, B. S.; Alon, N.; Rozmahel, R.; Grzelczak, Z.; Zielenski, J.; Lok, S.; Plavsic, N.; Chou, J. L.; Drumm, M. L.; Iannuzzi, M. C.; Collins, F. S.; Tsui, L. C.: Identification of the Cystic-Fibrosis Gene - Cloning and Characterization of Complementary-DNA. *Science.* **1989**, 245, 1066-1072.

23. Wang, X. D.; Venable, J.; LaPointe, P.; Hutt, D. M.; Koulov, A. V.; Coppinger, J.; Gurkan, C.; Kellner, W.; Matteson, J.; Plutner, H.; Riordan, J. R.; Kelly, J. W.; Yates, J. R.; Balch, W. E.: Hsp90 cochaperone Aha1 downregulation rescues misfolding of CFTR in cystic fibrosis. *Cell.* **2006**, 127, 803-815.

24. Hutt, D. M.; Herman, D.; Rodrigues, A. P. C.; Noel, S.; Pilewski, J. M.; Matteson, J.; Hoch, B.; Kellner, W.; Kelly, J. W.; Schmidt, A.; Thomas, P. J.; Matsumura, Y.; Skach, W. R.; Gentzsch, M.; Riordan, J. R.; Sorscher, E. J.; Okiyoneda, T.; Yates, J. R.; Lukacs, G. L.; Frizzell,

R. A.; Manning, G.; Gottesfeld, J. M.; Balch, W. E.: Reduced histone deacetylase 7 activity restores function to misfolded CFTR in cystic fibrosis. *Nat. Chem. Biol.* **2010**, *6*, 25-33.

25. Jiang, H.; Ramos, A. A.; Yao, X. D.: Targeted Quantitation of Overexpressed and Endogenous Cystic Fibrosis Transmembrane Conductance Regulator Using Multiple Reaction Monitoring Tandem Mass Spectrometry and Oxygen Stable Isotope Dilution. *Anal. Chem.* **2010**, 82, 336-342.

26. Addona, T. A.; Abbatiello, S. E.; Schilling, B.; Skates, S. J.; Mani, D. R.; Bunk, D. M.; Spiegelman, C. H.; Zimmerman, L. J.; Ham, A. J. L.; Keshishian, H.; Hall, S. C.; Allen, S.; Blackman, R. K.; Borchers, C. H.; Buck, C.; Cardasis, H. L.; Cusack, M. P.; Dodder, N. G.; Gibson, B. W.; Held, J. M.; Hiltke, T.; Jackson, A.; Johansen, E. B.; Kinsinger, C. R.; Li, J.; Mesri, M.; Neubert, T. A.; Niles, R. K.; Pulsipher, T. C.; Ransohoff, D.; Rodriguez, H.; Rudnick, P. A.; Smith, D.; Tabb, D. L.; Tegeler, T. J.; Variyath, A. M.; Vega-Montoto, L. J.; Wahlander, A.; Waldemarson, S.; Wang, M.; Whiteaker, J. R.; Zhao, L.; Anderson, N. L.; Fisher, S. J.; Liebler, D. C.; Paulovich, A. G.; Regnier, F. E.; Tempst, P.; Carr, S. A.: Multi-site assessment of the precision and reproducibility of multiple reaction monitoring-based measurements of proteins in plasma. *Nat. Biotechnol.* **2009**, 27, 633-U85.

27. Whiteaker, J. R.; Zhao, L.; Anderson, L.; Paulovich, A. G.: An Automated and Multiplexed Method for High Throughput Peptide Immunoaffinity Enrichment and Multiple Reaction Monitoring Mass Spectrometry-based Quantification of Protein Biomarkers. *Mol. Cell. Proteomics* **2010**, 9, 184-196.

28. Carr, S. A.; Abbatiello, S. E.; Ackermann, B. L.; Borchers, C.; Domon, B.; Deutsch, E. W.; Grant, R. P.; Hoofnagle, A. N.; Huttenhain, R.; Koomen, J. M.; Liebler, D. C.; Liu, T.; MacLean, B.; Mani, D.; Mansfield, E.; Neubert, H.; Paulovich, A. G.; Reiter, L.; Vitek, O.; Aebersold, R.;

Anderson, L.; Bethem, R.; Blonder, J.; Boja, E.; Botelho, J.; Boyne, M.; Bradshaw, R. A.; Burlingame, A. L.; Chan, D.; Keshishian, H.; Kuhn, E.; Kinsinger, C.; Lee, J. S. H.; Lee, S. W.; Moritz, R.; Oses-Prieto, J.; Rifai, N.; Ritchie, J.; Rodriguez, H.; Srinivas, P. R.; Townsend, R. R.; Van Eyk, J.; Whiteley, G.; Wiita, A.; Weintraub, S.: Targeted Peptide Measurements in Biology and Medicine: Best Practices for Mass Spectrometry- based Assay Development Using a Fit- for- Purpose Approach. *Mol. Cell. Proteomics* **2014**, 13, 907-917.

29. Yao, X. D.: Derivatization or Not: A Choice in Quantitative Proteomics. *Anal. Chem.* **2011**, 83, 4427-4439.

30. Bruscia, E.; Sangiuolo, F.; Sinibaldi, P.; Goncz, K. K.; Novelli, G.; Gruenert, D. C.: Isolation of CF cell lines corrected at Delta F508-CFTR locus by SFHR-mediated targeting. *Gene Ther.* **2002**, 9, 683-685.

31. Ong, S. E.; Blagoev, B.; Kratchmarova, I.; Kristensen, D. B.; Steen, H.; Pandey, A.; Mann, M.: Stable isotope labeling by amino acids in cell culture, SILAC, as a simple and accurate approach to expression proteomics. *Mol. Cell. Proteomics* **2002**, 1, 376-386.

32. Swiatecka-Urban, A.; Moreau-Marquis, S.; Maceachran, D. P.; Connolly, J. P.; Stanton, C. R.; Su, J. R.; Barnaby, R.; O'Toole G, A.; Stanton, B. A.: Pseudomonas aeruginosa inhibits endocytic recycling of CFTR in polarized human airway epithelial cells. *Am. J. Physiol. Cell Physiol.* **2006**, 290, C862-72.

33. MacLean, B.; Tomazela, D. M.; Abbatiello, S. E.; Zhang, S. C.; Whiteaker, J. R.; Paulovich, A. G.; Carr, S. A.; MacCoss, M. J.: Effect of Collision Energy Optimization on the Measurement of Peptides by Selected Reaction Monitoring (SRM) Mass Spectrometry. *Anal. Chem.* **2010**, 82, 10116-10124.

34. Yao, X. D.; Bajrami, B.; Shi, Y.: Ultrathroughput Multiple Reaction Monitoring Mass Spectrometry. *Anal. Chem.* **2010**, 82, 794-797.

35. Hopkins, A. L.; Groom, C. R.: The druggable genome. *Nat. Rev. Drug Discovery.* **2002**, 1, 727-730.

36. Bajrami, B.; Farrokhi, V.; Zhang, M. T.; Shehu, A.; Yao, X. D.: Back to deuterium: Utility of H-2-labeled peptides for targeted quantitative proteomics. *Int. J. Mass Spectrom.* **2012**, 312, 17-23.

37. Cheng, S. H.; Gregory, R. J.; Marshall, J.; Paul, S.; Souza, D. W.; White, G. A.; Oriordan, C. R.; Smith, A. E.: Defective Intracellular-Transport and Processing of Cftr Is the Molecular-Basis of Most Cystic-Fibrosis. *Cell.* **1990**, 63, 827-834.

38. Marmagne, A.; Rouet, M.-A.; Ferro, M.; Rolland, N.; Alcon, C.; Joyard, J.; Garin, J.; Barbier-Brygoo, H.; Ephritikhine, G.: Identification of new intrinsic proteins in Arabidopsis plasma membrane proteome. *Mol. Cell. Proteomics.* **2004**, 3, 675-691.

39. Ferro, M.; Salvi, D.; Brugiere, S.; Miras, S.; Kowalski, S.; Louwagie, M.; Garin, J.; Joyard, J.; Rolland, N.: Proteomics of the chloroplast envelope membranes from Arabidopsis thaliana. *Mol. Cell. Proteomics.* **2003**, 2, 325-345.

40. Lu, X.; Zhu, H.: Tube-gel digestion. A novel proteomic approach for high throughput analysis of membrane proteins. *Mol. Cell. Proteomics.* **2005**, 4, 1948-1958.

41. Cao, R.; He, Q.; Zhou, J.; Liu, Z.; Wang, X.; Chen, P.; Xie, J.; Liang, S.: High-throughput analysis of rat liver plasma membrane proteome by a nonelectrophoretic in-gel tryptic digestion coupled with mass spectrometry identification. *J. Proteome Res.* **2008**, 7, 535-45.

42. Kuzyk, M. A.; Smith, D.; Yang, J. C.; Cross, T. J.; Jackson, A. M.; Hardie, D. B.; Anderson, N. L.; Borchers, C. H.: Multiple Reaction Monitoring-based, Multiplexed, Absolute Quantitation of 45 Proteins in Human Plasma. *Mol. Cell. Proteomics.* **2009**, 8, 1860-1877.

43. Hare, J. F.; Taylor, K.: Mechanisms of Plasma-Membrane Protein-Degradation - Recycling Proteins Are Degraded More Rapidly Than Those Confined to the Cell-Surface. *Proc. Natl. Acad. Sci. U.S.A.* **1991**, 88, 5902-5906.

44. Doherty, M. K.; Hammond, D. E.; Clague, M. J.; Gaskell, S. J.; Beynon, R. J.: Turnover of the Human Proteome: Determination of Protein Intracellular Stability by Dynamic SILAC. *J. Proteome Res.* **2009**, 8, 104-112.

45. Fierro-Monti, I.; Racle, J.; Hernandez, C.; Waridel, P.; Hatzimanikatis, V.; Quadroni, M.: A Novel Pulse-Chase SILAC Strategy Measures Changes in Protein Decay and Synthesis Rates Induced by Perturbation of Proteostasis with an Hsp90 Inhibitor. *PloS one.* **2013**, 8, e80423.

Chapter 3

Ultrathroughput Multiple Reaction Monitoring Mass Spectrometry of Cystic Fibrosis Transmembrane Conductance Regulator in Cells

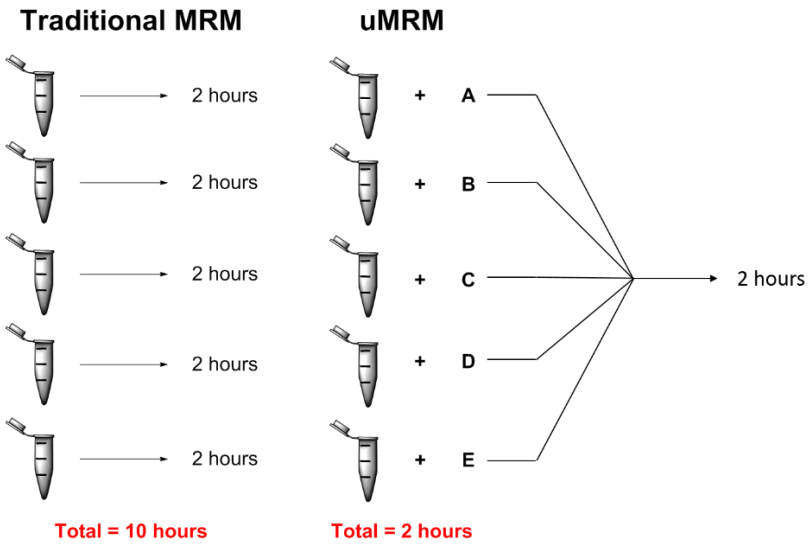

3.1 Introduction

Multiple reaction monitoring (MRM) mass spectrometry (MS) has provided a versatile and relatively low-cost platform to promptly develop quantitative proteomics methods [1]. The analytical advantages of MRM-MS over traditional immunoassays, for protein quantitation, has been well documented [2]. These include the increased precision and accuracy of measurements, with dramatically lower coefficients of variation (CV) [3] and interlaboratory reproducibility [4]. However, the sample throughput of immunoassays are incomparable. Enzyme-linked immunosorbent assays (ELISA), are capable of 100s of samples being simultaneously quantified [5]. Towards increasing sample throughput for MRM-MS, several technologies have emerged that contain high-cost derivatizing reagents that depend on expensive isotopologues [6-12]. The integrated design of these reagents (sample-throughput and quantitation modules combined) renders statistically-significant numbers to be cost prohibitive for monitoring changes. When subtle changes are observed across proteomes, an increase in replicates is needed to give statistical significance to the data [13]. To achieve increased sample throughput (i.e. replicates), a modular design was adopted (sample-throughput and quantitation modules separated), dubbed ultrathroughput MRM (uMRM) [14]. This approach is adaptable for a handful of samples to potentially 100s. To achieve sample throughput, inexpensive, non-isotopic reagents are used to derivatize proteolytic digests. These reagents act as mass tags that allows each sample to be distinguishable in a mass spectrometer. This gives uMRM an economic advantage over other integrated designs, and is not restricted to isotopologues. Potentially infinite chemically diverse structures are available as derivatizing reagents.

The second module, quantitation, is accomplished independent of the derivatizing reagents. This can be achieved by any number of techniques familiar to the proteomics field; such as, AQUA

peptides, ^{18}O, metabolic labelling, etc... [15,16]. Since the sample-throughput and quantitation modules are separated, only one common reference standard is required. The common reference standard in each sample would then go through the same derivatization as the sample. This cheapens the analysis to a fraction of the price, transforming a triple quadrupole mass spectrometer's intrinsic multiplexing capability to sample throughput. Statistically significant numbers are now available through the increased throughput.

This separated modular approach was applied to the quantitation of cystic fibrosis transmembrane conductance regulator (CFTR) protein. Approximately 90% of patients with cystic fibrosis (CF) have a gene deletion of F508del that causes the subsequent premature degradation of CFTR, before reaching the plasma membrane [17]. We have previously described a targeted proteomic quantitation of CFTR, in the apical plasma membrane of mammalian cells [18]. The intrinsic difficulty of preparing large, hydrophobic membrane proteins was mitigated by using a dual enrichment strategy that involved cell-surface biotinylation and gel electrophoretic enrichment (GEE). A whole protein internal standard (IS) was generated by the stable isotope labelling by amino acids in cell culture (SILAC) method [19].

In the current work, the sample throughput will be increased with uMRM technology. This will be demonstrated by 5 samples (varying ratios of IS to native) being quantified in triplicates. For traditional MRM MS analysis, this would require 15 MS experiments (5 samples x 3 replicates, ~30 hours); however, using uMRM MS this would take 3 MS experiments (5-plex sample x 3 replicates, ~6 hours). This drastically decreases the instrument time needed for quantitation. To achieve this throughput, non-isotopic amino acid reagents will be used to derivatize the free amines of the proteolytic digests. The modular design is exploited by using the SILAC strategy for the quantitation module and the derivatizing reagents as the sample-throughput module.

To achieve near 100% coupling of the derivatizing reagents with the proteolytic peptides, a large molar excess of the reagents is required. This renders a complicated sample, such as a cell lysate, to be additionally complicated with respect to precise, accurate MRM MS quantitation. The measurement is further challenged by dilution. An N-in-1 experiment requires sample pooling, thus an N-times dilution. To enrich the analytes of interest and to simplify a difficult matrix, a biotin pull-down technique was utilized. Similar to the ICAT® reagents [6], the thiols of cysteine-containing peptides were alkylated with a biotin moiety. The biotin moiety is easily added to thiols by replacing the typical alkylating reagents during trypsin digestion (e.g., iodoacetamide or iodoacetic acid) with iodoacetyl-LC-biotin. After derivatization, the cysteinyl peptides are enriched by exploiting the well-known avidin/biotin affinity [20]. This affinity enrichment step not only removes the derivatizing reagents, but also simplifies the baseline matrix to only peptides containing cysteine. Thus, improving the limit of quantitation.

This N-in-1 experiment will allow 5 different samples with 3 replicates per sample to be quantified in 3 MS experiments. Traditional MRM MS was performed requiring 15 MS experiments. A comparison of precision will be made between the 2 methods. This work will highlight the versatility and adaptability of the uMRM technology. This will be the first time for uMRM MS, a whole protein IS is used as the quantitation module. Furthermore, a biotin enrichment strategy is applied, to allow enrichment without a specific antibody, thus broader applications of this method are possible.

3.2 Experimental

3.2.1 Materials

All reagents were purchased from Sigma-Aldrich (St. Louis, MO) or Fisher Scientific (Fair Lawn, NJ) unless otherwise specified below. Direct-Q3 water system (Millipore, Billerica, MA)

was used to purify deionized water. FMOC-Xxx-Osu amino acids were purchased from Chem-Impex International (Wood Dale, IL). Proteomics grade recombinant trypsin was purchased from Roche Applied Science (Indianapolis, IN). The iodoacetyl-LC-biotin was purchased from ApexBio Technology (Houston, TX). The cell line, baby hamster kidney overexpressing wild type CFTR (BHK-wtCFTR), was a gift from the Cystic Fibrosis Foundation. Purified full-length CFTR samples were gifts from Dr. L. J. DeLucas (University of Alabama at Birmingham) and Dr. J. He (Accelagen, San Diego, CA). Purification of the later full-length CFTR sample was performed according to a procedure developed by Dr. J. R. Riordan at the University of North Carolina, Chapel Hill. Amino acid analysis for the highly-purified, native CFTR was performed at the Keck Biotechnology Resource Laboratory at Yale University. DMEM, Ham's F-12, DME/Low media deficient in L-arginine, L-leucine and L-lysine, and fetal bovine serum (FBS) were purchased from Thermo Scientific HyClone (Logan, UT). Dialyzed FBS and NeutrAvidin were purchased from Life Technologies (Thermo, Carlsbad, CA).

3.2.2 Cell culture and lysate preparation

BHK-wtCFTR cells were cultured in DMEM/Ham's F-12 with 550 μM methotrexate, 5% FBS, and 1% of each of the following reagents: pen-strep, non-essential amino acids, and sodium pyruvate. The lysis buffer (600 μL) containing 1% (v/v) Triton X-100, 150 mM NaCl, 20 mM Tris-HCl at pH 7.2, and 1% (v/v) protease inhibitors was used for the lysis of BHK-wtCFTR cells.

3.2.3 SILAC internal standard preparation

The heavy isotope labeled, full-length CFTR was obtained, by SILAC, from BHK-wtCFTR cells cultured in DME/Low deficient in L-lysine, L-leucine, and L-arginine supplemented with 550 μM methotrexate, 0.4 mM L-arginine-$^{13}C_6$•HCl (Cambridge Isotopes, Andover, MA), 0.8 mM L-lysine-$^{13}C_6{}^{15}N_2$•2HCl (Cambridge Isotopes, Andover, MA), 0.8 mM L-leucine, and 5%

of dialyzed fetal bovine serum. Cells grown in this heavy media were allowed at least 7 doublings prior to harvesting.

3.2.4 Gel-based electrophoretic enrichment

Gel electrophoresis was performed using a resolving gel consisting of 10% acrylamide and a stacking gel of 3% acrylamide. BioRad glass plates with 1.5 mm spacer plates and a 5-well comb were used. CFTR samples were mixed with Laemmli sample buffer and incubated at 30^{o}C for 20 min. Gel electrophoresis was carried out at 120 V (constant voltage) for 35 min.

3.2.5 Digestion

Gel pieces at the interface between the resolving and the stacking gels were excised. The gel pieces were washed (50 mM ammonium bicarbonate in H_2O/acetonitrile), reduced (10 mM DTE), and alkylated (2 mM iodoacetyl-LC-biotin, see next section) before trypsinization (20 ng/µL). The resulting digestion solution was dried via SpeedVac (Savant, Farmingdale, NY) and overnight lyophilization (Labconco, Kansas City, MO).

3.2.6 Biotin alkylation of thiols

The iodoacetyl-LC-biotin was first dissolved in pure DMSO, then diluted to a 2 mM concentration with 25 mM ammonium bicarbonate. To determine the time necessary for alkylation of thiols, a time point study was accomplished. Immediately after alkylation with iodoacetyl-LC-biotin the gel pieces were washed, and 20 mM iodoacetamide (IAA) was added. Transitions for iodoacetyl-LC-biotin and iodoacetamide alkylation were monitored. Time points collected were 0, 0.75, 1.5, 2.5, 5, 8, and 16 hr.

3.2.7 Peptide derivatization

Each sample was assigned a unique amino acid reagent for sample-specific derivatization. The activated FMOC-protected amino acid was dissolved in a solution of DIPEA/DMF at pH=8.

This solution was added to the dried digests, and incubated overnight at room temperature. The reaction was then quenched with ice-cooled 20% formic acid and dried via SpeedVac and overnight lyophilization.

3.2.8 Biotinylated peptide enrichment

The dried, derivatized, and biotinylated digest was dissolved in 0.1 M borate buffer (boric acid adjusted to pH=7.4 with NaOH), added to 0.1 mg of NeutrAvidin, and incubated at RT for 60 min. The solution was then added to a 10 kDa MWCO Vivacon 500 (SartoriusStedim, Goettingen, Germany) membrane filter. After washing with 0.1X PBS in 10% methanol, the derivatized, biotinylated peptides were eluted with 20% acetic acid in 30% methanol. The product was then dried via SpeedVac and overnight lyophilization

3.2.9 NanoLC-MRM MS

The optimization and data analysis of this work was assisted by the Skyline software. An Eksigent NanoLC-Ultra $2D^{+}$ (Redwood City, CA) was used at a flow rate of 250 nL/min with a self-packed Picofrit column (New Objective, Woburn, MA) filled with 15 cm of 2.7 μM diameter, 160Å pore Halo resin (MacMod, Chadds Ford, PA). Solvent A was composed of 98.8% H_2O, 1.0% acetonitrile, and 0.2% formic acid (v/v) and solvent B's composition was 98.8% acetonitrile, 1.0% water, and 0.2% formic acid (v/v). A typical gradient was 2%B at 0 min → 2%B at 20 min → 47%B at 100 min → 80%B at 120 min with 10 min equilibration. Samples were loaded on the trap column at a flow rate of 3.5 μL/min at 1% solvent B for 10 min. A triple quadrupole mass spectrometer was used, 4000 QTrap from ABSCIEX (Foster City, CA).

3.3 Results and discussion

3.3.1 Enrichment of whole CFTR protein from cell lysates

A modified CFTR enrichment strategy from a previous work was applied [18]. A gel was poured that localized CFTR protein to the interface between the stacking (3% acrylamide) and resolving (10% acrylamide) gels that lacked sodium dodecyl sulfate (SDS) **(Figure 3.1a)**. After mixing the sample buffer with the BHK-wtCFTR cell lysate, it was incubated at a gentle temperature of 30^{o}C for 20 min to prevent CFTR degradation. The total complexity reduction was calculated to be approximately 89% based on Ponceau S whole protein staining **(Figure 3.1b)**. Since this method depends on the pull down of biotinylated peptides, endogenous biotinylated proteins were located **(Figure 3.1c)** to determine if they are co-localized with CFTR **(Figure 3.1d)**. Ultimately, if a region of interest is biotin-rich, then more avidin should be used to ensure proper capture of all the biotinylated peptides. For CFTR, the region above the orange marker (~148 kDa) was excised for in-gel trypsin digestion. This region has no strong bands for endogenously biotinylated proteins.

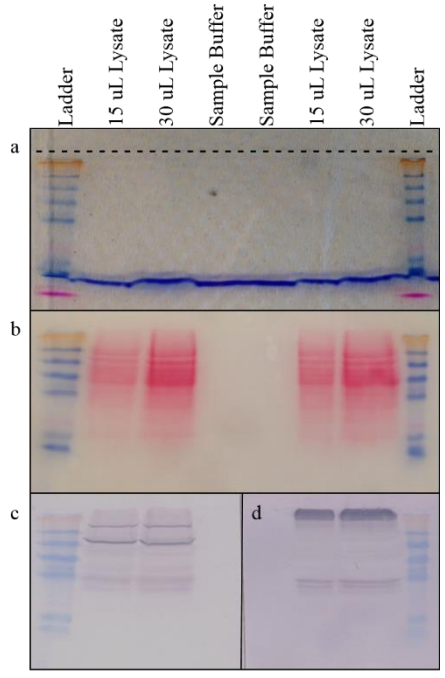

Figure 3.1: Localization of CFTR and endogenously biotinylated proteins in BHK-wtCFTR triton X-100 cell lysate during modified SDS-PAGE: lysate incubation with Laemmli sample buffer containing 20% β-mercaptoethanol for 20 minutes at 30^{o}C, 10% acrylamide resolving gel with no SDS, 3% acrylamide stacking gel with no SDS, 1 mm thickness gel with 10 wells (44 µL/well), and a 35 minute run time at 120V. (a) GEE [18] with the dotted line marking the interface between the stacking and resolving gel (b) Ponceau S staining of the total proteins on the PVDF membrane after transferring from gel: 90 minute transfer at 30V. After blocking, the PVDF membrane was cut, and the protein detection was performed in 2 separate dishes. (c) BCIP/NBT staining after 60 minute incubation with avidin conjugated with alkaline phosphatase (d) BCIP/NBT staining after 60 minute incubation with an anti-CFTR mAb-596 (J. Riordan, UNC, NC) and a 30 minute incubation with a secondary antibody conjugated with alkaline phosphatase.

3.3.2 Biotinylation of cysteine-containing peptides during in-gel digestion and peptide selection for MRM MS

The increase in sample complexity and sample dilution, from the respective derivatizing reagents and sample pooling, renders an enrichment strategy necessary. A biotin handle is added to cysteinyl peptides by alkylating with iodoacetyl-LC-biotin **(Figure 3.2)**. This is similar the ICAT method, but the biotin alkylation does not possess isotopes and therefore is not responsible for quantitation [6]. From all possible biotinylated signature peptides, only those with one cysteine, 6-18 amino acids in length, and no cysteine at the N-terminus were chosen for MRM screening. This criteria was chosen to ensure only one biotin moiety, allowable quadrupole *m/z* range, and no steric hindrance at the N-terminus for future derivatization, respectively. From those 8 peptides, 4 were able to be monitored by MRM MS **(Table 3.1 and Figure 3.3)**.

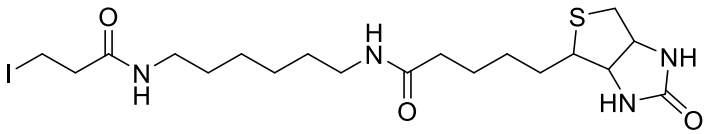

Figure 3.2: Structure of iodoacetyl-LC-biotin.

Signature Cysteinyl CFTR Peptides		
LMGCDSFDQFSAER	LDFVLVDGGCVLSHGHK	EIFESCVCK
QAFADCTVILCEHR	ACQLEEDISK	AYCWEEAMEK
IFTTISFCIVLR	IEAMLECQQFLVIEENK	ISFCSQFSWIMPGTIK
SIAIYLGIGLCLLFIVR	QLMCLAR	ECFFDDMESIPAVTTWNTYLR

Table 3.1: Signature cysteinyl CFTR peptides after trypsin digestion. The peptides in red were monitored in uMRM MS.

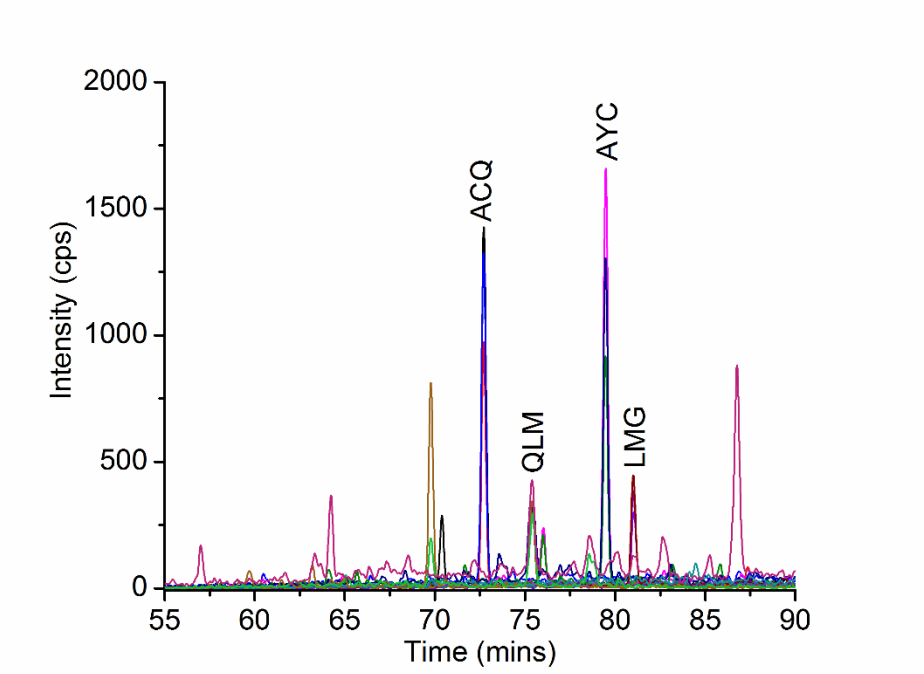

Figure 3.3: Chromatogram of signature cysteinyl peptides monitored by nanoLC-MRM MS without NeutrAvidin enrichment.

3.3.3 Iodoacetyl-LC-biotin versus iodoacetamide alkylation of cysteines

To determine the incubation period for full iodoacetyl-LC-biotin alkylation of cysteines, a time trial was performed. After the iodoacetyl-LC-biotin alkylation, iodoacetamide was added. Once trypsinization was completed, transitions for iodoacetyl-LC biotin and iodoacetamide alkylation were monitored by MRM MS. After 45 min, no iodoacetamide alkylation was seen. Digests from separately alkylated digests (IAA and iodoacetyl-LC-biotin) are comparable for both cysteinyl (ACQ, AYC, and LMG) and non-cysteinyl peptides (CFTR01 and CFTR02) **(Figure 3.4)**.

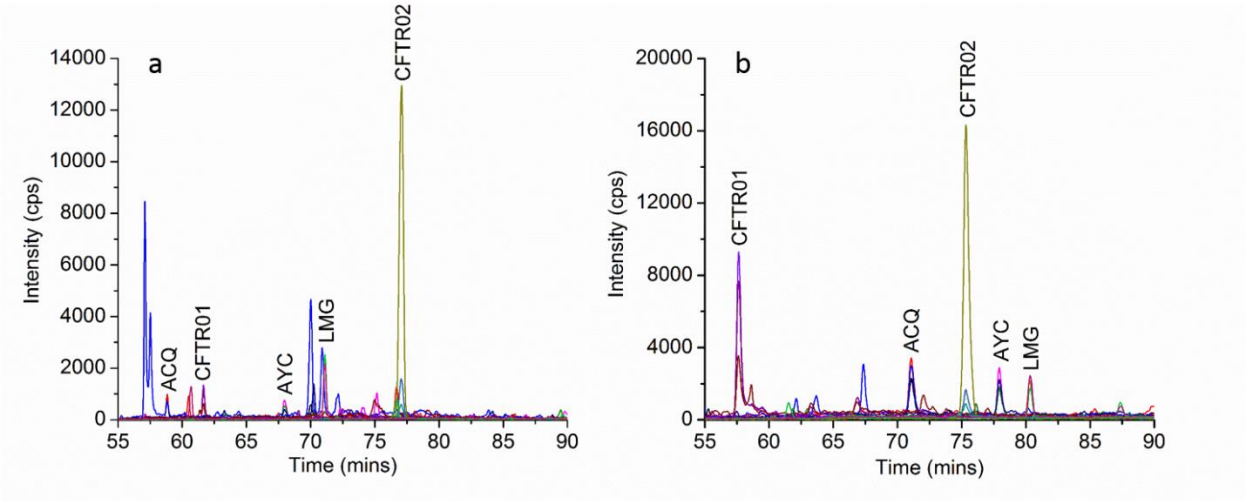

Figure 3.4: Thiol alkylation with iodoacetamide (a) and iodoacetyl-LC-biotin (b) before trypsinization. ACQ, AYC, and LMG are cysteine-containing peptides of CFTR, where CFTR01 and CFTR02 are not.

3.3.4 Pull down of biotin-containing peptides to reduce sample complexity

The biotin-containing peptides were pulled down with free NeutraAvidin (a deglycosylated avidin) protein. This provided a scalable approach to economically enrich large amounts of biotinylated peptides, and also eliminate non-specific binding to the immobilization matric of solid-phase avidin reagents. According to bicinchonimic acid (BCA) analysis, the protein concentration from the BHK-wtCFTR lysates are 2.05±0.03 mg/mL (NanoDrop 2000c, ThermoScientific, Wilmington, DE). Only 10.5% of the proteins exist at the excised, interfacial band **(Figure 3.1b)**. Assuming all the protein at the interface is CFTR and digested at 100% efficiency, 40.9 µg of cysteine-containing peptides are present in the digest. Therefore using 0.1 mg of NeutrAvidin is over double what is required. After incubating the avidin and biotinylated peptides together, they were placed on a 10 kDa molecular weight cut off filter and centrifuged. The non-biotinylated peptides were washed away with methanol/water washes. The biotinylated peptides were separated from the NeutrAvidin with an acidic solution. The filtrate was then dried and stored at -20^{o}C until MRM MS analysis. This simple filter-assisted method was quite effective as shown in **Figure 3.5**. This enrichment step is essential because of the increase in sample

complexity caused by the derivatizing reagents. A large excess of reagents is required to ensure a chemical conversion of the biotinylated, derivatized peptide. Secondly, when pooling the samples for uMRM analysis, a dilution occurs that is overcome by this enrichment step.

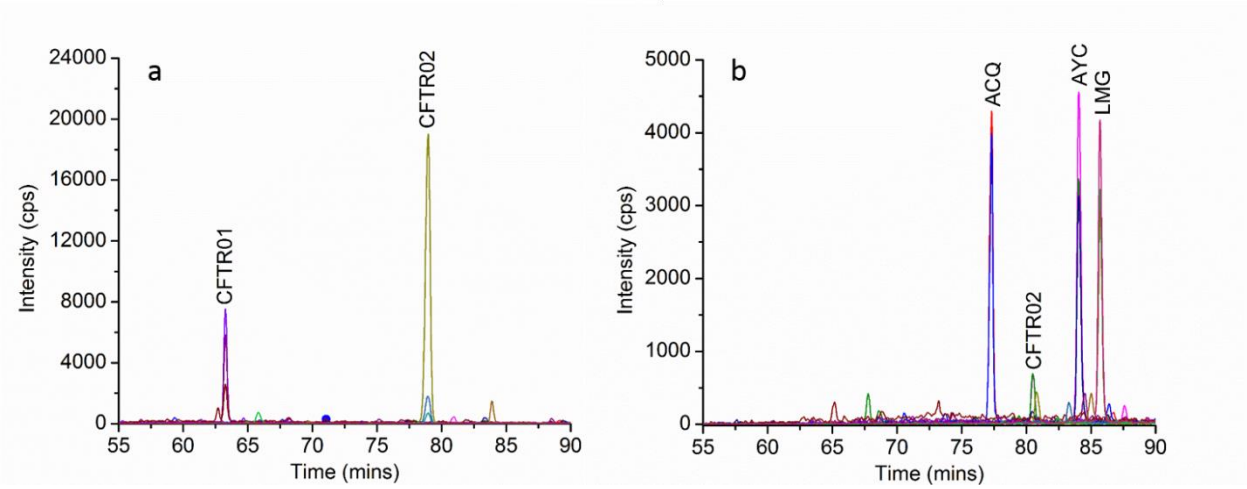

Figure 3.5: Enrichment of cysteinyl peptides with NeutrAvidin on a 10 kDa molecular weight cut off filter. (a) Filtrate after 30 min incubation of the CFTR digest with NeutrAvidin. This step washes away the non-cysteinyl peptides (CFTR01 and CFTR02) with the cysteinyl peptides (ACQ, AYC, and LMG) bound to the NeutrAvidin. No cysteinyl peptides were seen in this filtrate ensuring a proper amount of NeutrAvidin was utilized (b) Filtrate after 10 min incubation with 20% acetic acid in a 30% methanol solution. This step separates the cysteinyl peptides (ACQ, AYC, and LMG) from the NeutrAvidin. Very little non-cysteinyl peptides are seen (only a weak CFTR02 signal). This ensures that we are able to separate cysteinyl from non-cysteinyl peptides.

3.3.5 Derivatization of biotinylated peptides

To achieve the sample throughput module of uMRM, a derivatizing step is needed. In this study, the derivatizing reagents were FMOC-Xxx-OSu amino acids. The N-terminus alkylation prevents polymerization, when the coupling agents are added to the digests. In the near future, 5 different FMOC-Xxx-Osu amino acids will be used to derivatize 5 different BHK-wtCFTR digests. This will be accomplished in biological triplicates.

3.3.6 BHK-wtCFTR lysate preparation for CFTR quantitation

Five different ratios of native BHK-wtCFTR and SILAC BHK-wtCFTR lysate were combined to compare traditional MRM MS to uMRM MS. The ratios in **Table 3.2** were made

from common stocks of the appropriate lysate. Each ratio was quantified in triplicate via traditional MRM MS; i.e., gel-fractionated, digested, desalted, and nanoLC-MRM MS separately. A triplicate uMRM MS measurement will also be made; i.e. each sample gel-fractionated, digested, and derivatized separately, but then pooled before enrichment and nanoLC-MRM MS **(Figure 3.6)**. This will yield a 5 times reduction in analysis time, and enable analytical significant numbers more feasible.

Ratio (Native/SILAC)	Volume of BHK-wCFTR Lysate (uL)	Volume of SILAC BHK-wtCFTR Lysate (uL)
0.33	150	450
0.50	200	400
1.0	300	300
2.0	400	200
3.0	450	150

Table 3.2: Sample ratios of the native BHK-wtCFTR to the SILAC BHK-wtCFTR lysate. The lysates were of common stock for both the traditional and uMRM MS experiments. Triplicates of each sample were prepared for both experiments.

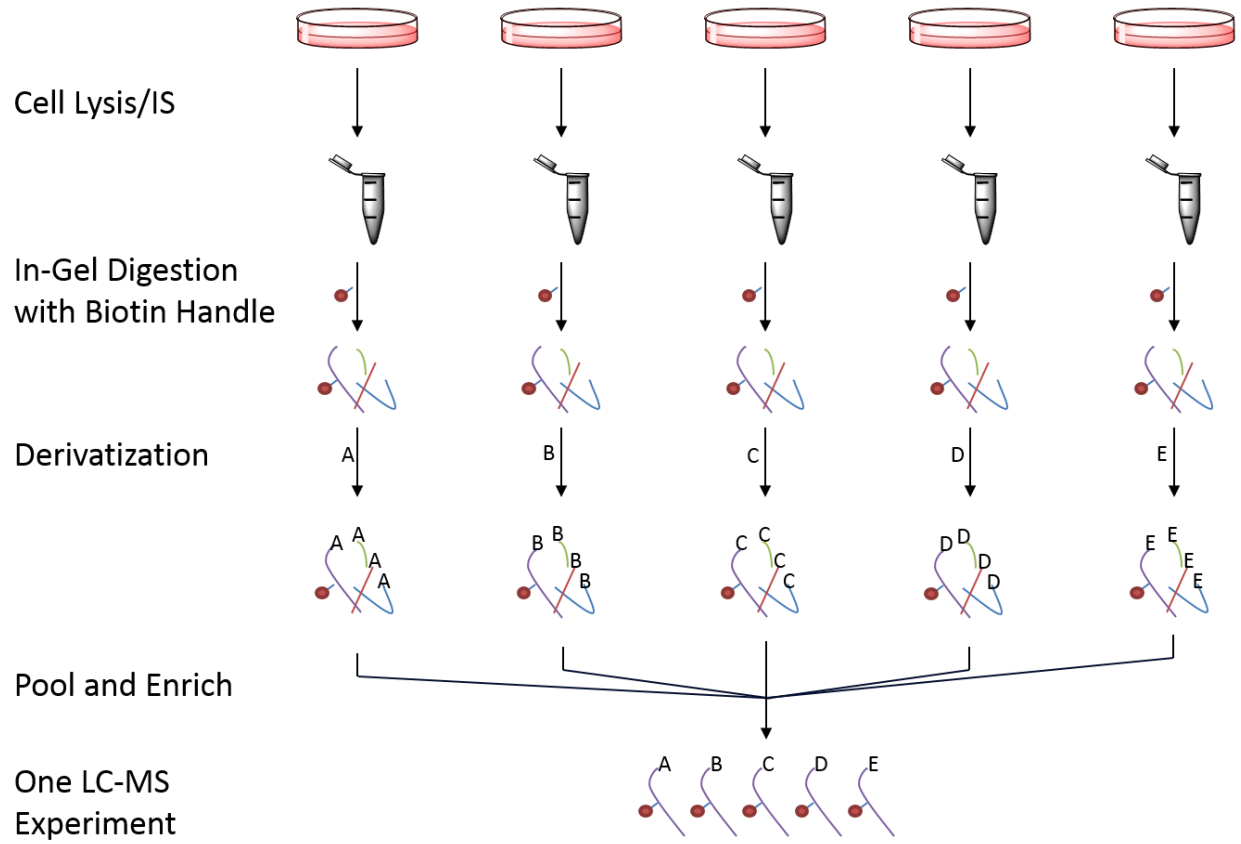

Figure 3.6: Five-plex uMRM MS strategy. A sample-specific amino acid will be added to each sample to create the multiplexing module of the design. Each sample will be analyzed in triplicates, and compared to traditional MRM MS.

3.3.7 Traditional MRM MS of the mixed lysate solutions

The 5 ratios of native to SILAC BHK-wtCFTR lysates (0.33, 0.50, 1.0, 2.0, and 3.0) were gel fractionated, in-gel digested, and desalted in triplicate before nanoLC-MRM MS measurements were accomplished. Peptides CFTR01 through CFTR04 were used for quantitation with 3 transitions monitored from each individual peptide [18]. The peak area ratios of the native to SILAC CFTR were averaged and plotted in **Figure 3.7**. The peak area ratios and the volume ratios of native to SILAC BHK-wtCFTR lysate correlated linearly with an adjusted R^2 of 0.9984. This represents that the experiment parameters are well within the limit of linearity. Also the standard error is very minimal for each ratio demonstrating the precision of the CFTR quantitation method.

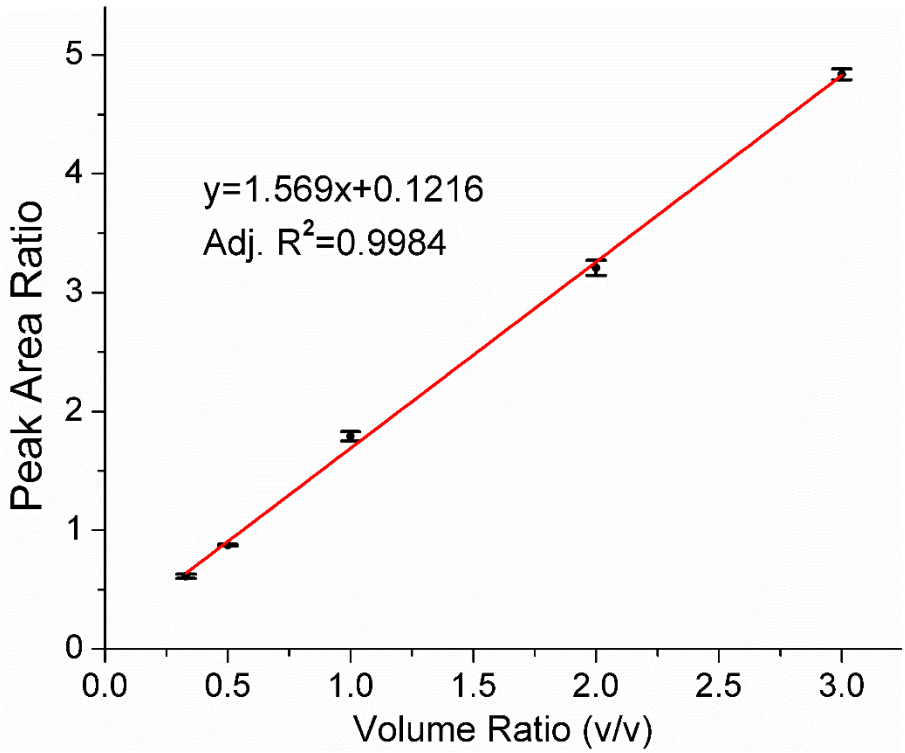

Figure 3.7: Relationship between the peak area ratios and the lysate solutions. Five different lysate ratios of native and SILAC BHK-wtCFTR lysates were made: 0.33, 0.50, 1.0, 2.0, and 3.0 (native/SILAC). Biological triplicates of each ratio were then acquired from gel fractionation to nanoLC-MRM MS measurement.

3.3.8 Future work

The completed traditional MRM MS experiments will serve as the basis of comparison to the uMRM MS analyses. The 5 different lysate solutions, from a common stock with the MRM MS analyses, was gel fractionated and in-gel digested. However, a biotin handle was added during the alkylation of the cysteine residues. These were prepared in triplicate, and ready for the next step of the uMRM MS strategy, derivatization. In the future, each ratio will be alkylated with a specific FMOC-Xxx-Osu. The derivatized, biotinylated peptides will then be combined and pulled down with NeutrAvidin. After elution and drying, the sample will be analyzed via nanoLC-uMRM MS. A comparison will then be made between the MRM and uMRM MS.

3.7 Conclusion

By using non-isotopic, inexpensive derivatizing reagents affordable and immensely expandable sample throughput is possible for MRM MS. With this uMRM methodology, a single common IS allows for concurrent quantitation of the same surrogate peptides in multiple samples via sample-specific derivatization. The amount of multiplexing is controlled by the mass spectrometrist from a few samples to potentially hundreds. The analysis of a statistically significant number of samples or proteomes with a large protein concentration (e.g. serum) are now more practical. This technology has the potential to shift the paradigm of derivatization-based methods for improving sample throughput.

3.8 References

1. Whiteaker, J. R.; Halusa, G. N.; Hoofnagle, A. N.; Sharma, V.; MacLean, B.; Yan, P.; Wrobel, J. A.; Kennedy, J.; Mani, D. R.; Zimmerman, L. J.; Meyer, M. R.; Mesri, M.; Rodriguez, H.; Clinical Proteomic Tumor Analysis Consortium (CPTAC); Paulovich, A. G. CPTAC Assay Portal: A Repository of Targeted Proteomic Assays. *Nat. Methods.* **2014**, 11, 703-704.

2. Wu, A. H.; French, D. Implementation of Liquid Chromatography/Mass Spectrometry into the Clinical Laboratory. *Clin. Chim. Acta.* **2013**, 420, 4-10.

3. Yau, Y. Y.; Duo, X.; Leong, R. W.; Wasinger, V. C. Reverse-Polynomial Dilution Calibration Methodology Extends Lower Limit of Quantification and Reduces Relative Residual Error in Targeted Peptide Measurements in Blood Plasma. *Mol. Cell. Proteomics.* **2015**, 14, 441-454.

4. Addona, T. A.; Abbatiello, S. E.; Schilling, B.; Skates, S. J.; Mani, D. R.; Bunk, D. M.; Spiegelman, C. H.; Zimmerman, L. J.; Ham, A. J.; Keshishian, H.; Hall, S. C.; Allen, S.; Blackman, R. K.; Borchers, C. H.; Buck, C.; Cardasis, H. L.; Cusack, M. P.; Dodder, N. G.; Gibson, B. W.; Held, J. M.; Hiltke, T.; Jackson, A.; Johansen, E. B.; Kinsinger, C. R.; Li, J.; Mesri, M.; Neubert, T. A.; Niles, R. K.; Pulsipher, T. C.; Ransohoff, D.; Rodriguez, H.; Rudnick, P. A.; Smith, D.; Tabb, D. L.; Tegeler, T. J.; Variyath, A. M.; Vega-Montoto, L. J.; Wahlander, A.; Waldemarson, S.; Wang, M.; Whiteaker, J. R.; Zhao, L.; Anderson, N. L.; Fisher, S. J.; Liebler, D. C.; Paulovich, A. G.; Regnier, F. E.; Tempst, P.; Carr, S. A. Multi-Site Assessment of the Precision and Reproducibility of Multiple Reaction Monitoring-Based Measurements of Proteins in Plasma. *Nat. Biotechnol.* **2009**, 27, 633-641.

5. Kingsmore, S. F. Multiplexed Protein Measurement: Technologies and Applications of Protein and Antibody Arrays. *Nat. Rev. Drug Discov.* **2006**, 5, 310-320.

6. Gygi, S. P.; Rist, B.; Gerber, S. A.; Turecek, F.; Gelb, M. H.; Aebersold, R. Quantitative Analysis of Complex Protein Mixtures using Isotope-Coded Affinity Tags. *Nat. Biotechnol.* **1999**, 17, 994-999.

7. Thompson, A.; Schafer, J.; Kuhn, K.; Kienle, S.; Schwarz, J.; Schmidt, G.; Neumann, T.; Johnstone, R.; Mohammed, A. K.; Hamon, C. Tandem Mass Tags: A Novel Quantification Strategy for Comparative Analysis of Complex Protein Mixtures by MS/MS. *Anal. Chem.* **2003**, 75, 1895-1904.

8. Ross, P. L.; Huang, Y. N.; Marchese, J. N.; Williamson, B.; Parker, K.; Hattan, S.; Khainovski, N.; Pillai, S.; Dey, S.; Daniels, S.; Purkayastha, S.; Juhasz, P.; Martin, S.; Bartlet-Jones, M.; He, F.; Jacobson, A.; Pappin, D. J. Multiplexed Protein Quantitation in Saccharomyces Cerevisiae using Amine-Reactive Isobaric Tagging Reagents. *Mol. Cell. Proteomics.* **2004**, 3, 1154-1169.

9. Xiang, F.; Ye, H.; Chen, R.; Fu, Q.; Li, L. N,N-Dimethyl Leucines as Novel Isobaric Tandem Mass Tags for Quantitative Proteomics and Peptidomics. *Anal. Chem.* **2010**, 82, 2817-2825.

10. Sohn, C. H.; Lee, J. E.; Sweredoski, M. J.; Graham, R. L.; Smith, G. T.; Hess, S.; Czerwieniec, G.; Loo, J. A.; Deshaies, R. J.; Beauchamp, J. L. Click Chemistry Facilitates Formation of Reporter Ions and Simplified Synthesis of Amine-Reactive Multiplexed Isobaric Tags for Protein Quantification. *J. Am. Chem. Soc.* **2012**, 134, 2672-2680.

11. Zhou, Y.; Shan, Y.; Wu, Q.; Zhang, S.; Zhang, L.; Zhang, Y. Mass Defect-Based Pseudo-Isobaric Dimethyl Labeling for Proteome Quantification. *Anal. Chem.* **2013**, 85, 10658-10663.

12. McShane, A. J.; Shen, Y.; Castillo, M. J.; Yao, X. Peptide Dimethylation: Fragmentation Control Via Distancing the Dimethylamino Group. *J. Am. Soc. Mass Spectrom.* **2014**, 25, 1694-1704.

13. Levin, Y. The Role of Statistical Power Analysis in Quantitative Proteomics. *Proteomics.* **2011**, 11, 2565-2567.

14. Yao, X.; Bajrami, B.; Shi, Y. Ultrathroughput Multiple Reaction Monitoring Mass Spectrometry. *Anal. Chem.* **2010**, 82, 794-797.

15. Yao, X. Derivatization Or Not: A Choice in Quantitative Proteomics. *Anal. Chem.* **2011**, 83, 4427-4439.

16. McShane, A. J.; Farrokhi, V.; Nemati, R.; Li, S.; Yao, X. An Overview of Quantitative Proteomic Approaches. Comprehensive Analytical Chemistry, Oxford, UK; Elsevier, **2014**; p. 111-135.

17. Collawn, J. F.; Matalon, S. CFTR and Lung Homeostasis. *Am. J. Physiol. Lung Cell. Mol. Physiol.* **2014**, 307, L917-23.

18. McShane, A. J.; Bajrami, B.; Ramos, A. A.; Diego-Limpin, P. A.; Farrokhi, V.; Coutermarsh, B. A.; Stanton, B. A.; Jensen, T.; Riordan, J. R.; Wetmore, D.; Joseloff, E.; Yao, X. Targeted Proteomic Quantitation of the Absolute Expression and Turnover of Cystic Fibrosis Transmembrane Conductance Regulator in the Apical Plasma Membrane. *J. Proteome Res.* **2014**, 13, 4676-4685.

19. Ong, S. E.; Blagoev, B.; Kratchmarova, I.; Kristensen, D. B.; Steen, H.; Pandey, A.; Mann, M. Stable Isotope Labeling by Amino Acids in Cell Culture, SILAC, as a Simple and Accurate Approach to Expression Proteomics. *Mol. Cell. Proteomics.* **2002**, 1, 376-386.

20. Lesch, H. P.; Kaikkonen, M. U.; Pikkarainen, J. T.; Yla-Herttuala, S. Avidin-Biotin Technology in Targeted Therapy. *Expert Opin. Drug Deliv.* **2010**, 7, 551-564.

Chapter 4

Peptide Dimethylation: Fragmentation Control via Distancing the Dimethylamino Group

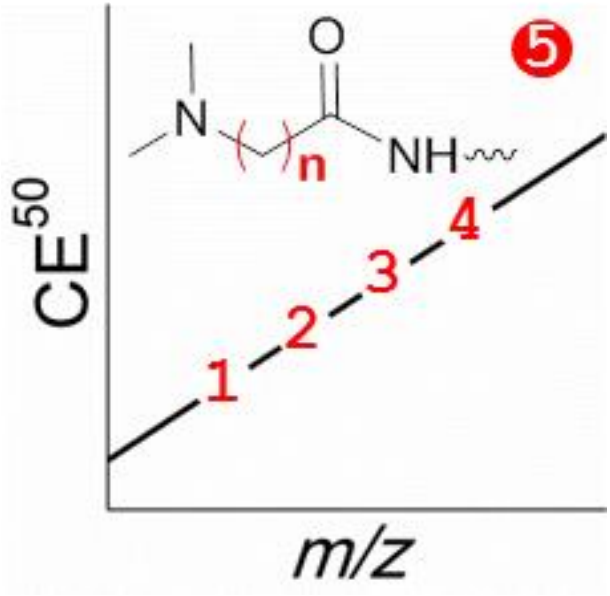

4.1 Introduction

The use of peptide derivatization is a staple of proteomic quantitation [1]. Derivatization-based mass spectrometry (MS) quantitation is characterized by its sample-throughput capabilities allowing multiple samples to be analyzed simultaneously. Different applications are dependent upon fragmentation control of the derivatized peptide. In applications of isobaric mass tagging reagents [1,2], the derivatized peptides are isobaric, but after fragmentation produce differentiable reporter ions in tandem MS (MS/MS) spectra. Peptide derivatization with these types of reagents are Type I active derivatizations (**Scheme 4.1**), classified by the strong signals directly observed from the fragmented derivatization group [3]. One significant pitfall of these reagents is the limited dynamic range, which is caused by all the derivatized peptides sharing common reporter ions; therefore, peptides with similar masses and elution time produce elevated background for the peptides in quantitation [4,5].

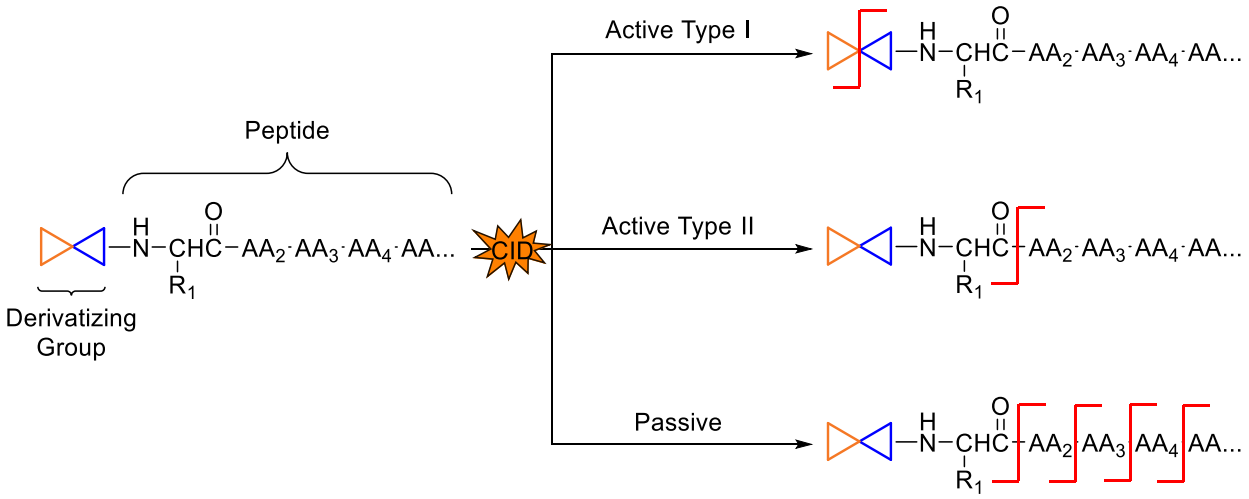

Scheme 4.1: Categorization of peptidyl chemical derivatizations.

Reductive methylation has been used as both mass-difference tagging for MS quantitation [6-8] and recently isobaric mass tagging for MS/MS quantitation [9-11]. Dimethylation is a relatively simple reaction only requiring a reducing agent and formaldehyde. This reaction is

expeditious without any substantial formation of side products. When stable isotope labels are used in the reducing agent and/or formaldehyde, peptides can be introduced with a designed number of stable isotope labels for MS-based quantitative measurements. This method has been broadly applicable due to its easy implementation [12].

The molecular basis for MS/MS quantitation of peptides with direct dimethylation is the facile collisional cleavage of the first N-terminal amino acid residues. Strong signals for derivatized a_1 ions (stable quaternary amine ions) are characteristic in MS/MS spectra of the derivatized peptides [13-15]. Dimethylation of peptides is considered a Type II active derivatization, where the derivatizing group promotes the cleavage of the first amide bond of peptides (**Scheme 4.1**). Collisional fragmentation of directly dimethylated peptides has been studied in detail [14,15]. When the methyl groups carry differential stable isotope labels, the derivatized peptides can, in principle, be quantified based on the correspondingly labeled a_1 ions. This quantitation using MS/MS measurement could be advantageous. These a_1 ions are peptide-specific and thus lessen the interference from co-eluting peptides experienced for peptides derivatized with isobaric mass tagging reagents. In order to observe such interference, derivatized peptides would need to have similar elution times and masses as well as the same first N-terminal amino acid residue; a rare occurrence. However, authentic quadrupole sampling of dimethylated peptide ions with different numbers of isotope labels as precursors can be problematic. Efforts have been made to develop an isobaric mass tagging capability using peptide dimethylation. One method derivatizes peptides at both N- and C-termini, but with complementary numbers of stable isotope labels. In this method, triplex isobaric peptide termini labeling with dimethylation, peptide precursors are isobaric and fragment ions carry differentiable stable isotope labels and thus the ion intensity of the fragments can be used for quantitation [9].

In line with recent advancements in the utilization of ultra-high resolving MS for proteomics, differences in mass defects of carbon, hydrogen, oxygen, and nitrogen isotopes have been exploited [10, 11, 16-19]. The scope of isobaric mass tagging is thus being expanded, opening exciting new opportunities in proteome quantitation. In principle, all of the currently practiced, derivatization-based quantitative proteomic methods can be adapted to better utilize contemporary mass spectrometers. Two recent reports use peptide dimethylation. Peptides in comparison carry derivatizing groups with different isotopologue labels, i.e., two atoms of ^{13}C versus ^{2}H. Therefore, during the low-resolution selection of precursor ions, the differentially-labeled peptides are co-selected authentically. However, when MS/MS are recorded with ultra-high resolving power, fragment ions can be baseline-separated for quantitation. Both works use Lys-C for protein digestion so that each resulting peptide carries two derivatizing groups. It is interesting to note that there are more derivatized y ions than b ions available to be used for quantitation [10,11]; in other words the ε-dimethylamino group on the lysine side chain at the peptide C-terminus is more stable than the α-dimethylamino group at the N-terminus.

Multiple reaction monitoring (MRM) MS is at the forefront of targeted, quantitative MS due to its high selectivity, sensitivity, and method robustness [20]. Stable isotope labeled references are commonly used to assemble methods for stable isotope dilution (SID) MRM MS. The generation of quantitation reference peptides can be achieved by derivatizing peptides with stable isotope labeled chemicals for mass-difference tagging [21,22]. Although the quantitation utility of the derivatized reference peptides can be comparable to those produced by metabolic labeling techniques [23], these reagents have yet to be broadly adopted. The limited adoption of the commercial reagents for MRM MS exemplifies a common problem for using active derivatizations of peptides for MRM-based MS quantitation: the derivatizing groups are not

efficiently held as intact mass tags for the precursor ions of the derivatized peptides or for their fragments.

MRM-based methods require the detection of strong signals for both precursor ions and fragment ions to obtain low quantitation limits. Furthermore, multiple distinguishable fragment ions are preferred to secure the method's specificity. If the derivatizing group is cleaved from the fragment ions, these fragments are no longer distinguishable among peptides with differential derivatizations. Therefore, MRM-based quantitation can benefit from passive derivatization of peptides (**Scheme 4.1**) [3]: during MRM analysis, derivatized peptides preserve the derivatizing groups on the intact peptide precursor ions in the ionization region of the instrument and keep these derivatizing groups on multiple fragment ions during fragmentation of the derivatized peptides in the collision cell. We hypothesize that if the dimethylamino group on derivatized peptides is disengaged from the adjacent amide bond, then a passive derivatization will be achieved for MRM-based peptide analysis. This derivatization will keep the increased gas-phase basicity of dimethylamino peptides, from the tertiary amine of the dimethylamino group, and accordingly the enhanced MS signals [24], but not activate particular peptide bonds in a biased manner. Herein, we present a systematic study of how diversely a dimethylamino group participates in collisional fragmentation of peptides with the increased distance from the first N-terminal amino acid residue. In addition, the change of role for the dimethylamino group from an active participant in fragmentation to a passive mass tagging one is reported.

4.2 Experimental

4.2.1 Chemicals

2-aminoacetic acid (>99%), 3-aminopropanoic acid (99%), 4-aminobutanoic acid (>99%), 5-aminopentanoic acid (>97%), 6-aminohexanoic acid (>99%), methanol (>99.9%), diethyl ether

(>99%), glacial acetic acid (>99.7%), N,N-diisopropylethylamine (99.5%, DIEA), N-hydroxysuccinimide (98%, NHS), dimethyl sulfoxide (>99.7%, DMSO), anhydrous N,N-dimethylformamide (>99.8%, DMF), 4-(4,6-dimethoxy-1, 3, 5-triazin-2-yl)-4-methylmorpholinium chloride (≥96.0%, DMTMM), N- (3-dimethylaminopropyl)-N'-ethylcarbodiimide hydrochloride (≥98.0%, EDC), and anhydrous dichloromethane (>99.5%, DCM) were purchased from Sigma-Aldrich (St. Louis, MO). Formic acid (88% and 99.5%), trifluoroacetic acid (97%, TFA), acetonitrile (99.9%, ACN), and formaldehyde (37%) were purchased from Fisher (Hanover Park, IL). Concentrated hydrogen chloride acid (36.5% - 38%) was purchased from J.T. Baker (Center Valley, PA). N, N'-diisopropylcarbodiimide (99%, DIC) was purchased from Alfa Aesar (Ward Hill, MA). The ultrapure water was obtained from a Direct-Q 3 UV water purification system (EMD Millipore, Billerica, MA). The peptides LSLVPDSEQGEAILPR (95%), LSEPAELTDAVK (99%), YGGFLR (98%), and SVILLGR (99%) were purchased from Peptide 2.0 (Chantilly, VA). The peptide NSILTETLHR (95%) was purchased from Anaspec (Fremont, CA). The isotopic peptide SVIL[L-$^{13}C_6{}^{15}N$]GR (99%) was purchased from Thermo Fisher (Rockford, IL).

4.2.2 Dimethylamino acid synthesis

Each amino acid (8 mmol) was dissolved in formic acid (5 mL, 88%) and formaldehyde (1 mL). The synthesis of 3-(dimethylamino)-propanoic acid (denoted as dim-3), 4-(dimethylamino)-butanoic acid (denoted as dim-4), 5-(dimethylamino)-pentanoic acid (denoted as dim-5), and 6-(dimethylamino)-hexanoic acid (denoted as dim-6) was carried out in a microwave reactor (CEM Discover-S, Matthews, NC), with the following conditions: 100 W, 110 °C, 20 to 120 min. 2-(Dimethylamino)-acetic acid (denoted as dim-2) was conventionally refluxed at 100 °C for 1 hour. Concentrated HCl (1 mL) was added after heating. The solvent was dried *in vacuo*. After drying,

a white precipitate was obtained and washed with glacial acetic acid (5 mL) three times. The dimethylamino acid was then recrystallized with methanol and diethyl ether. After purification, the reagents were characterized with nuclear magnetic resonance (NMR) spectroscopy (Avance III 400 MHz, Bruker, Billerica, MA) and high-resolution MS (AccuTOF™ DART, JEOL, Peabody, MA, USA). Detailed syntheses and characterizations can be found in **Appendix-1 Text A1.1-A1.5**.

4.2.3 Peptide derivatization

The dimethylamino acid (1.0 equivalent), NHS (1.2 equivalents), and DIC (1.0 equivalent) were first dissolved in DMSO, and then diluted with anhydrous DCM. The solution was incubated overnight at room temperature. A solution containing five peptides, NSILTETLHR, LSLVPDSEQGEAILPR, LSEPAELTDAVK, YGGFLR, and SVILLGR dissolved in 10% DIEA/DMF, was added to the activated dimethylamino acid. The solution was incubated overnight at room temperature. The coupling was then quenched with 20% formic acid/H_2O on ice. The solution was first dried with a speed-vac (Savant SC100, Thermo Fisher) then lyophilized (Labconco FreeZone Plus, Kansas City, MO, USA). After drying, the sample was desalted via an empty spin column (Thermo Fisher) packed with hydrophilic-lipophilic-balanced (HLB, Oasis®, Waters, Milford, MA, USA) reversed-phase sorbent. The sample was then dried and reconstituted with FA/H_2O for liquid chromatography (LC)-MS analysis (Shimadzu HPLC pumps/controller, Kyoto, KYT, Japan and HTC PAL autosampler, Carrboro, NC).

4.2.4 LC-MS and LC-MS/MS studies

A 10 cm, 1.0 mm I.D. Hypersil Gold HPLC column (Thermo Fisher Scientific, Inc., USA) with 175 Å, 3 μm C18resin was used. Solvent A was composed of 98.8% H_2O, 1.0% ACN, and 0.2% FA and solvent B was 98.8% ACN, 1.0% H_2O, and 0.2% FA. The LC gradient was 5% to

35% solvent B for 45 minutes. The column temperature was 60 °C. The hybrid mass spectrometer used was a QSTAR® Elite (AB Sciex, Framingham, MA). Positive electrospray ionization (ESI) was used, with parameters of 5.5 kV for the spray voltage and source temperature of 300 °C. The initial collision energies (CE) for the doubly- and triply-charged peptides were obtained from **Equations 4.1** and **4.2**, respectively [25].

Equation 4.1: $CE = (0.057 \times m/z) - 4.265$

Equation 4.2: $CE = (0.031 \times m/z) + 7.082$

These equations were empirically adjusted for the non-derivatized peptides (**Appendix-1 Table A1.1**), and for dim-2-peptides (**Appendix-1 Table A1.2**). The new equations from the dim-2-peptides were applied to the dim-3- through dim-6-peptides.

4.2.5 Energy resolved (ER)-MS studies

An AB SCIEX 4000 QTRAP® (AB SCIEX, Framingham, MA) triple quadrupole mass spectrometer with direct syringe infusion of the sample solutions was used for the ER-MS studies. The ESI was in positive mode with parameters of 5.5 kV for the ion spray and a source temperature of 200 °C. Each peptide (500 fmol/µL) was individually infused with a flow rate at 5 µL/min. The DP was optimized before the collision studies were started. The CE was ramped from 5 to 40 V in 0.5 V/s increments. The resolution was set to unit for Q1 and high for Q3. The dwell time was 200 msec. Three replicates were taken for each peptide measured (non-derivatized YGGFLR through dim-6-YGGFLR).

4.3 Results and discussion

4.3.1 Microwave-assisted synthesis of dimethylamino acids

The established Eschweiler-Clarke reaction [26,27] was used to dimethylate the primary amines of five amino acids: 2-aminoacetic acid, 3-aminopropanoic acid, 4-aminobutanoic acid, 5-

aminopentanoic acid, and 6-aminohexanoic acid. They have increasing numbers of methylene groups, one through five (dim-2 through dim-6, respectively), distancing the amino group from the carboxylic acid. Full conversion of 3-aminopropanoic acid to dim-3 required 8 hours of conventional refluxing. Other amino acids were even less reactive towards amine dimethylation. In an attempt to expedite the dimethylation of 3-aminopropanoic acid to 6-aminohexanoic acid, microwave irradiation was utilized. All of the initial five substrates were converted to the corresponding products within 20 to 120 minutes of irradiation (**Appendix-1 Text A1.1-A1.5**).

4.3.2 Preparation of dimethylamino peptides

Five synthetic peptides were used as models to investigate collisional fragmentation mechanisms of dimethylated peptides: NSILTETLHR, LSLVPDSEQGEAILPR, LSEPAELTDAVK, YGGFLR, and SVILLGR. They possess a wide variety of properties (**Appendix-1 Table A1.3**). Peptide LSEPAELTDAVK was chosen as a model peptide for lysine-containing peptides, which have two primary amines. Tandem mass spectra for these non-derivatized peptides are shown in **Appendix-1 Figures A1.1a-A1.1f**.

Peptidyl amino groups on the model peptides were derivatized with dimethylamino acids whose carboxylic groups were activated *in situ* (**Scheme 4.2**). The activation of carboxylic groups was mediated by DIC and NHS. Solvent played a dominating role in this peptide derivatization. The dimethylamino acids were soluble in aqueous solution. However, derivatization of the peptides using water-soluble mediation reagents, including EDC/NHS and DMTMM, resulted in low and varying yields for the derivatization products. A mixed solvent of DMSO and DCM served well for activating the dimethylamino acids using DIC/NHS. This solvent system was miscible with the mixture of DIEA and DMF, which was used as the solvent for preparing peptide solutions for derivatization.

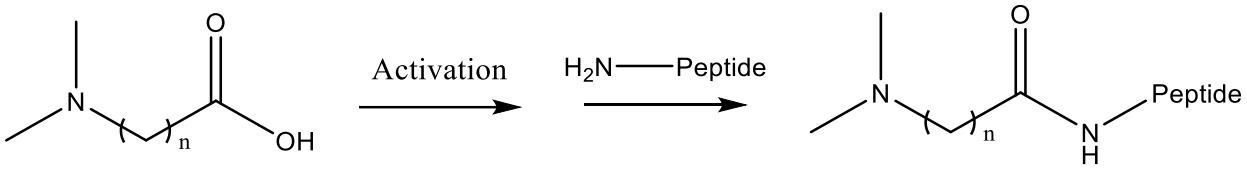

n = 1 for dim-2, 2 for dim-3, 3 for dim-4, 4 for dim-5, and 5 for dim-6

Scheme 4.2: General reaction for derivatizing peptidyl amines with dimethylated amino acids.

4.3.3 MS signal enhancement of dimethylamino peptides

The percentage of chemical conversion (PCC) and signal yield for mass spectrometry (SYMS) were quantitatively measured for peptides dim-2-SVILLGR through dim-6-SVILLGR. After quenching the derivatization reaction, an equal amount of isotopically labeled SVIL[L-$^{13}C_6{}^{15}N$]GR was added as the quantitation reference, although GSVIL[L-$^{13}C_6{}^{15}N$]GR would be a closer reference. The MS signal for the residual unreacted SVILLGR, compared to that for the isotopic quantitation reference, allowed for calculation of the PCC value for each derivatization. The average PCC for all five derivatizations of SVILLGR was 85% (**Appendix-1 Equation A1.1**). Further optimization of derivatization reactions was not performed in this work, because these reactions were used to generate sufficient amounts of dimethylated peptides for mechanistic investigations not to be directly applied for proteome quantitation. The SYMS value for a derivatization was calculated based on the MS signal of the derivatized peptide, e.g., dim-2-SVILLGR, and that of the isotopic quantitation reference. The average SYMS for all five derivatized peptides was 170% (**Appendix-1 Equation A1.2**). This average SYMS was further corrected for the derivatization completeness (or average PCC), giving an adjusted SYMS of 200% (**Appendix-1 Equation A1.3**), for the addition of dimethylamino acids to the N-terminus of SVILLGR.

The enhanced MS signal for the derivatized peptides can be attributed to the increased gas-phase basicity, compared to the underivatized SVILLGR. These derivatizations convert a primary

N-terminal amino group to a tertiary amine which is more basic and results in more favorable protonation in the gas phase. Signal enhancement of 130% to 240% was also reported for peptides with dimethylated lysine side chains, compared to their non-dimethylated counterparts [24]. The increased basicity of peptides carrying the dimethylamino group is likely also attributing to the charge-state shift from a mixture of singly- and doubly-charged ions for SVILLGR and YGGFLR to the mostly doubly charged for their derivatized counterparts, and predominantly doubly-charged LSLVPDSEQGEAILPR to a doubly and triply-charged mixture (**Appendix-1 Figure A1.7a-A1.7c**). The coalescence to doubly-charged SVILLGR from the singly- and doubly-charged mixture could also attribute to the increase in SYMS.

4.3.4 Fragmentation dependence of dimethylamino peptides on alkyl chain length

Tandem MS was performed on a QqTOF mass spectrometer for all of the derivatized peptides. The derivatized YGGFLR peptides are used as the exemplary peptides for discussion, with all others in the SI (**Appendix-1 Figures A1.1-A1.6**). The CE was empirically adjusted using **Equations 4.1** and **4.2** to ensure proper fragment ion production. The dim-2-peptides were used for the empirical adjustment, and the CE was increased by 1.1 to 1.5 times, compared to the suggested values from the equations (**Appendix-1 Table A1.3**). The CE was adjusted until an approximate <10% precursor ion was observed after collision-induced dissociation (CID). **Equations 4.1** and **4.2** were then corrected accordingly for other dimethylamino peptides. As shown in **Scheme 4.3**, fragment ions are denoted with typical nomenclature except for the following: (1) b and a ions carrying the derivatizing group are denoted as *b and *a respectively, (2) b and a ions carrying a cyclization product of the derivatizing group are denoted as ^{c}b and ^{c}a respectively, (3) ions from the bond cleavage between the α and β carbon from the dimethylamino group is denoted as f_1, (4) b and a ions carrying an acetyl group (the complementary products

from the α-β cleavage) are denoted as ^{a}b and ^{a}a, respectively, and (5) the ions from the amide bond cleavage between the derivatizing group and the original N-terminus of the peptide is denoted as f_2, and the corresponding production of the singly-charged ion as the original peptide is denoted as ^{o}M. A general trend of the increased coverage of b and derivatized b ions was observed for the derivatized peptides compared to their underivatized counterparts (**Appendix-1 Figures A1.1-A1.6**) [6].

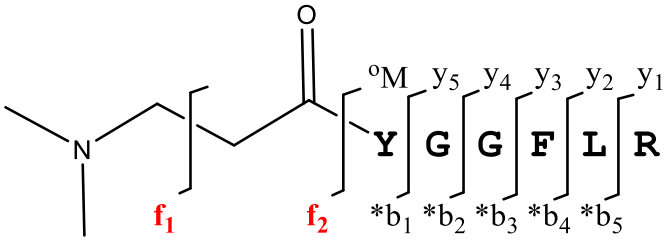

Scheme 4.3: Nomenclature of fragment ions as represented by dim-3-YGGFLR.

Dim-2 derivatization results in peptides with the same chemical structure as peptides with direct reductive dimethylation; collisional fragmentation mechanism for the directly methylated peptides has been studied in detail (**Scheme 4.4a**) [14,15]. For instance, dim-2-YGGFLR (MS/MS spectrum shown in **Figure 4.1**) is the same as dimethylated GYGGFLR. Dimethylated peptides are known to produce enhanced signals for *a_1 ions [13-15]. In the nomenclature system used in this paper, the f_1 ion was observed for dim-2-YGGFLR (or *a_1 for dimethylated GYGGFLR) at *m/z* 58.06 (**Figure 4.1**; **Scheme 4.4**). Generation of f_2 ions (or *b_1 for dimethylated GYGGFLR) at *m/z* 86.20 can be accounted for by the oxozolium mechanism [28] or the aziridin-2-one pathway (**Scheme 4.4b**) which further produces the f_1 ion [29]. Generation of f_2 ions suggests the favorable protonation of the dimethylamino group and a facile intramolecular proton transfer to activate the adjacent amide group in the derivatized peptides (**Scheme 4.4b**). In other words, there is an active participation of the derivatizing group in the peptide fragmentation.

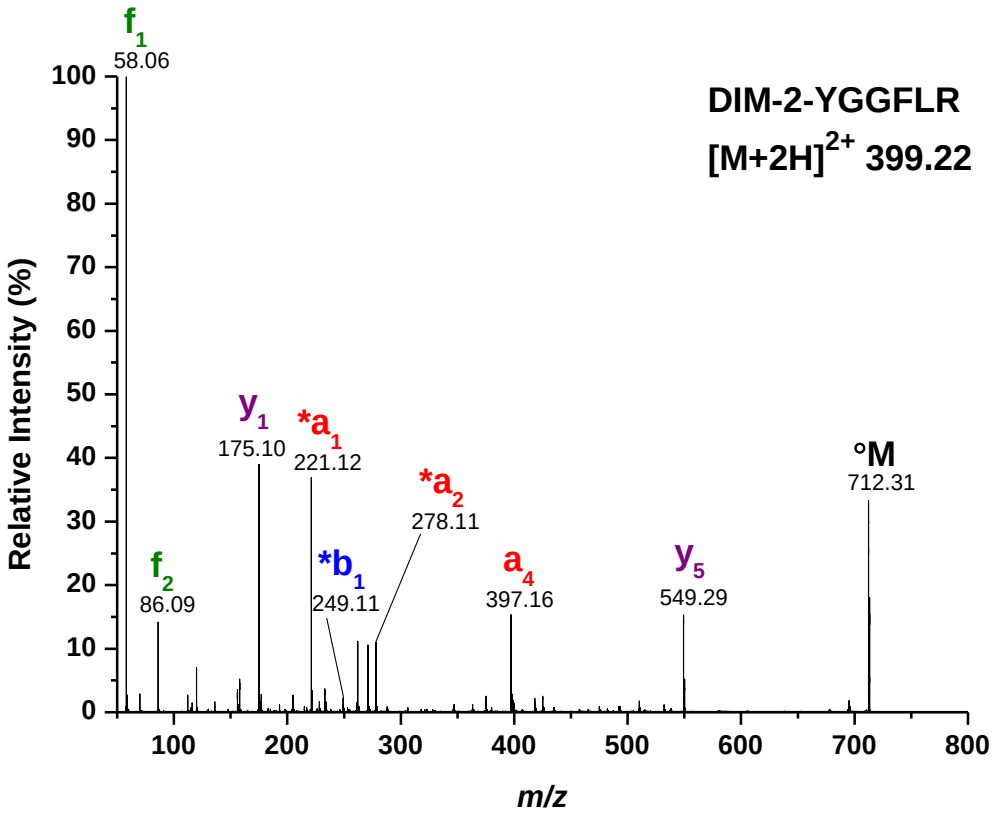

Figure 4.1: MS/MS spectrum of dim-2-YGGFLR.

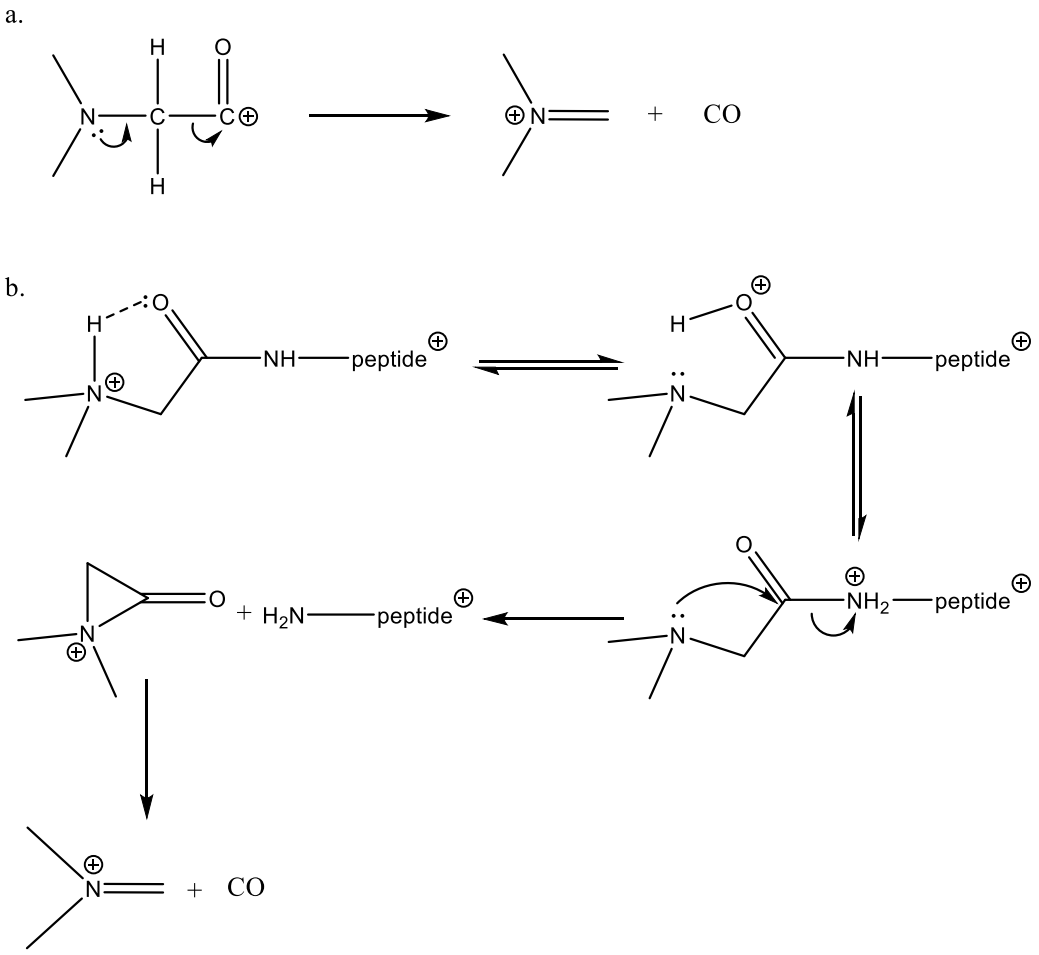

Scheme 4.4: Mechanism of f_1 production from dim-2 derivatized peptides.

Dim-3 derivatization extends the distance by one additional methylene group between the dimethylamino group and the first amide group on the derivatized peptides, which is formed upon the attachment of a dimethylamino propionic acid. Two intense ions at *m/z* 58.06 (f_1) and *m/z* 754.36 $[MH\text{-}f_1]^+$ were observed for dim-3-YGGFLR, together with significant signals for acetyl b ions ($^a b_1$, $^a b_2$, $^a b_3$, and $^a b_4$), shown in **Figure 4.2**. The sum of *m/z* 58.06 and *m/z* 754.36 made up the mass balance for dim-3-YGGFLR, suggesting the existence of a labile bond. Generation of these 2 ions can be readily explained by the McLafferty-type rearrangement (**Scheme 4.5**) [30]. It should be noted that although the ion structure for f_1 ions for dim-2-peptides and dim-3-peptides are the same, mechanisms for the ion generation are different (**Schemes 4.4** and **4.5**). In general, the f_1 ion

was observed for all dim-3 peptides (**Figure 4.2** and **Appendix-1 Figure A1.3**). On the other hand, not all of the corresponding $[MH\text{-}f_1]^+$ ions were observed (**Appendix-1 Figure A1.3**), which could be due to further breakage of the primary $[MH\text{-}f_1]^+$ fragment ions under experimental conditions. According to the categorization of peptide derivatization shown in **Scheme 4.1**, the dim-3 reaction would be classified as a Type I active derivatization, where there is preferential cleavage within the derivatizing group.

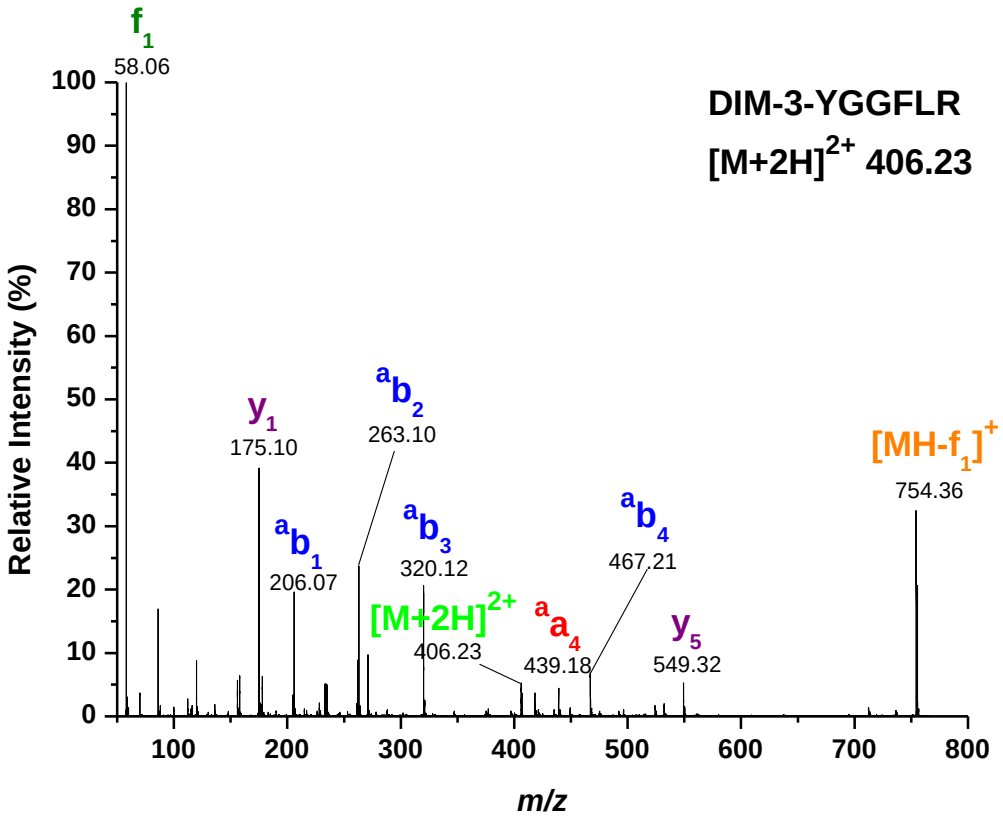

Figure 4.2: MS/MS spectrum of dim-3-YGGFLR.

A common, neutral loss of dimethylamine was observed for doubly-charged ions of dim-4-, dim-5-, and dim-6-YGGFLR, producing corresponding doubly-charged fragments (**Scheme 4.6**). Dim-4 derivatization produced a very strong fragment ion at *m/z* 390.75 (cyc^{2+}, **Figure 4.3**). Dim-5-YGGFLR gave a doubly-charged ion at *m/z* 397.73 (cyc^{2+}) as the most intense fragment (**Figure 4.4**). These two ions are proposed as YGGFLR carrying an imido lactone at the N-

terminus (**Scheme 4.6**). A complement of b and a ions carrying the imido lactone, i.e., ^{c}b and ^{c}a ions, were observed for dim-4- and dim-5-YGGFLR. Formation of these ions can be explained by nucleophilic substitution of the amide oxygen to the α-methylene carbon of the dimethylamino group (**Scheme 4.6**). Similar mechanisms were reported in a fragmentation study of lysylglycine [31] and used for explaining the charge mobilization of peptides derivatized with a quaternary amine [32] and loss of dimethylamine from N^{ε}-dimethyllysine [33]. Dim-6-YGGFLR produced a similar cyclization product at *m/z* 404.72 (cyc^{2+}, **Figure 4.5**), but at a much reduced intensity and without observable complementary ^{c}a and ^{c}b ions. The intensity differences could be related to the stability of imido lactone rings.

Doubly-charged dim-6-YGGFLR, compared to dim-4- and dim-5-YGGFLR, produced full series of *a and *b ions carrying the derivatization group, together with y ions (**Figures 4.3-4.5**). This suggests that in the dim-6-peptide the preferential cleavage via the mechanism in **Scheme 4.5** becomes much less competitive. In other words, the dim-6 derivatization is passive (**Scheme 4.1**). Similar results were also observed for other dim-6 derivatized peptides (**Appendix-1 Figure A1.6**). It is also interesting to note that the intensity for the residual doubly-charged precursor was high (**Figure 4.5**), using the collision energy obtained from the same calculation as those for other derivatized peptides (**Appendix-1 Table A1.2**), dim-2-YGGFLR through dim-5-YGGFLR.

Double derivatization of LSEPAELTDAVK was obtained at both the N-terminus and the lysine side chain. For example, dim-4-LSEPAELTDAVK (**Appendix-1 Figure A1.4d**) produced fragments that corresponded to the cyclization occurring at both sites. The first cyclization product (m/z 727.45) was 80% relative intensity and the second (m/z 704.90) was 30% relative intensity. In comparison, one cyclization product (m/z 741.43) was observed for dim-5-LSEPAELTDAVK

at 15% relative intensity (**Appendix-1 Figure A1.5e**), which reports the bond cleavage at the N-terminus.

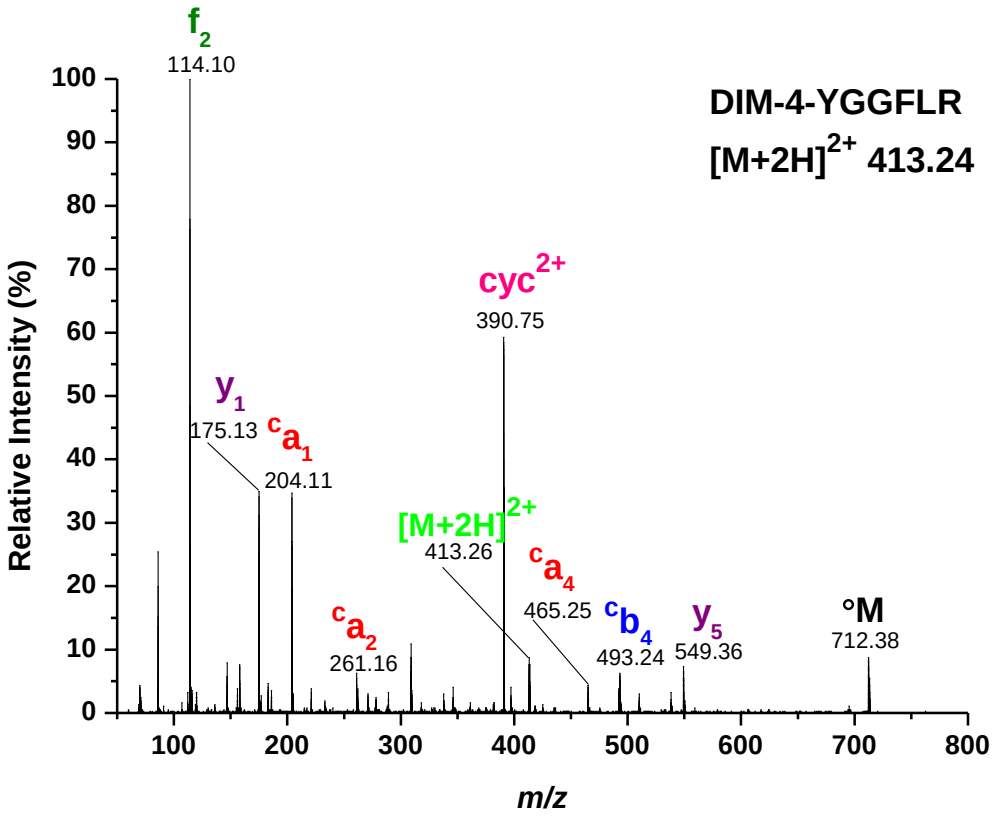

Figure 4.3: MS/MS spectrum of dim-4-YGGFLR.

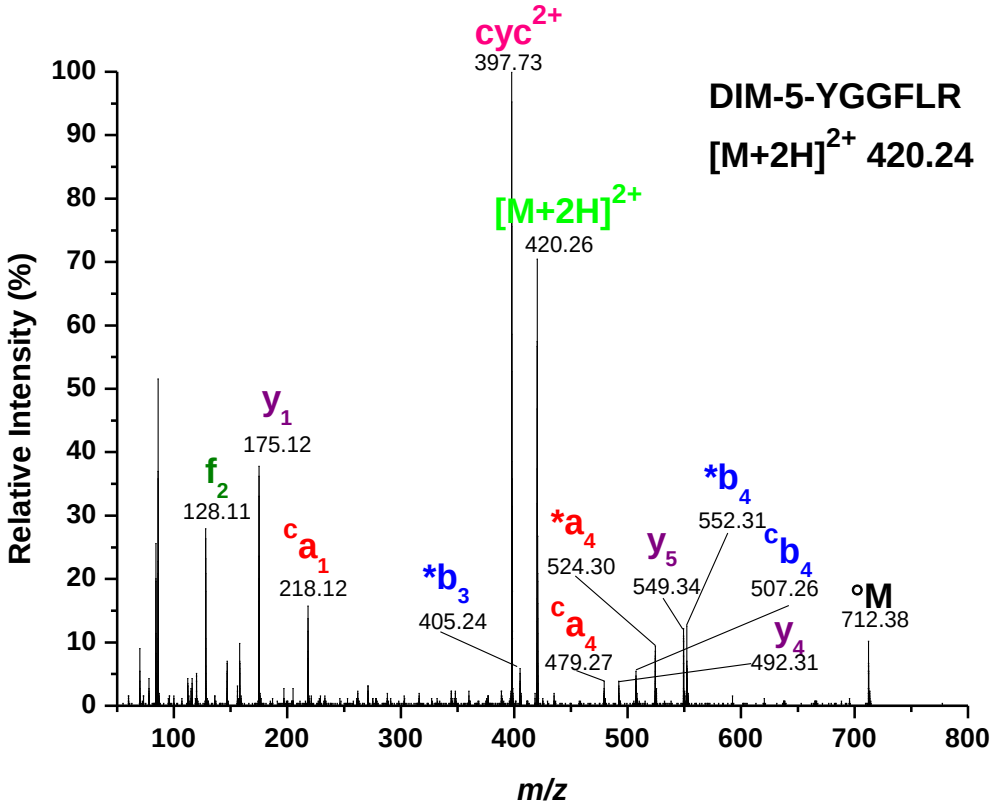

Figure 4.4: MS/MS spectrum of dim-5-YGGFLR.

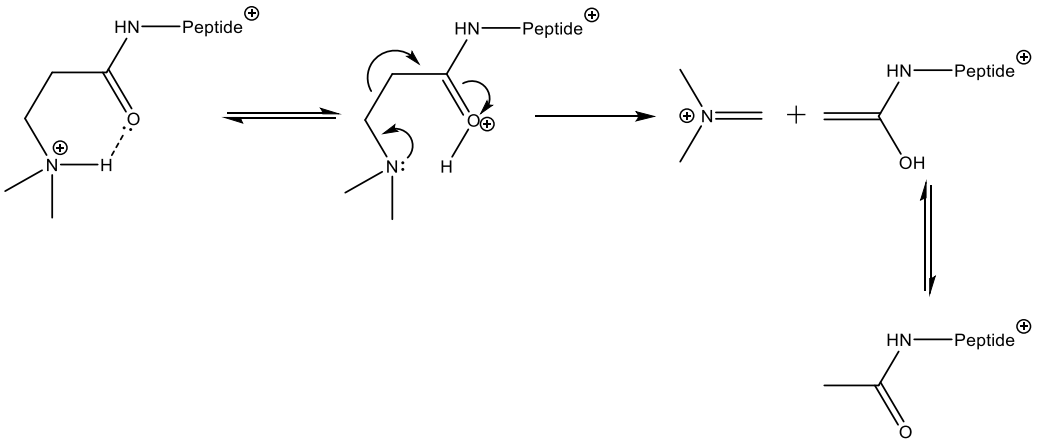

Scheme 4.5: Mechanism of f_1 production from dim-3 derivatized peptides.

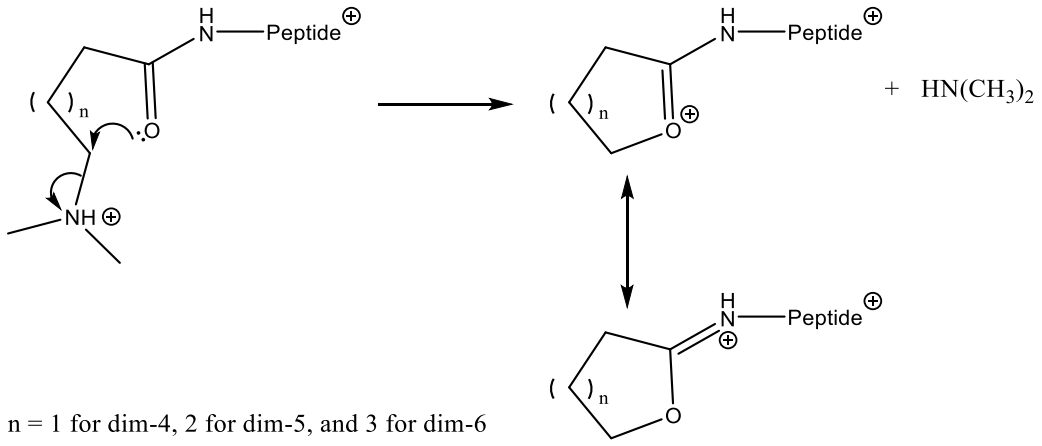

Scheme 4.6: Imido lactone formation at the N-terminus of dim-4-, dim-5-, and dim-6-YGGFLR.

4.3.5 Another preferential cleavage pathway of dim-4-, dim-5-, and dim-6-Peptides

Two ions related to cleavage of the derivatizing group from the doubly-charged dim-4-YGGFLR precursor were observed; one dominantly at *m/z* 114.10 (f_2) and the other strong ion at *m/z* 712.38 (^oM, **Figure 4.3**). Dim-5-YGGFLR and dim-6-YGGFLR, cleaving at the same amide bond, also produced ion pairs at *m/z* 128.15 and 712.38 and at *m/z* 142.12 and 712.34, respectively. However, the relative ion intensities for the corresponding f_2 ions, although strong, were not dominantly high for dim-5- and dim-6-YGGFLR (**Figures 4.4 and 4.5**). The favorable cleavage of the amide bond can be accounted for by the mechanism proposed in **Scheme 4.7**. The intensity differences among these ions are on the same order of the facility for intramolecular proton transfer, requiring the formation of a pseudo ring of 7, 8, or 9 atoms, with the increasing entropy penalty. Although dim-2- and dim-3-peptides have a more facile intramolecular proton transfer through a pseudo 5- or 6-membered ring (**Schemes 4.4b** and **4.5**), the nucleophilic attack of the deprotonated dimethylamine to the carbon of protonated amide would experience high ring constraints; the generation of similar f_2 ions would require the formation of a ring with three or four atoms following the mechanism in **Scheme 4.7**. Protonated aziridin-2-ones, however, are viable intermediates for a_1 ions of peptides upon collisional dissociation (**Scheme 4.4b**) [29].

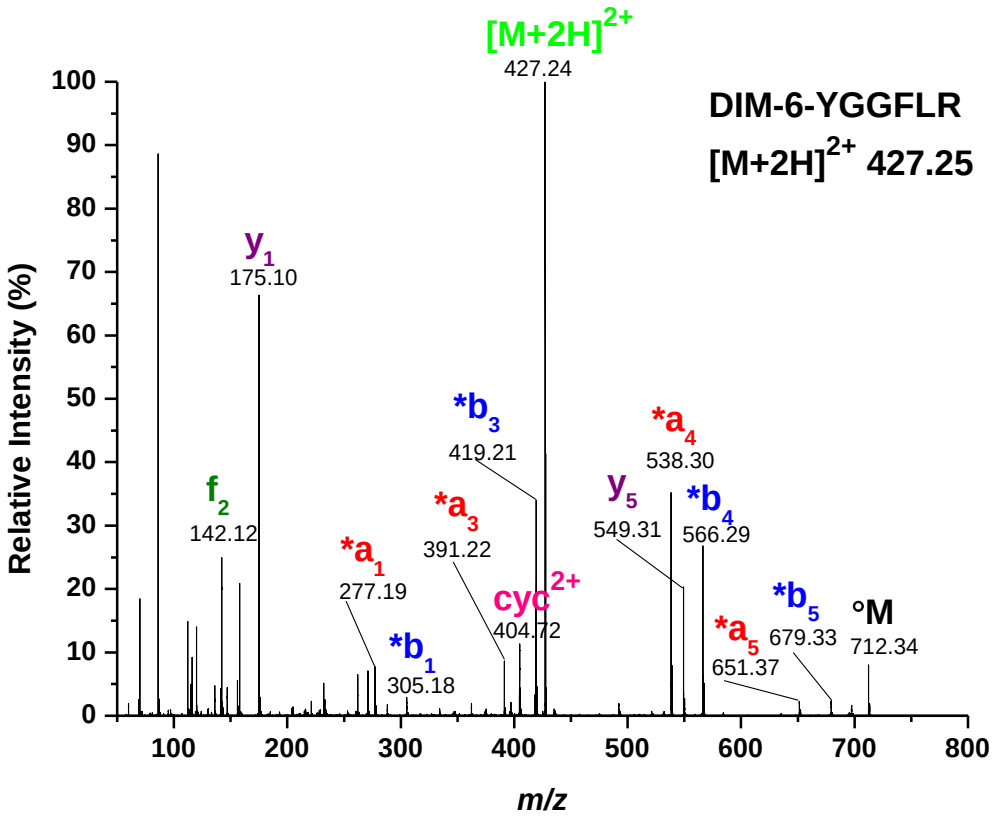

Figure 4.5: MS/MS spectrum of dim-6-YGGFLR.

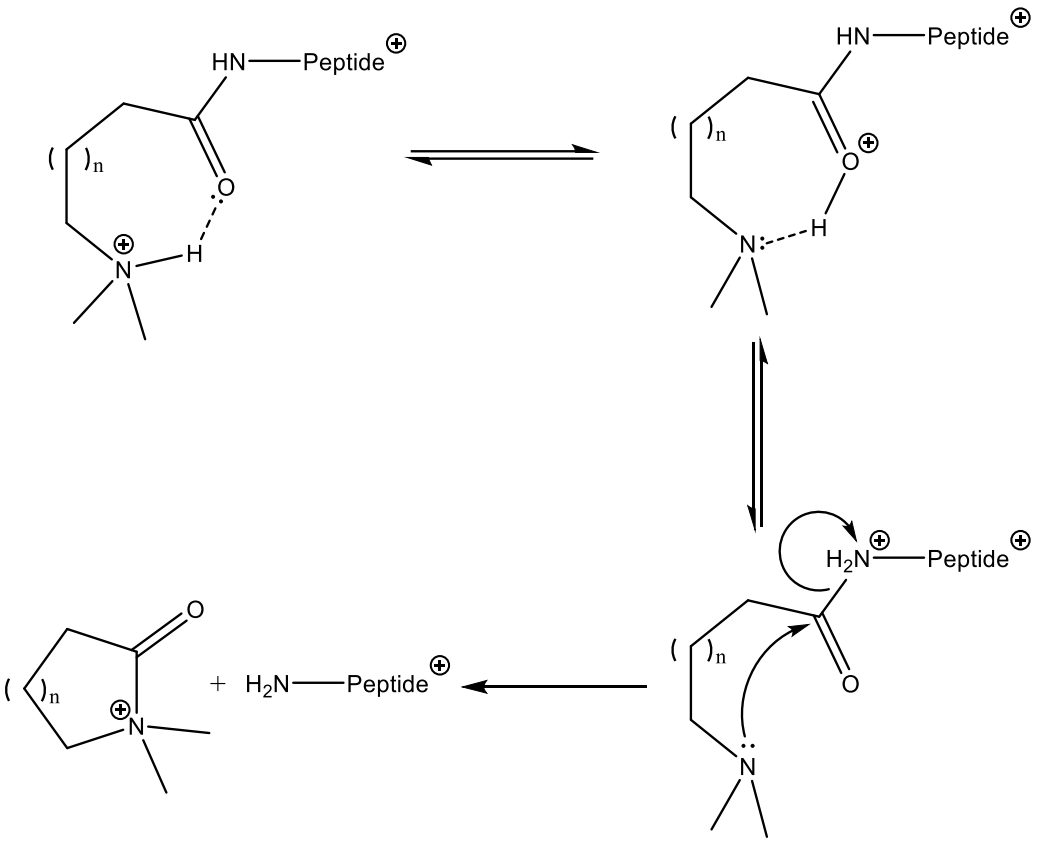

n = 1 for dim-4, 2 for dim-5, and 3 for dim-6

Scheme 4.7: N,N-Dimethyl lactam ion loss from dim-4-, dim-5-, and dim-6-YGGFLR.

4.3.6 ER-MS to categorize peptides into active and passive derivatization groups

ER-MS is an excellent tool to evaluate the energy requirements for the generation of fragment ions and elucidation of fragmentation patterns and mechanisms [28]. ER-MS was performed for YGGFLR and dim-2- through dim-6-YGGFLR. The CE profiles, in the laboratory frame, for the breakdown of the derivatized peptides were recorded on a triple quadrupole instrument. After normalization to the initial precursor ion intensity, triplicate measurements were combined as a single data set for sigmoidal dose-response fitting to produce the survival curve (**Figure 4.6**), giving a CE value at 50% (CE^{50}) of residual precursor ions. Fitting plots for all of the six YGGLFR peptides are shown in **Appendix-1 Figure A1.8** and the formulae and the goodness of fitting are reported in **Appendix-1 Table A1.4**. CE^{50} values for these peptides were

plotted against *m/z* values of doubly-charged precursor ions (**Figure 4.7**). Dim-2-, dim-3-, dim-4-, and dim-5-YGGFLR correlated linearly with a slope of 0.153 and adjusted R^2 of 0.9994. Together with the fact that different pathways operate to preferentially produce f_1 and/or f_2 ions and their complementary fragment ions (**Schemes 4.4-4.7**), this linear correlation suggests that these different mechanisms result in minimal differential effects on CE required for the breakage of doubly-charged precursor ions.

The underivatized YGGFLR showed positive deviation of 1.81 volts from the linear correlation (**Figure 4.7**). This deviation signifies the peptide as a mechanistic indicator, reporting that there is no special bond in the peptide which is particularly labile to gas-phase collision. The same is true for the positive deviation of 2.59 volts for dim-6-YGGFLR (**Figure 4.7**). Although dim-4- to dim-6-YGGFLR share a common fragmentation pathway releasing the derivatizing groups as N,N-dimethyl lactams (**Scheme 4.7**), the increased distance between the dimethylamino group and the amide bond formed upon the peptide derivatization leads to a discrete increase in the stability of intact precursors from dim-5- to dim-6-YGGFLR, shown as the positive deviation (**Figure 4.7**). This agrees with the observation that the ε-dimethylamino group on the lysine side chain is a passive mass tag (**Appendix-1 Figure A1.2e**), stable to collisional fragmentation in the gas phase [10,11].

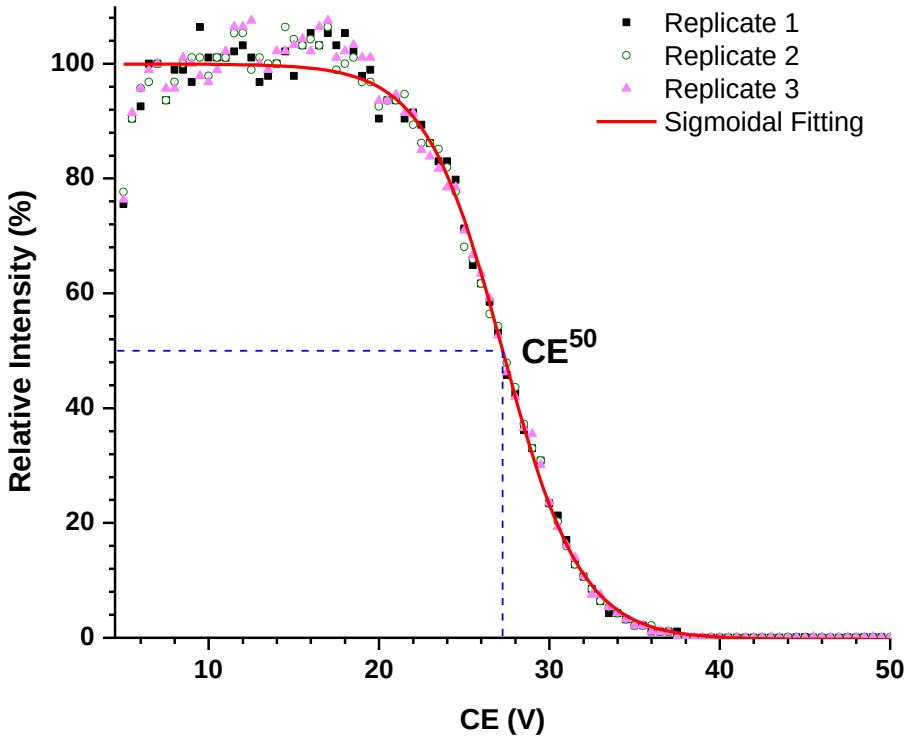

Figure 4.6: Survival curve of dim-6-YGGFLR. The precursor was selected in Q1 and Q3 with the CE being ramped from 5 to 35 volts in 0.5 V/s increments. Three replicates were obtained for each YGGFLR peptide, and the data was normalized to the maximum intensity. After sigmoidal dose-response fitting the CE^{50} was obtained.

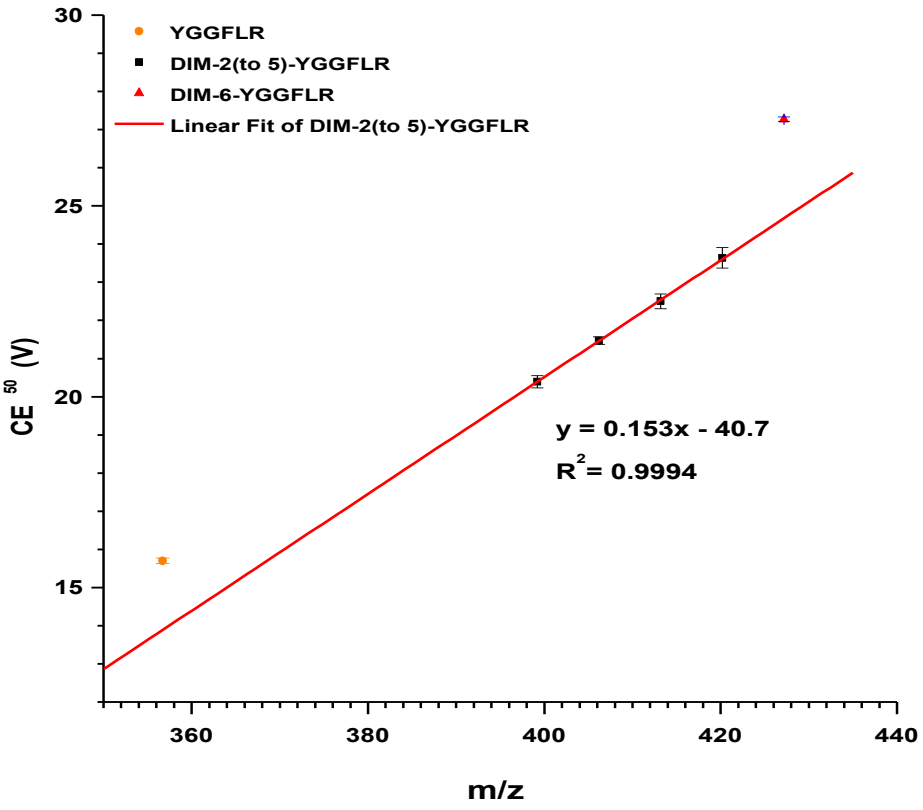

Figure 7: CE^{50} and *m/z* Correlation for Dimethylamino YGGFLR Peptides

4.3.7 Two routes for selective activation of dimethylamino peptides

There are two general mechanisms for a derivatizing group actively participating in preferential fragmentations around the N-termini of derivatized peptides. Both start from the preferential protonation of the dimethylamino group. This proton then either: (1) transfers to the adjacent amide group acting as an acid catalyst to facilitate fragmentation reactions (the mobile-proton regime) as in **Schemes 4.4b**, **4.5**, and **4.7**, or (2) directly polarizes the α-methylene carbon of the protonated dimethylamino group for the nucleophilic substitution by the adjacent amide oxygen (the charge-directed regime) as in **Scheme 4.6**. Proton migration from basic amino acids, including histidine, lysine, and arginine, has been shown to promote preferential neighboring cleavages [34-36]. The first general mechanism also operates in the preferential fragmentation of peptides derivatized with isothiocyanates [37,38]. The importance of the intramolecular proton

transfer is evident in this study. When the intramolecular proton transfer becomes less favorable for dim-6-YGGFLR, the preferential activation of the adjacent amide bond diminishes and so do the subsequent fragmentation products. In comparison, proton transfer from non-methylated ε-amine at the peptide N-terminus faces competing paths due to the complex intramolecular solvation of the protonated amine group [39]; therefore activation of the first amide group via acid catalysis confronts similar competitions.

For the second general mechanism, although activation of the α-methylene carbon of the protonated dimethylamino group stays the same more or less, the direct nucleophilic substitution by the amide oxygen becomes less entropically favorable with the distancing of the protonated dimethylamino group from the neighboring amide. Succinctly, a quantized change happens from dim-5-YGGFLR to dim-6-YGGFLR or from active derivatization to passive derivatization (**Scheme 4.1**).

4.4 Conclusion

Reagents for quantitative MS are essential tools in proteomic technologies. Full utilization of contemporary MS advancement requires a clear appreciation of chemical principles governing the gas-phase fragmentation of derivatized peptides [40]. In certain applications, *active* cleavage of the derivatizing group is preferred to produce quantitative reporter ions and simple spectra of sequence ions for concurrent peptide identification; common examples are proteomic peptides derivatized with tandem mass tagging reagents. In other applications like MRM MS, it is advantageous to have the derivatizing group associated with multiple fragment ions. This requires a derivatizing group staying *passive* as a ubiquitous mass tag during fragmentation processes of derivatized peptides [3]. Understanding the underlying principles of gas-phase chemistry of

derivatized peptides, as revealed by the investigational reagents in this study, can guide rational design of novel reagents for quantitative MS.

4.5 References

1. Yao, X. Derivatization Or Not: A Choice in Quantitative Proteomics. *Anal. Chem.* **2011**, 83, 4427-4439.

2. Ross, P. L.; Huang, Y. N.; Marchese, J. N.; Williamson, B.; Parker, K.; Hattan, S.; Khainovski, N.; Pillai, S.; Dey, S.; Daniels, S.; Purkayastha, S.; Juhasz, P.; Martin, S.; Bartlet-Jones, M.; He, F.; Jacobson, A.; Pappin, D. J. Multiplexed Protein Quantitation in Saccharomyces Cerevisiae using Amine-Reactive Isobaric Tagging Reagents. *Mol. Cell. Proteomics.* **2004**, 3, 1154-1169.

3. Shi, Y.; Bajrami, B.; Yao, X. Passive and Active Fragment Ion Mass Defect Labeling: Distinct Proteomics Potential of Iodine-Based Reagents. *Anal. Chem.* **2009**, 81, 6438-6448.

4. Ow, S. Y.; Salim, M.; Noirel, J.; Evans, C.; Rehman, I.; Wright, P. C. iTRAQ Underestimation in Simple and Complex Mixtures: "The Good, the Bad and the Ugly". *J. Proteome Res.* **2009**, 8, 5347-5355.

5. Karp, N. A.; Huber, W.; Sadowski, P. G.; Charles, P. D.; Hester, S. V.; Lilley, K. S. Addressing Accuracy and Precision Issues in iTRAQ Quantitation. *Mol. Cell. Proteomics.* **2010**, 9, 1885-1897.

6. Hsu, J. L.; Huang, S. Y.; Chow, N. H.; Chen, S. H. Stable-Isotope Dimethyl Labeling for Quantitative Proteomics. *Anal. Chem.* **2003**, 75, 6843-6852.

7. Boersema, P. J.; Raijmakers, R.; Lemeer, S.; Mohammed, S.; Heck, A. J. Multiplex Peptide Stable Isotope Dimethyl Labeling for Quantitative Proteomics. *Nat. Protoc.* **2009**, *4*, 484-494.

8. Wu, Y.; Wang, F.; Liu, Z.; Qin, H.; Song, C.; Huang, J.; Bian, Y.; Wei, X.; Dong, J.; Zou, H. Five-Plex Isotope Dimethyl Labeling for Quantitative Proteomics. *Chem. Commun. (Camb).* **2014**, 50, 1708-1710.

9. Koehler, C. J.; Arntzen, M. O.; de Souza, G. A.; Thiede, B. An Approach for Triplex-Isobaric Peptide Termini Labeling (Triplex-IPTL). *Anal. Chem.* **2013**, 85, 2478-2485.

10. Bamberger, C.; Pankow, S.; Park, S. K.; Yates, J. R. Interference-Free Proteome Quantification with MS/MS-Based Isobaric Isotopologue Detection. *J. Proteome Res.* **2014**, 13, 1494-1051.

11. Zhou, Y.; Shan, Y.; Wu, Q.; Zhang, S.; Zhang, L.; Zhang, Y. Mass Defect-Based Pseudo-Isobaric Dimethyl Labeling for Proteome Quantification. *Anal. Chem.* **2013**, *85*, 10658-10663.

12. Kovanich, D.; Cappadona, S.; Raijmakers, R.; Mohammed, S.; Scholten, A.; Heck, A. J. Applications of Stable Isotope Dimethyl Labeling in Quantitative Proteomics. *Anal. Bioanal Chem.* **2012**, 404, 991-1009.

13. Hsu, J. L.; Huang, S. Y.; Shiea, J. T.; Huang, W. Y.; Chen, S. H. Beyond Quantitative Proteomics: Signal Enhancement of the A1 Ion as a Mass Tag for Peptide Sequencing using Dimethyl Labeling. *J. Proteome Res.* **2005**, *4*, 101-108.

14. Fu, Q.; Li, L. De Novo Sequencing of Neuropeptides using Reductive Isotopic Methylation and Investigation of ESI QTOF MS/MS Fragmentation Pattern of Neuropeptides with N-Terminal Dimethylation. *Anal. Chem.* **2005**, 77, 7783-7795.

15. Locke, S. J.; Leslie, A. D.; Melanson, J. E.; Pinto, D. M. Deviation from the Mobile Proton Model in Amino-Modified Peptides: Implications for Multiple Reaction Monitoring Analysis of Peptides. *Rapid Commun. Mass Spectrom.* **2006**, 20, 1525-1530.

16. Rose, C. M.; Merrill, A. E.; Bailey, D. J.; Hebert, A. S.; Westphall, M. S.; Coon, J. J. Neutron Encoded Labeling for Peptide Identification. *Anal. Chem.* **2013**, 85, 5129-5137.

17. McAlister, G. C.; Huttlin, E. L.; Haas, W.; Ting, L.; Jedrychowski, M. P.; Rogers, J. C.; Kuhn, K.; Pike, I.; Grothe, R. A.; Blethrow, J. D.; Gygi, S. P. Increasing the Multiplexing

Capacity of TMTs using Reporter Ion Isotopologues with Isobaric Masses. *Anal. Chem.* **2012**, 84, 7469-7478.

18. Werner, T.; Becher, I.; Sweetman, G.; Doce, C.; Savitski, M. M.; Bantscheff, M. High-Resolution Enabled TMT 8-Plexing. *Anal. Chem.* **2012**, 84, 7188-7194.

19. Hebert, A. S.; Merrill, A. E.; Stefely, J. A.; Bailey, D. J.; Wenger, C. D.; Westphall, M. S.; Pagliarini, D. J.; Coon, J. J. Amine-Reactive Neutron-Encoded Labels for Highly Plexed Proteomic Quantitation. *Mol. Cell. Proteomics.* **2013**, 12, 3360-3369.

20. Abbatiello, S. E.; Mani, D. R.; Schilling, B.; Maclean, B.; Zimmerman, L. J.; Feng, X.; Cusack, M. P.; Sedransk, N.; Hall, S. C.; Addona, T.; Allen, S.; Dodder, N. G.; Ghosh, M.; Held, J. M.; Hedrick, V.; Inerowicz, H. D.; Jackson, A.; Keshishian, H.; Kim, J. W.; Lyssand, J. S.; Riley, C. P.; Rudnick, P.; Sadowski, P.; Shaddox, K.; Smith, D.; Tomazela, D.; Wahlander, A.; Waldemarson, S.; Whitwell, C. A.; You, J.; Zhang, S.; Kinsinger, C. R.; Mesri, M.; Rodriguez, H.; Borchers, C. H.; Buck, C.; Fisher, S. J.; Gibson, B. W.; Liebler, D.; Maccoss, M.; Neubert, T. A.; Paulovich, A.; Regnier, F.; Skates, S. J.; Tempst, P.; Wang, M.; Carr, S. A. Design, Implementation and Multisite Evaluation of a System Suitability Protocol for the Quantitative Assessment of Instrument Performance in Liquid Chromatography-Multiple Reaction Monitoring-MS (LC-MRM-MS). *Mol. Cell. Proteomics.* **2013**, 12, 2623-2639.

21. DeSouza, L. V.; Taylor, A. M.; Li, W.; Minkoff, M. S.; Romaschin, A. D.; Colgan, T. J.; Siu, K. W. Multiple Reaction Monitoring of mTRAQ-Labeled Peptides Enables Absolute Quantification of Endogenous Levels of a Potential Cancer Marker in Cancerous and Normal Endometrial Tissues. *J. Proteome Res.* **2008**, 7, 3525-3534.

22. DeSouza, L. V.; Krakovska, O.; Darfler, M. M.; Krizman, D. B.; Romaschin, A. D.; Colgan, T. J.; Siu, K. W. mTRAQ-Based Quantification of Potential Endometrial Carcinoma Biomarkers from Archived Formalin-Fixed Paraffin-Embedded Tissues. *Proteomics.* **2010**, 10, 3108-3116.

23. Oppermann, F. S.; Klammer, M.; Bobe, C.; Cox, J.; Schaab, C.; Tebbe, A.; Daub, H. Comparison of SILAC and mTRAQ Quantification for Phosphoproteomics on a Quadrupole Orbitrap Mass Spectrometer. *J. Proteome Res.* **2013**, 12, 4089-4100.

24. Gropengiesser, J.; Varadarajan, B. T.; Stephanowitz, H.; Krause, E. The Relative Influence of Phosphorylation and Methylation on Responsiveness of Peptides to MALDI and ESI Mass Spectrometry. *J. Mass Spectrom.* **2009**, 44, 821-831.

25. Maclean, B.; Tomazela, D. M.; Abbatiello, S. E.; Zhang, S.; Whiteaker, J. R.; Paulovich, A. G.; Carr, S. A.; Maccoss, M. J. Effect of Collision Energy Optimization on the Measurement of Peptides by Selected Reaction Monitoring (SRM) Mass Spectrometry. *Anal. Chem.* **2010**, 82, 10116-10124.

26. Eschweiler, W. Replacement of Hydrogen Atoms by the Methyl Group by Formaldehyde, Bound at Nitrogen. *BER.* **1905**, 38, 880-882.

27. Clarke, H. T.; Gillespie, H. B.; Weisshaus, S. Z. Action of Formaldehyde on Amines and Amino Acids. *J. Am. Chem. Soc.* **1933**, 55, 4571-4587.

28. Harrison, A. G. To B Or Not to B: The Ongoing Saga of Peptide B Ions. *Mass Spectrom. Rev.* **2009**, *28*, 640-654.

29. Harrison, A. G.; Csizmadia, I. G.; Tang, T. H.; Tu, Y. P. Reaction Competition in the Fragmentation of Protonated Dipeptides. *J. Mass Spectrom.* **2000**, *35*, 683-688.

30. McLafferty, F. W. Mass Spectrometric Analysis: Molecular Rearrangements. *Anal. Chem.* **1959**, 31, 82-87.

31. Csonka, I. P.; Paizs, B.; Lendvay, G.; Suhai, S. Proton Mobility and Main Fragmentation Pathways of Protonated Lysylglycine. *Rapid Commun. Mass Spectrom.* **2001**, *15*, 1457-1472.

32. He, Y.; Reilly, J. P. Does a Charge Tag really Provide a Fixed Charge? *Angew. Chem. Int. Ed. Engl.* **2008**, 47, 2463-2465.

33. Yalcin, T.; Harrison, A. G. Ion Chemistry of Protonated Lysine Derivatives. *J. Mass Spectrom.* **1996**, 31, 1237-1243.

34. Farrugia, J. M.; Taverner, T.; O'Hair, R. A. J. Side-Chain Involvement in the Fragmentation Reactions of the Protonated Methyl Esters of Histidine and its Peptides. *Int. J. Mass Spectrom.* **2001**, 209, 99-112.

35. Tsaprailis, G.; Nair, H.; Zhong, W.; Kuppannan, K.; Futrell, J. H.; Wysocki, V. H. A Mechanistic Investigation of the Enhanced Cleavage at Histidine in the Gas-Phase Dissociation of Protonated Peptides. *Anal. Chem.* **2004**, 76, 2083-2094.

36. Hiserodt, R. D.; Brown, S. M.; Swijter, D. F.; Hawkins, N.; Mussinan, C. J. A Study of b1+H2O and B1-Ions in the Product Ion Spectra of Dipeptides Containing N-Terminal Basic Amino Acid Residues. *J. Am. Soc. Mass Spectrom.* **2007**, 18, 1414-1422.

37. van der Rest, G.; He, F.; Emmett, M. R.; Marshall, A. G.; Gaskell, S. J. Gas-Phase Cleavage of PTC-Derivatized Electrosprayed Tryptic Peptides in an FT-ICR Trapped-Ion Cell: Mass-Based Protein Identification without Liquid Chromatographic Separation. *J. Am. Soc. Mass Spectrom.* **2001**, 12, 288-295.

38. Diego, P. A.; Bajrami, B.; Jiang, H.; Shi, Y.; Gascon, J. A.; Yao, X. Site-Preferential Dissociation of Peptides with Active Chemical Modification for Improving Fragment Ion Detection. *Anal. Chem.* **2010**, 82, 23-27.

39. Laskin, J.; Yang, Z.; Song, T.; Lam, C.; Chu, I. K. Effect of the Basic Residue on the Energetics, Dynamics, and Mechanisms of Gas-Phase Fragmentation of Protonated Peptides. *J. Am. Chem. Soc.* **2010**, 132, 16006-16016.

40. Barlow, C. K.; O'Hair, R. A. J. Gas-Phase Peptide Fragmentation: How Understanding the Fundamentals Provides a Springboard to Developing New Chemistry and Novel Proteomic Tools. *J. Mass Spectrom.* **2008**, 43, 1301-1319.

Chapter 5

Conclusion and Perspective

5.1 Novel mass spectrometric technologies for targeted membrane proteomics

Mass spectrometry-based proteomics was used to absolutely and precisely quantify CFTR, an important transmembrane protein for cystic fibrosis. Transmembrane proteins represent a very difficult analyte to accurately and precisely quantify due to their high molecular weight and hydrophobic domains. A surrogate, peptide-level measurement of CFTR was exploited, to avoid these quantitative problems. This was further enhanced by dual protein-level enrichment strategies: cell-surface biotinylation and GEE [1]. To increase sample throughput of CFTR, passive mass tags, which possess a signal-enhancing dimethylamino group, were synthesized, and their gas-phase fragmentation evaluated [2]. The collisional fragmentation of peptides whose amine groups were derivatized with five linear ω-dimethylamino acids, from 2-(dimethylamino)-acetic acid to 6-(dimethylamino)-hexanoic acid were investigated. A separation of five methylene groups, between the terminal dimethylamino group and the amide formed upon peptide derivatization, is required to shut down the active participation of the terminal dimethylamino group. These tags are potential, new reagents for uMRM MS. This throughput technology adapts a modular design that separates quantitation and sample throughput. This allows one common IS to be used as the quantitation standard. By using non-isotopic derivatizing reagents, inexpensive and unprecedented sample throughput is possible. This technique is adaptable from a few samples to potentially hundreds.

5.2 The need to rapidly develop tests in a clinical setting

With the ever-increasing catalog of biomarkers for disease and treatment, the desire to rapidly develop clinical assays is of upmost importance to scientist, clinicians, and patients [3,4]. Mass spectrometry provides a flexible platform to rapidly perform this quantitative analysis [5]. There is no need for the lengthy and expensive production of immunograde, monoclonal

antibodies. Also the multiplexing capabilities of mass spectrometers allows multiple analytes to be monitored in a single experiment. MRM MS has been shown to be reproducible in quantifying proteins across laboratories [6]. These attributes make MS in the clinical setting an attractive alternative to immunoassays. However, difficult or low abundance analytes, such as CFTR, represent quantitative challenges, which must be overcome by the development new tools, technologies, and methods.

5.3 References

1. McShane, A. J.; Bajrami, B.; Ramos, A. A.; Diego-Limpin, P. A.; Farrokhi, V.; Coutermarsh, B. A.; Stanton, B. A.; Jensen, T.; Riordan, J. R.; Wetmore, D.; Joseloff, E.; Yao, X. Targeted Proteomic Quantitation of the Absolute Expression and Turnover of Cystic Fibrosis Transmembrane Conductance Regulator in the Apical Plasma Membrane. *J. Proteome Res.* **2014**, 13, 4676-4685.

2. McShane, A. J.; Shen, Y.; Castillo, M. J.; Yao, X. Peptide Dimethylation: Fragmentation Control Via Distancing the Dimethylamino Group. *J. Am. Soc. Mass Spectrom.* **2014**, 25, 1694-1704.

3. Heegaard, N. H.; Ostergaard, O.; Bahl, J. M.; Overgaard, M.; Beck, H. C.; Rasmussen, L. M.; Larsen, M. R. Important Options Available--from Start to Finish--for Translating Proteomics Results to Clinical Chemistry. *Proteomics Clin. Appl.* **2015**, 9, 235-252.

4. Scherl, A. Clinical Protein Mass Spectrometry. *Methods.* **2015**, 15, 00088-2.

5. McShane, A. J.; Farrokhi, V.; Nemati, R.; Li, S.; Yao, X. An Overview of Quantitative Proteomic Approaches. Comprehensive Analytical Chemistry, Oxford, UK; Elsevier, **2014**; p. 111-135.

6. Addona, T. A.; Abbatiello, S. E.; Schilling, B.; Skates, S. J.; Mani, D. R.; Bunk, D. M.; Spiegelman, C. H.; Zimmerman, L. J.; Ham, A. J.; Keshishian, H.; Hall, S. C.; Allen, S.; Blackman, R. K.; Borchers, C. H.; Buck, C.; Cardasis, H. L.; Cusack, M. P.; Dodder, N. G.; Gibson, B. W.; Held, J. M.; Hiltke, T.; Jackson, A.; Johansen, E. B.; Kinsinger, C. R.; Li, J.; Mesri, M.; Neubert, T. A.; Niles, R. K.; Pulsipher, T. C.; Ransohoff, D.; Rodriguez, H.; Rudnick, P. A.; Smith, D.; Tabb, D. L.; Tegeler, T. J.; Variyath, A. M.; Vega-Montoto, L. J.; Wahlander, A.; Waldemarson, S.; Wang, M.; Whiteaker, J. R.; Zhao, L.; Anderson, N. L.; Fisher, S. J.;

Liebler, D. C.; Paulovich, A. G.; Regnier, F. E.; Tempst, P.; Carr, S. A. Multi-Site Assessment of the Precision and Reproducibility of Multiple Reaction Monitoring-Based Measurements of Proteins in Plasma. *Nat. Biotechnol.* **2009**, *27*, 633-641.

Appendix 1

Supplemental Information for Chapter 4

Text A1.1

2-aminoacetic acid (8 mmol) was dissolved in 5 mL of 88% formic acid (125 mmol) and 1 mL of 37% formaldehyde (36 mmol). The solution was refluxed at 100°C for 1h. After heating, 1 mL of concentrated HCl was added. The solvent was dried *in vacuo*, after which a white precipitate was obtained. The precipitate was washed with 5 mL of glacial acetic acid 3 times. The product was recrystallized in methanol and diethyl ether. The yield was 29.6%. ^{1}H NMR (400 MHz, D_2O, 25°C): δ = 4.06 (s, 2H), 3.01 (s, 6H) ppm; HRMS (DART) calculated $[M+H]^+$ 104.0712, found 104.0671.

Text A1.2

3-aminopropanoic acid (8 mmol) was dissolved in 5 mL of 88% formic acid (125 mmol) and 1 mL of 37% formaldehyde (36 mmol). The solution was heated via microwave irradiation at 110°C, 100 W for 1h. After microwave heating 1 mL of concentrated HCl was added. The solvent was dried *in vacuo*, after which a white precipitate was obtained. The precipitate was washed with 5 mL of glacial acetic acid 3 times. The product was recrystallized in methanol and diethyl ether. The yield was 86.7%. ^{1}H NMR (400 MHz, D_2O, 25°C): δ = 3.47 (t, J = 6.7 Hz, 2H), 2.96 (s, 6H), 2.93 (t, J = 6.7 Hz, 2H) ppm; HRMS (DART) calculated $[M+H]^+$ 118.0868, found 118.0871.

Text A1.3

4-aminobutanoic acid (8 mmol) was dissolved in 5 mL of 88% formic acid (125 mmol) and 1 mL of 37% formaldehyde (36 mmol). The solution was heated via microwave irradiation at 110°C, 100 W for 1h. After microwave heating 1 mL of concentrated HCl was added. The solvent was dried *in vacuo*, after which a white precipitate was obtained. The precipitate was washed with 5 mL of glacial acetic acid 3 times. The product was recrystallized in methanol and diethyl ether. The yield was 84.1%. ^{1}H NMR (400 MHz, D_2O, 25°C): δ = 3.22 (t, J = 8.2 Hz, 2H), 2.94 (s, 6H),

2.54 (t, J = 7.2 Hz, 2H), 2.12-2.01 (m, 2H) ppm; HRMS (DART) calculated $[M+H]^+$ 132.1025, found 132.1047.

Text A1.4

5-aminopentanoic acid (8 mmol) was dissolved in 5 mL of 88% formic acid (125 mmol) and 1 mL of 37% formaldehyde (36 mmol). The solution was heated via microwave irradiation at 110°C, 100 W for 1h. After microwave heating 1 mL of concentrated HCl was added. The solvent was dried *in vacuo*, after which a white precipitate was obtained. The precipitate was washed with 5 mL of glacial acetic acid 3 times. The product was recrystallized in methanol and diethyl ether. The yield was 29.2%. ^{1}H NMR (400 MHz, D_2O, 25°C): δ = 3.19 (t, J = 8.1 Hz, 2H), 2.91 (s, 6H), 2.49 (t, J = 7.1 Hz, 2H), 1.84-1.68 (m, 4H) ppm; HRMS (DART) calculated $[M+H]^+$ 146.1181, found 146.1166.

Text A1.5

6-aminohexanoic acid (8 mmol) was dissolved in 5 mL of 88% formic acid (125 mmol) and 1 mL of 37% formaldehyde (36 mmol). The solution was heated via microwave irradiation at 110°C, 100 W for 2h. After microwave heating 1 mL of concentrated HCl was added. The solvent was dried *in vacuo*, after which a white precipitate was obtained. The precipitate was washed with 5 mL glacial of acetic acid 3 times. The product was recrystallized in methanol and diethyl ether. The yield was 20.8%. ^{1}H NMR (400 MHz, D_2O, 25°C): δ = 3.17 (t, J = 8.1 Hz, 2H), 2.90 (s, 6H), 2.44 (t, J = 7.3 Hz, 2H), 1.82-1.63 (m, 4H), 1.48-1.38 (m, 2H) ppm; HRMS (DART) calculated $[M+H]^+$ 160.1338, found 160.1386.

Figure A1.1a: Non-derivatized NSILTETLHR $[M+2H]^{2+}$ MS/MS spectrum (y ions that are doubly charged are denoted as y^{2+}).

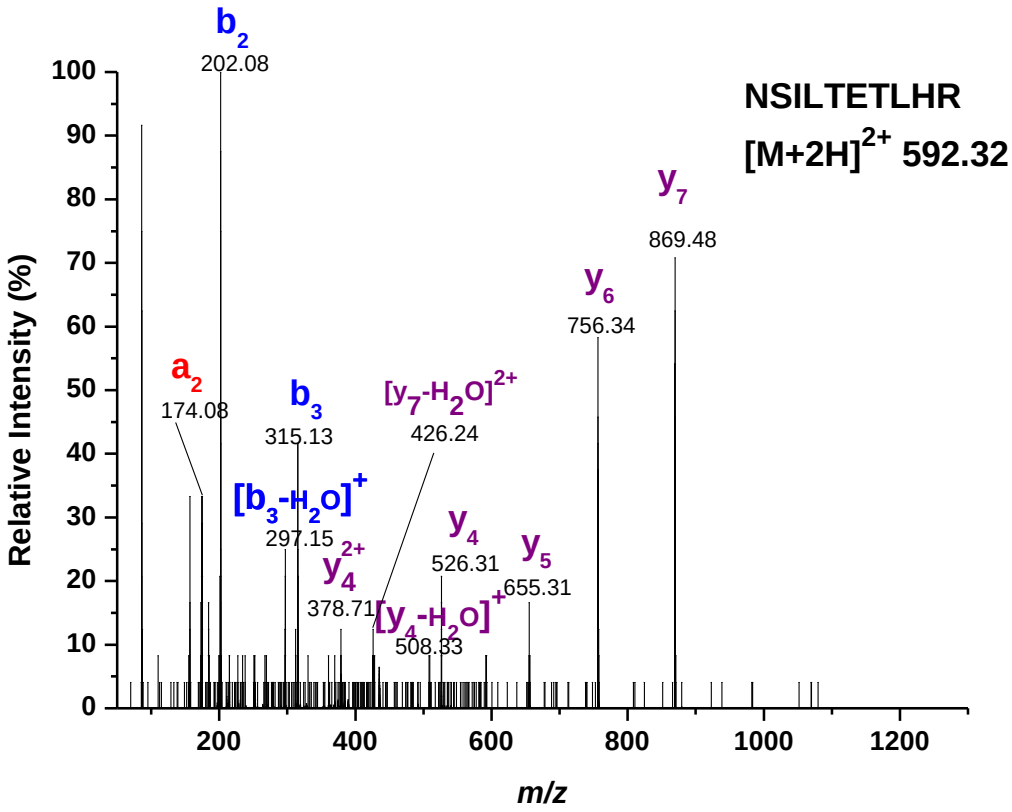

Figure A1.1b: Non-derivatized NSILTETLHR $[M+3H]^{3+}$ MS/MS spectrum (y ions that are doubly charged are denoted as y^{2+}).

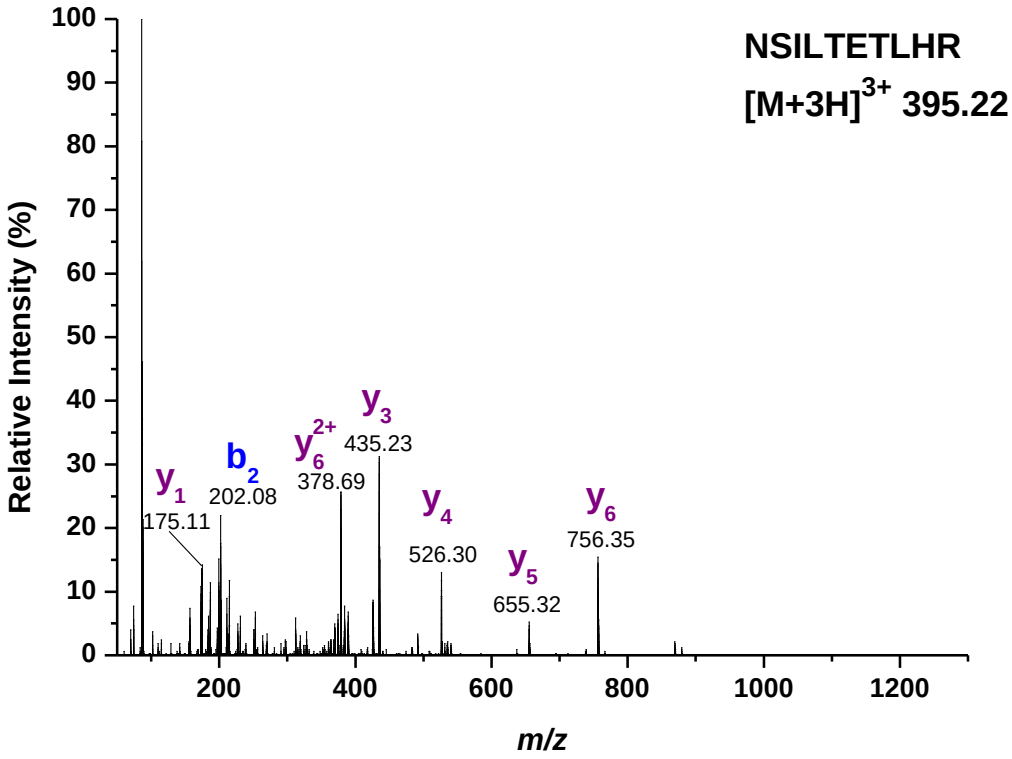

Figure A1.1c: Non-derivatized LSLVPDSEQGEAILPR $[M+2H]^{2+}$ MS/MS spectrum (y ions that are doubly charged are denoted as y^{2+}).

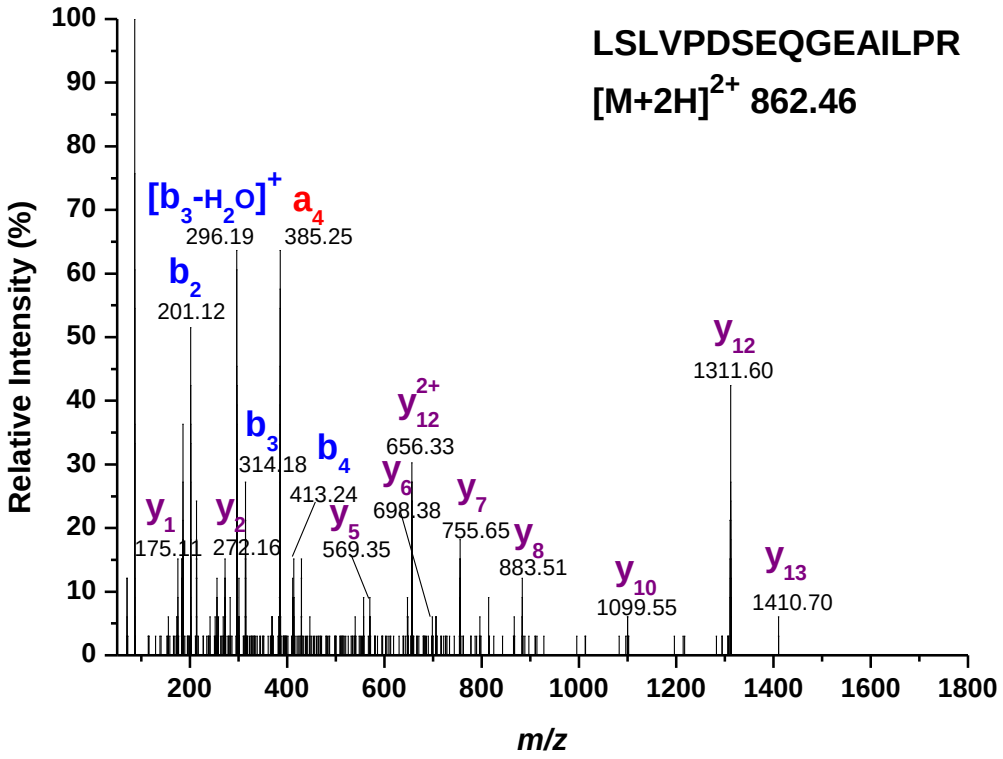

Figure A1.1d: Non-derivatized LSEPAELTDAVK $[M+2H]^{2+}$ MS/MS spectrum (y ions that are doubly charged are denoted as y^{2+}).

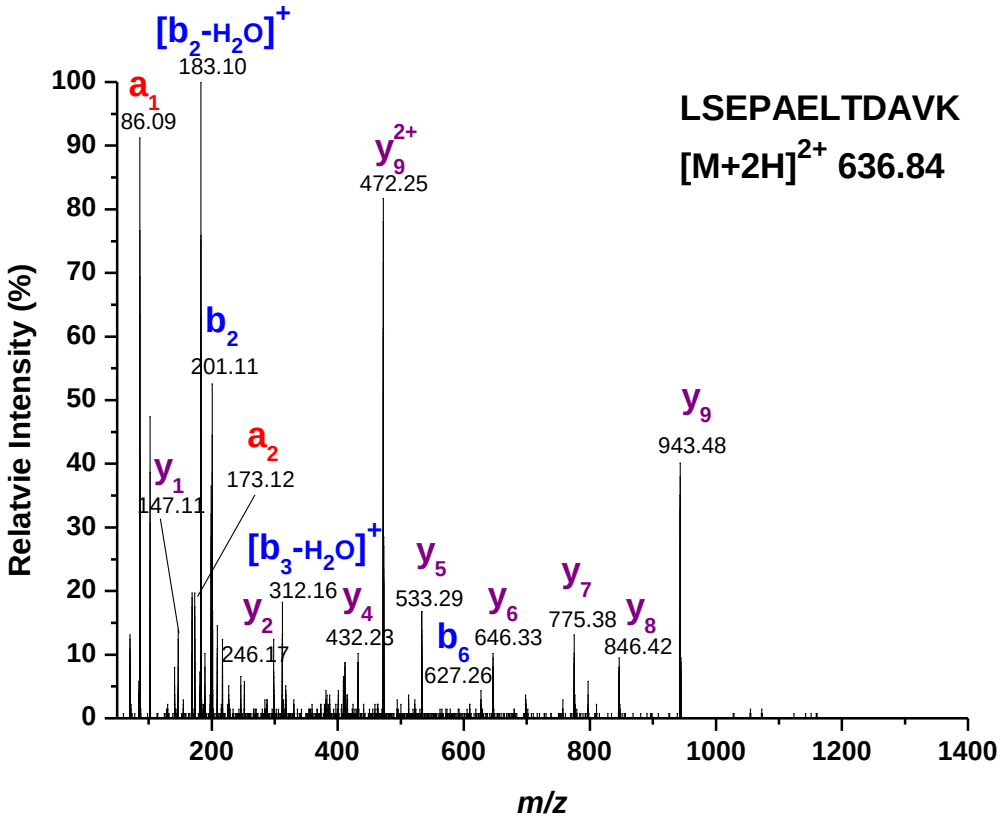

Figure A1.1e: Non-derivatized SVILLGR $[M+2H]^{2+}$ MS/MS spectrum (y ions that are doubly charged are denoted as y^{2+}).

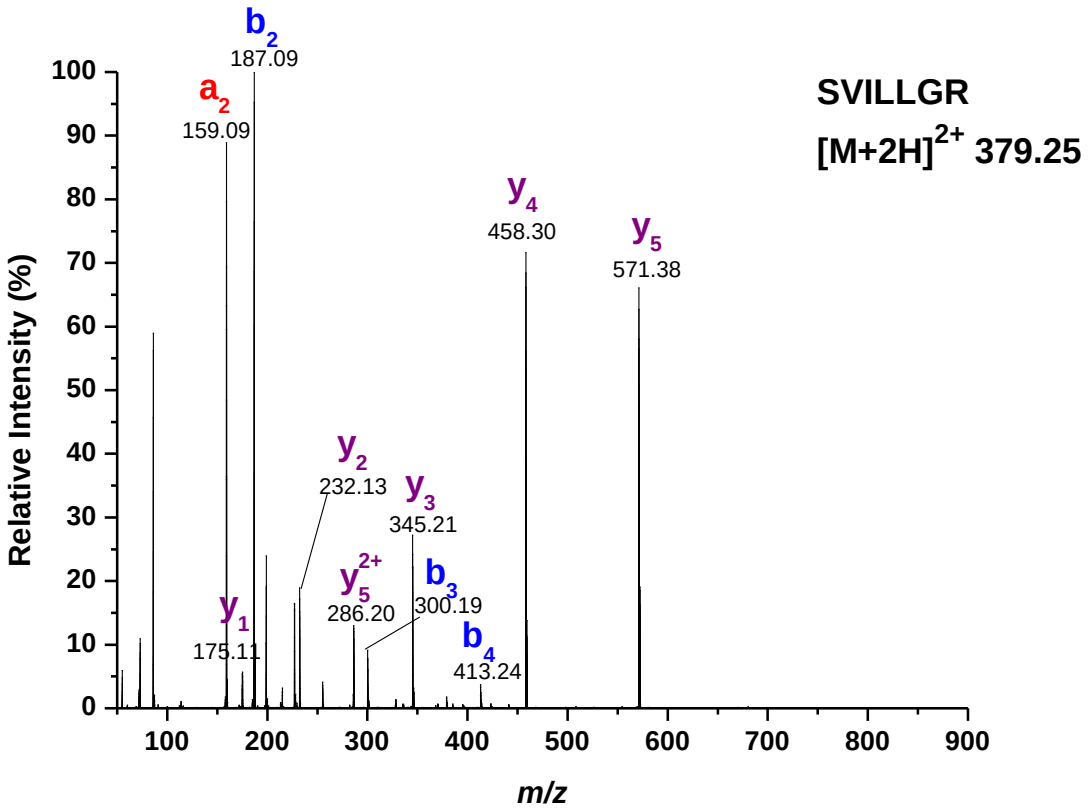

Figure A1.1f: Non-derivatized YGGFLR $[M+2H]^{2+}$ MS/MS spectrum.

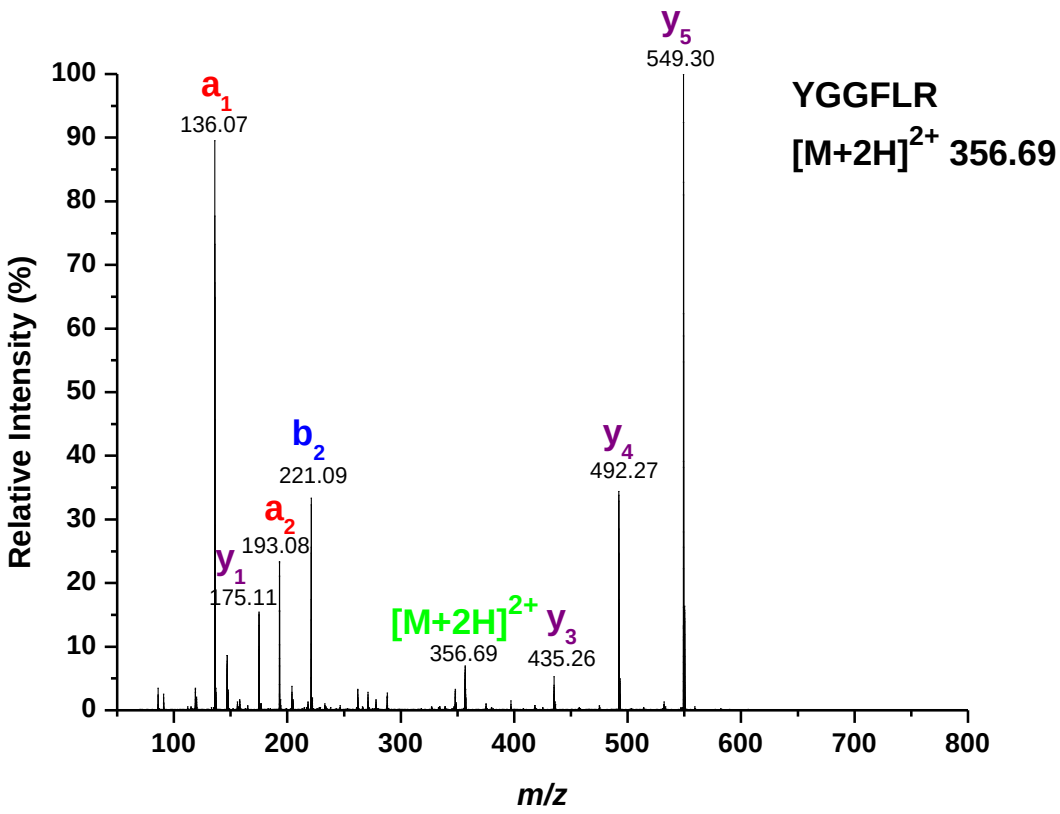

Figure A1.2a: Dim-2 derivatized NSILTETLHR $[M+2H]^{2+}$ MS/MS spectrum.

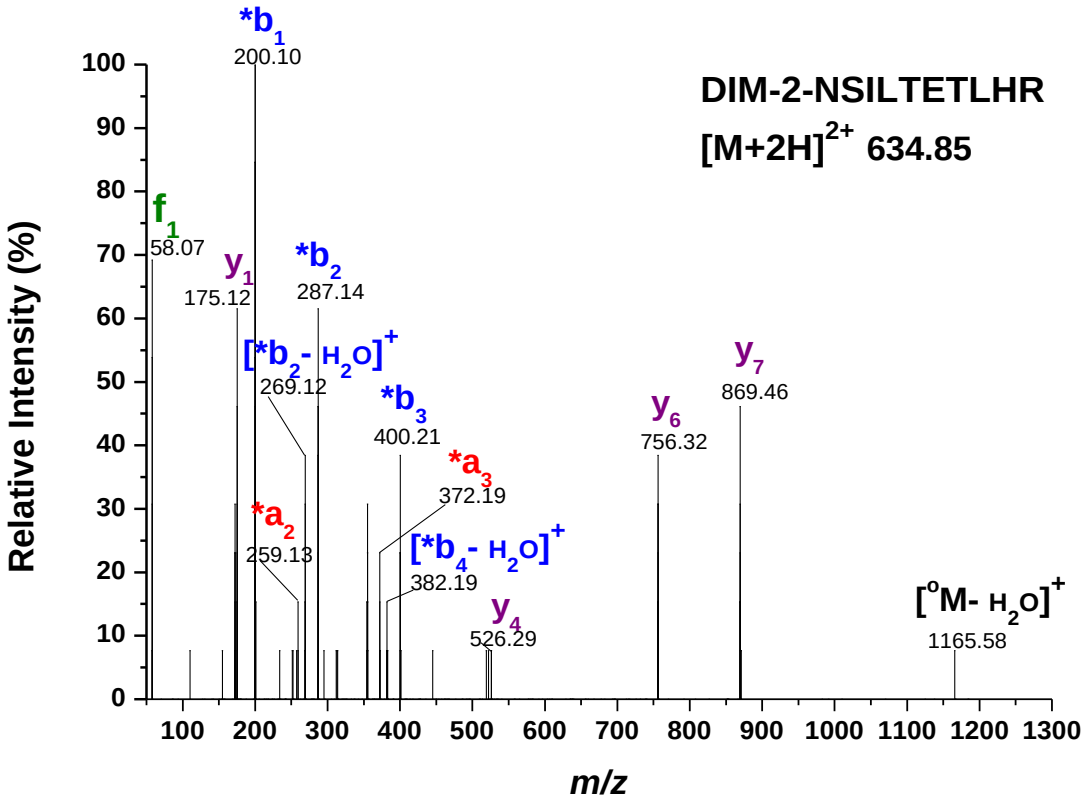

Figure A1.2b: Dim-2 derivatized NSILTETLHR $[M+3H]^{3+}$ MS/MS spectrum.

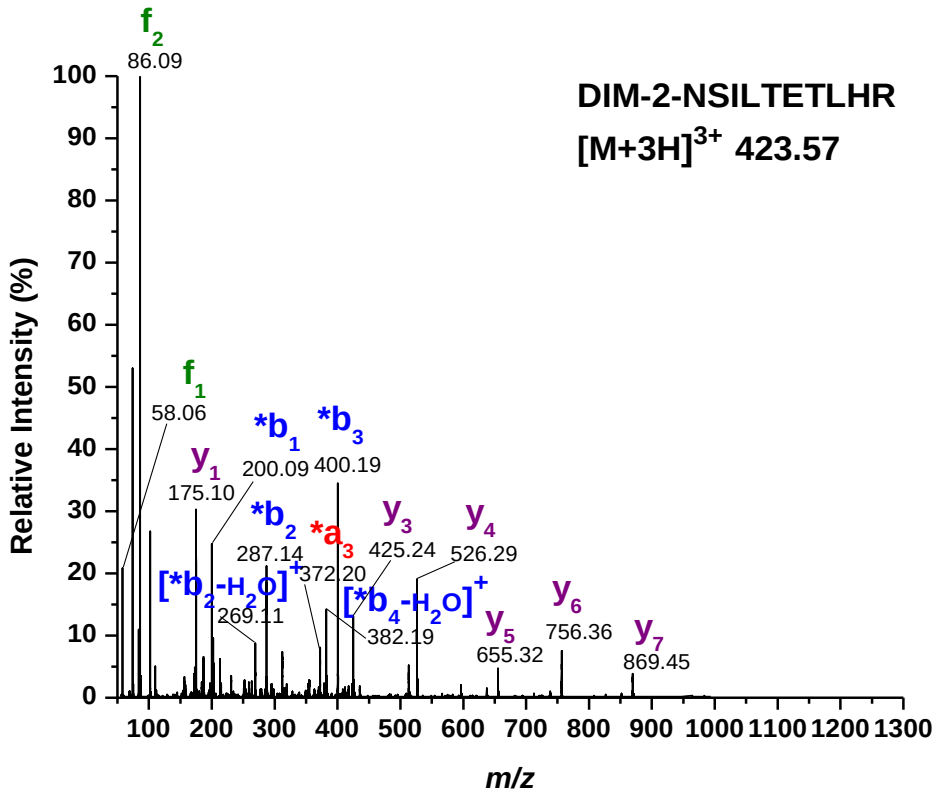

Figure A1.2c: Dim-2 derivatized LSLVPDSEQGEAILPR $[M+2H]^{2+}$ MS/MS spectrum.

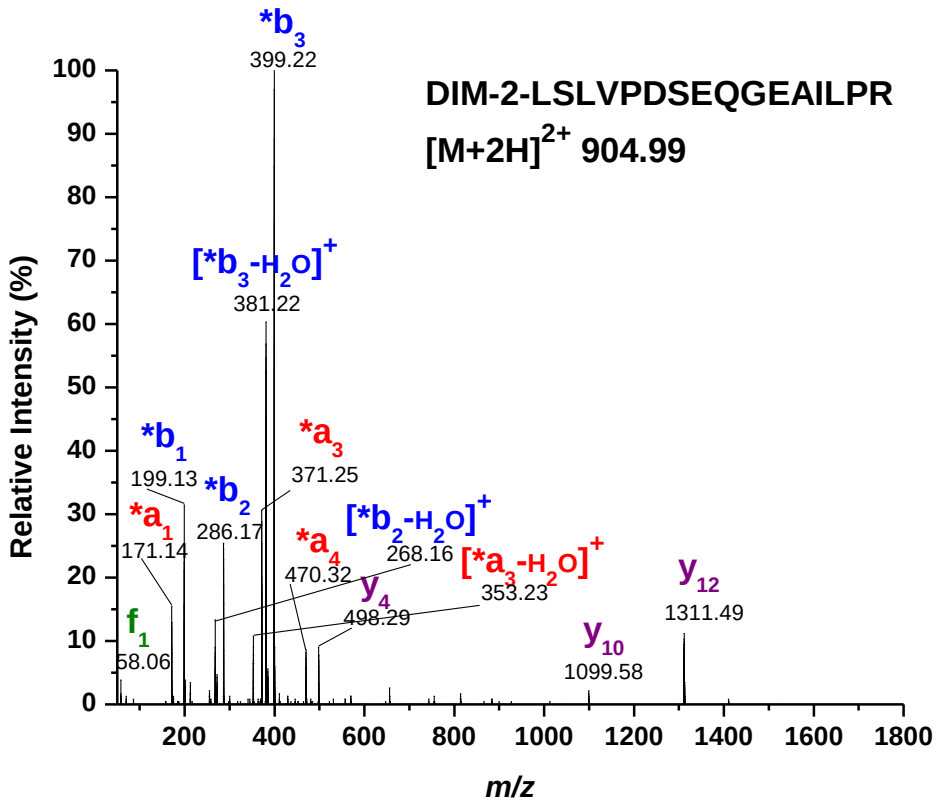

Figure A1.2d: Dim-2 derivatized LSLVPDSEQGEAILPR $[M+3H]^{3+}$ MS/MS spectrum.

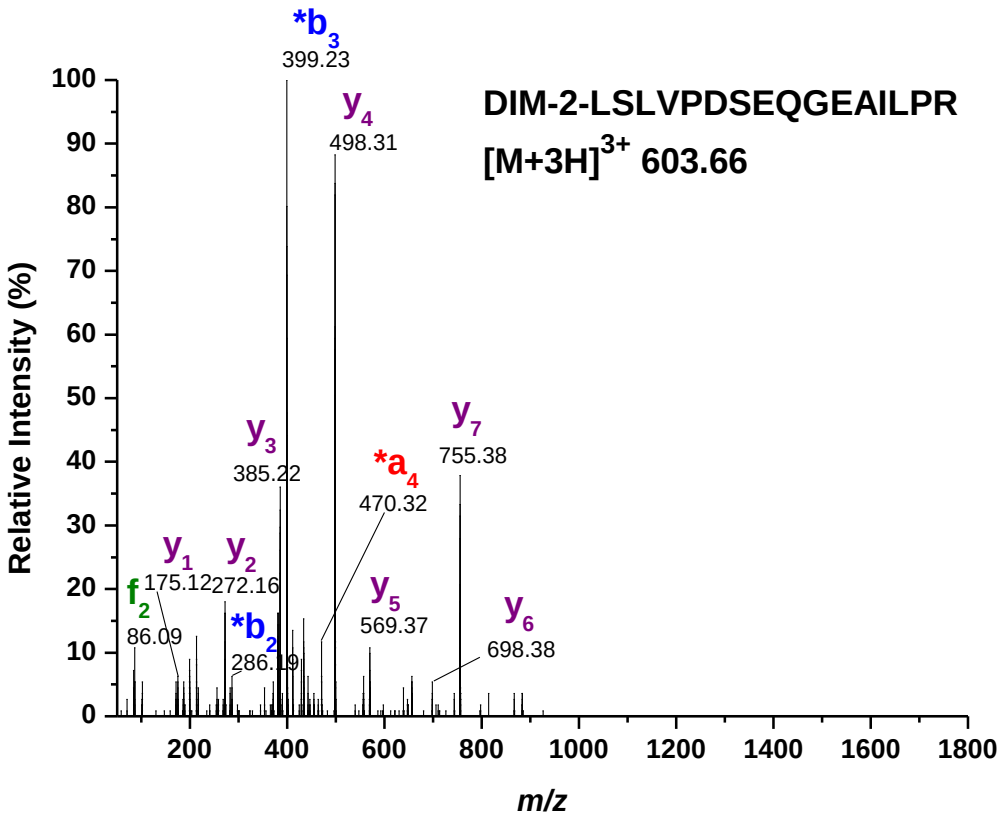

Figure A1.2e: Dim-2 derivatized LSEPAELTDAVK $[M+2H]^{2+}$ MS/MS spectrum (y ions carrying the derivatizing group, on the lysine's side chain amine, are denoted as *y).

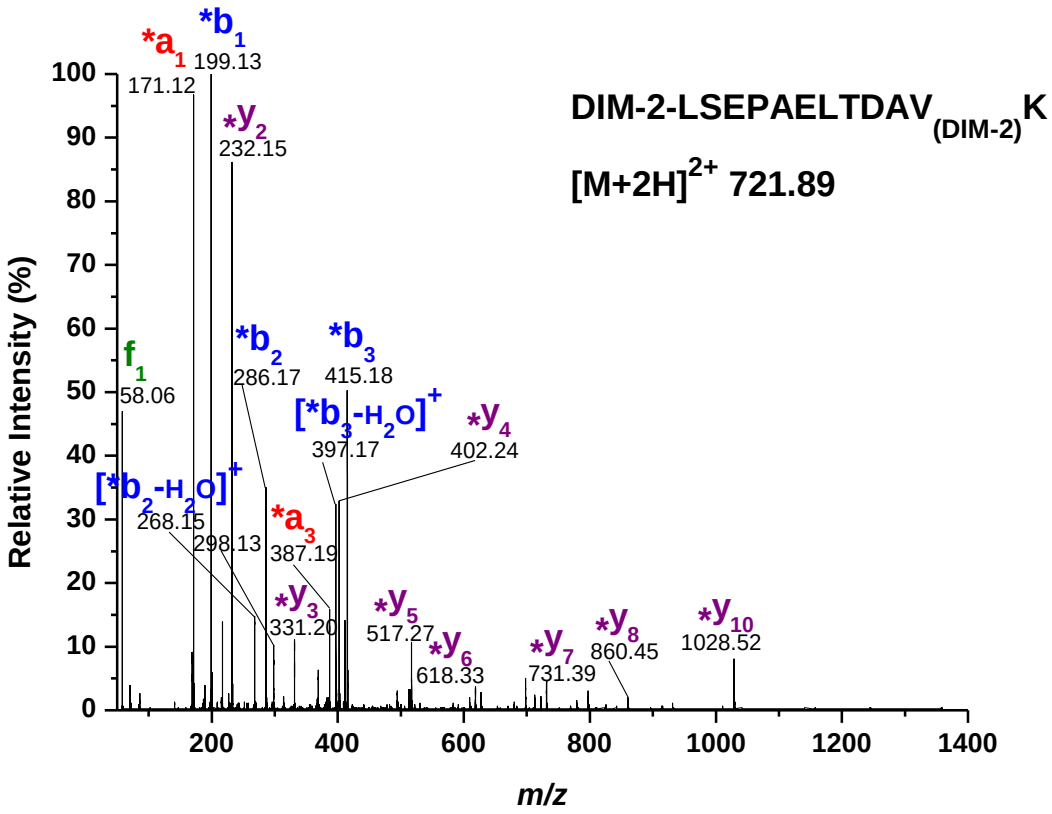

Figure A1.2f: Dim-2 derivatized SVILLGR $[M+2H]^{2+}$ MS/MS spectrum**.**

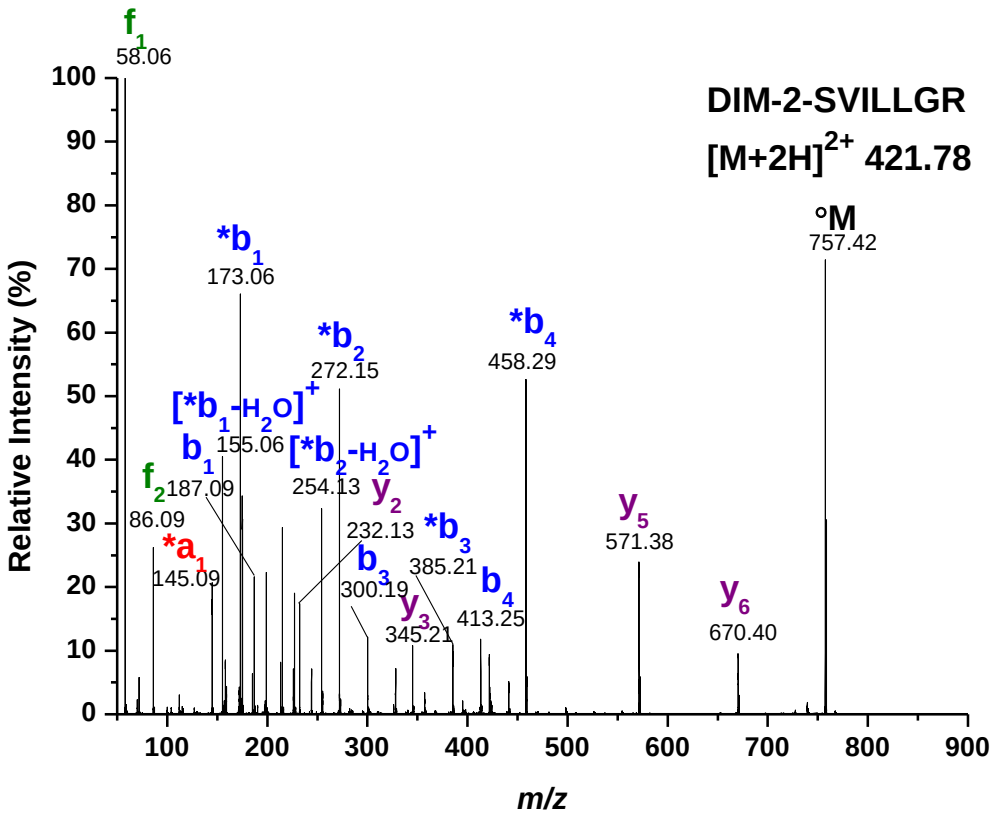

Figure A1.3a: Dim-3 derivatized NSILTETLHR $[M+2H]^{2+}$ MS/MS spectrum.

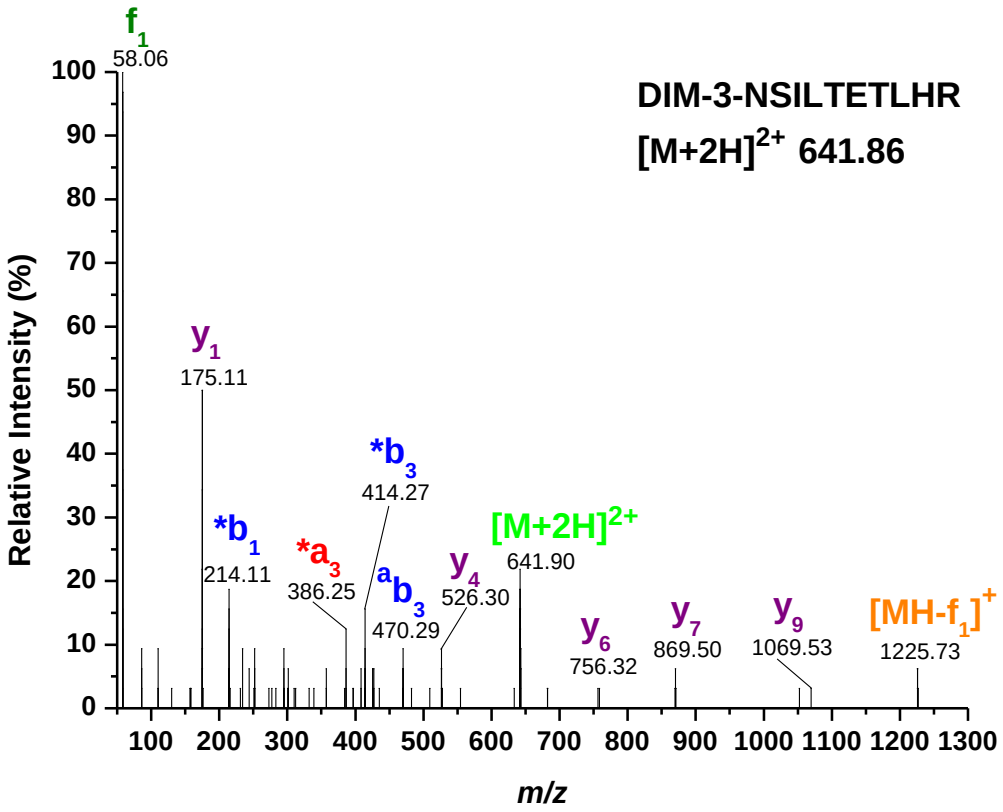

Figure A1.3b: Dim-3 derivatized NSILTETLHR $[M+3H]^{3+}$ MS/MS spectrum.

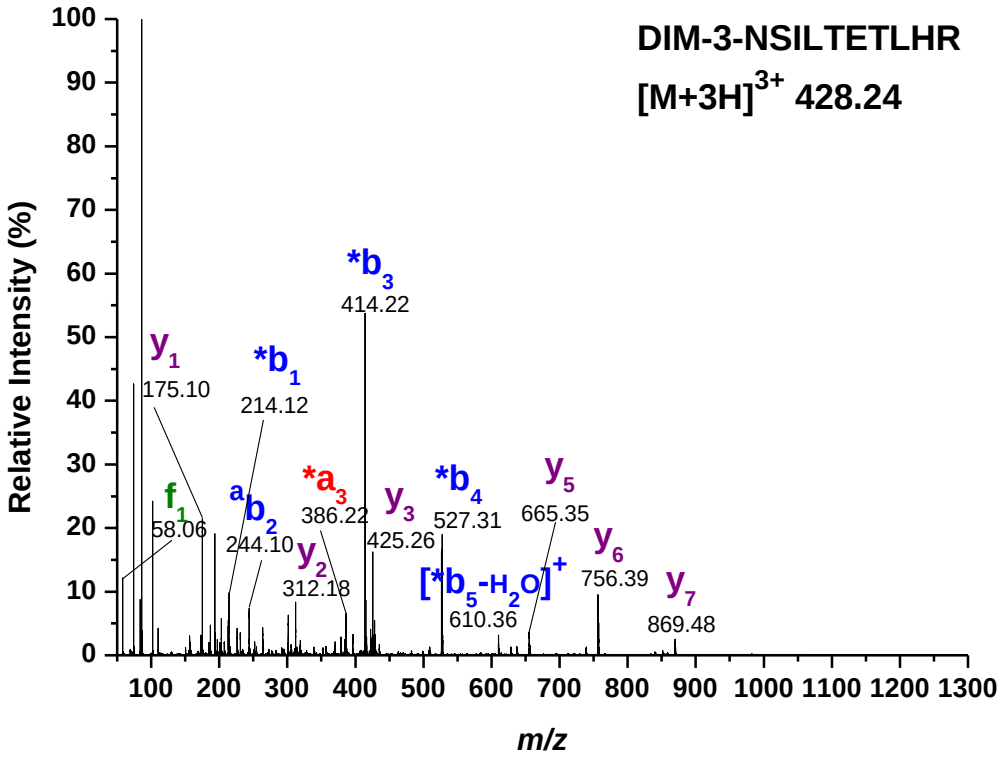

Figure A1.3c: Dim-3 derivatized LSLVPDSEQGEAILPR $[M+2H]^{2+}$ MS/MS spectrum.

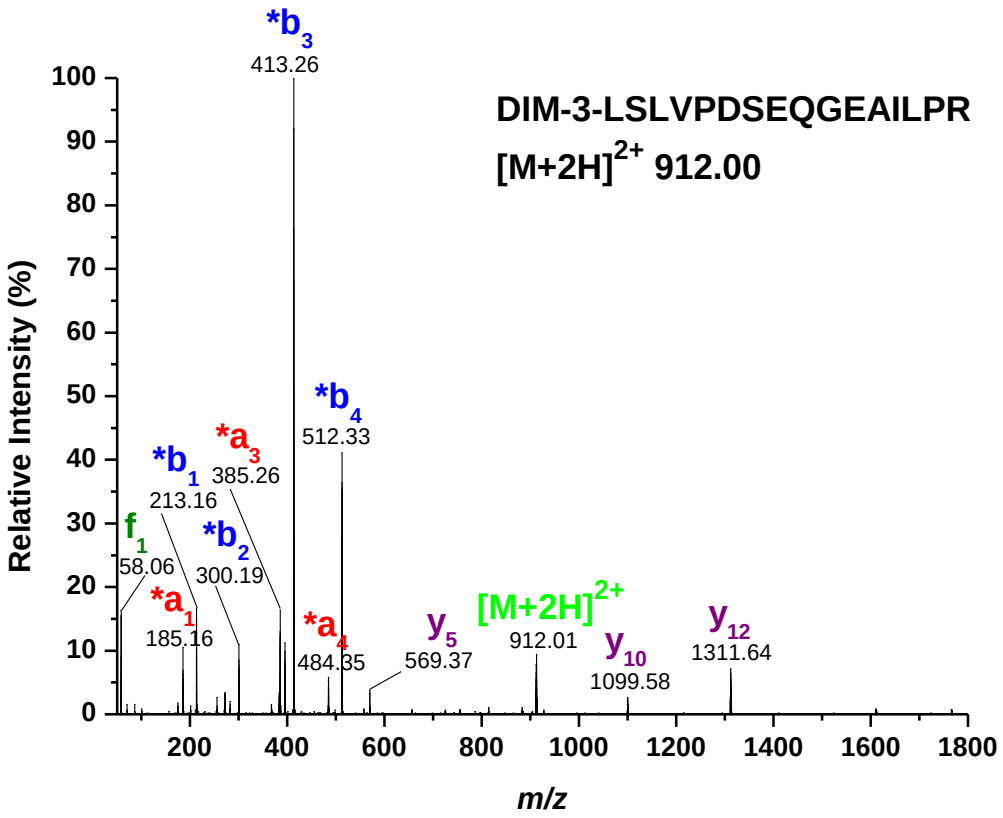

Figure A1.3d: Dim-3 derivatized LSLVPDSEQGEAILPR $[M+3H]^{3+}$ MS/MS spectrum.

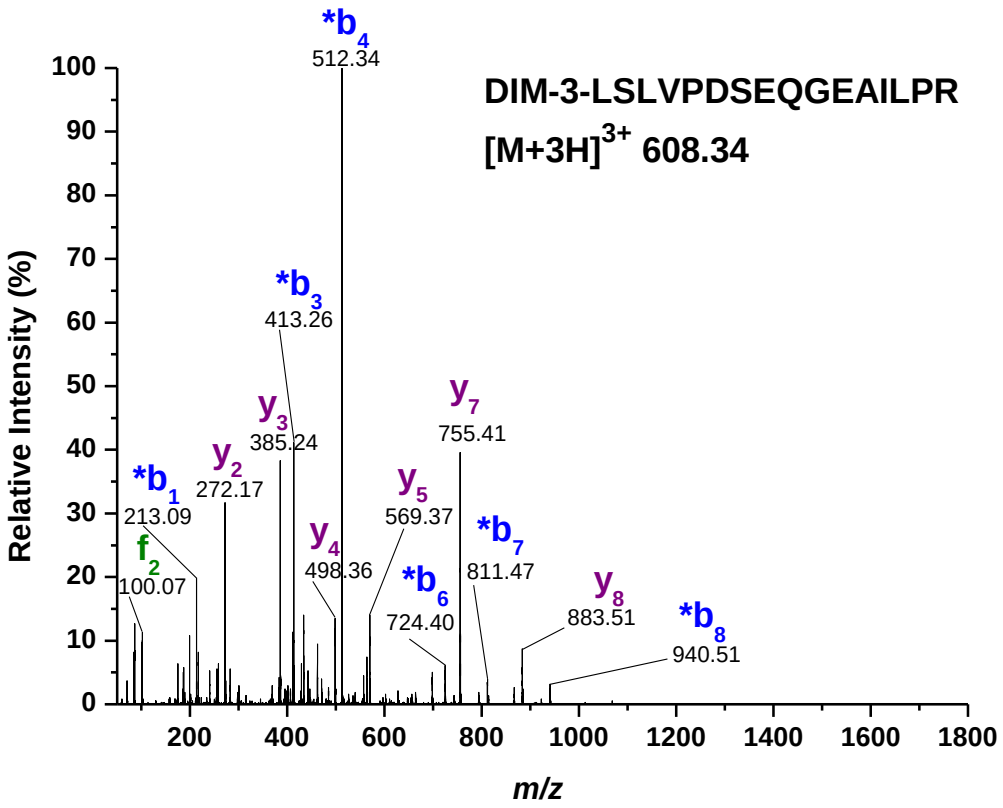

Figure A1.3e: Dim-3 derivatized LSEPAELTDAVK $[M+2H]^{2+}$ MS/MS spectrum (y ions carrying the derivatizing group, on the lysine's side chain amine, are denoted as *y).

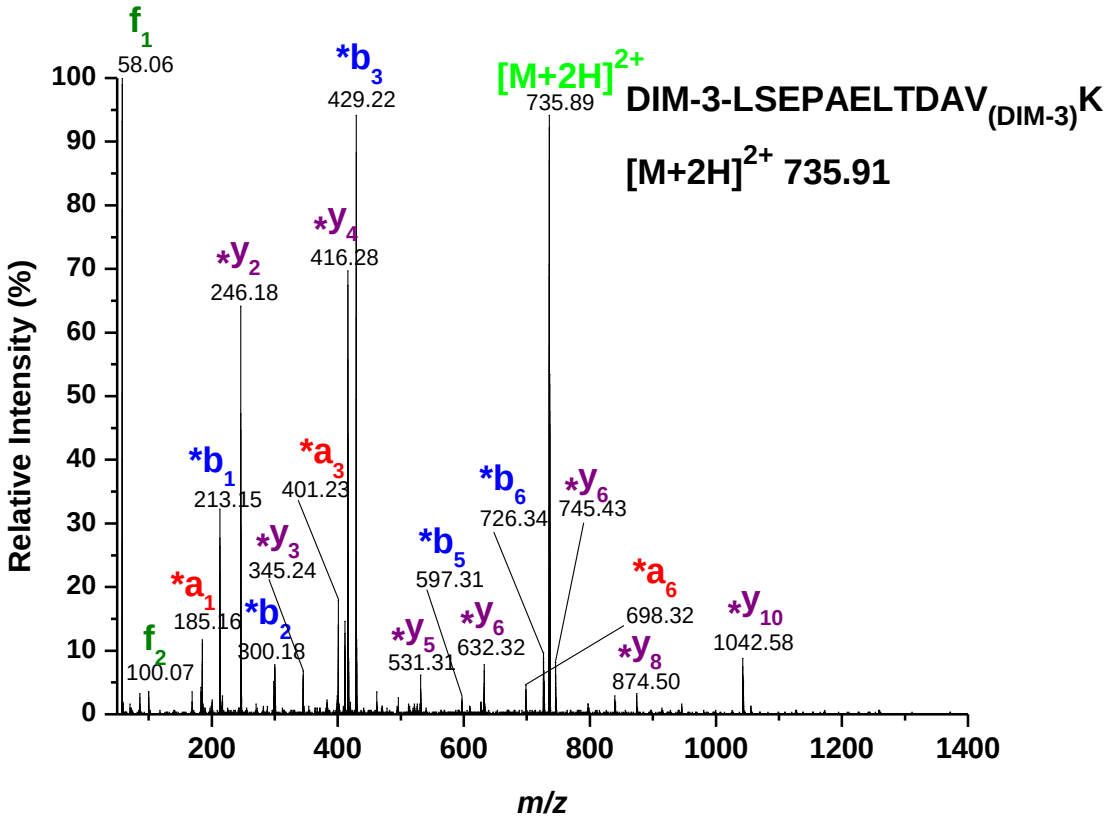

Figure A1.3f: Dim-3 derivatized SVILLGR $[M+2H]^{2+}$ MS/MS spectrum.

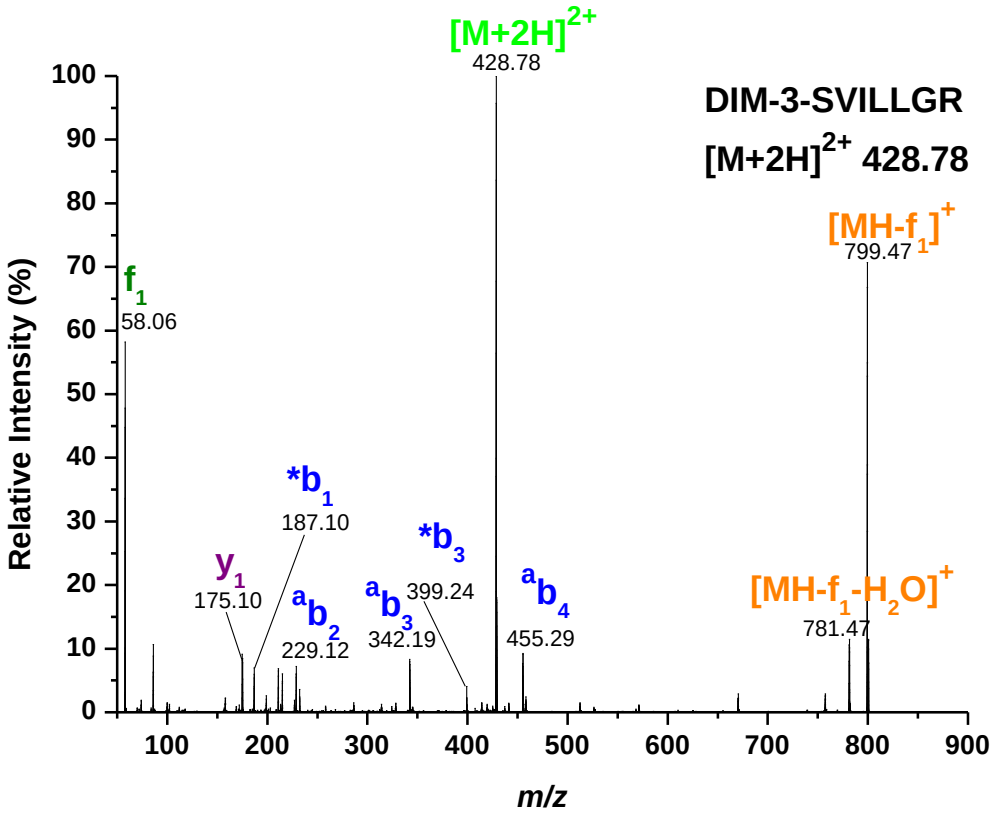

Figure A1.4a: Dim-4 derivatized NSILTETLHR $[M+3H]^{3+}$ MS/MS spectrum.

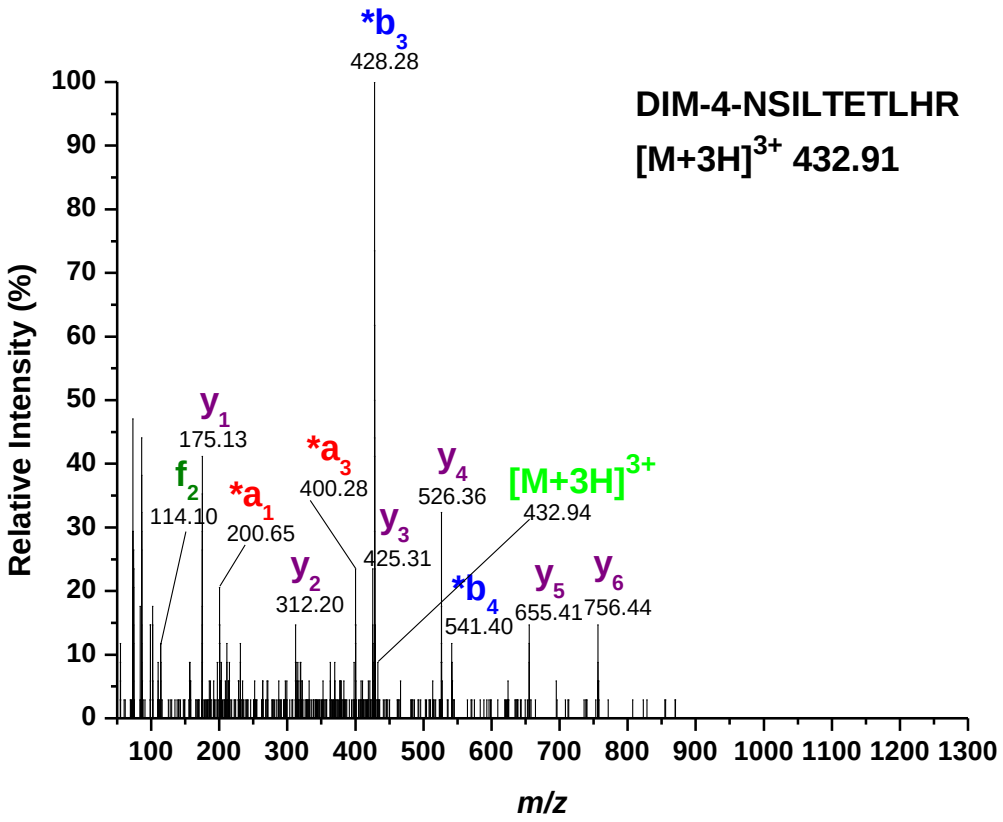

Figure A1.4b: Dim-4 derivatized LSLVPDSEQGEAILPR $[M+2H]^{2+}$ MS/MS spectrum.

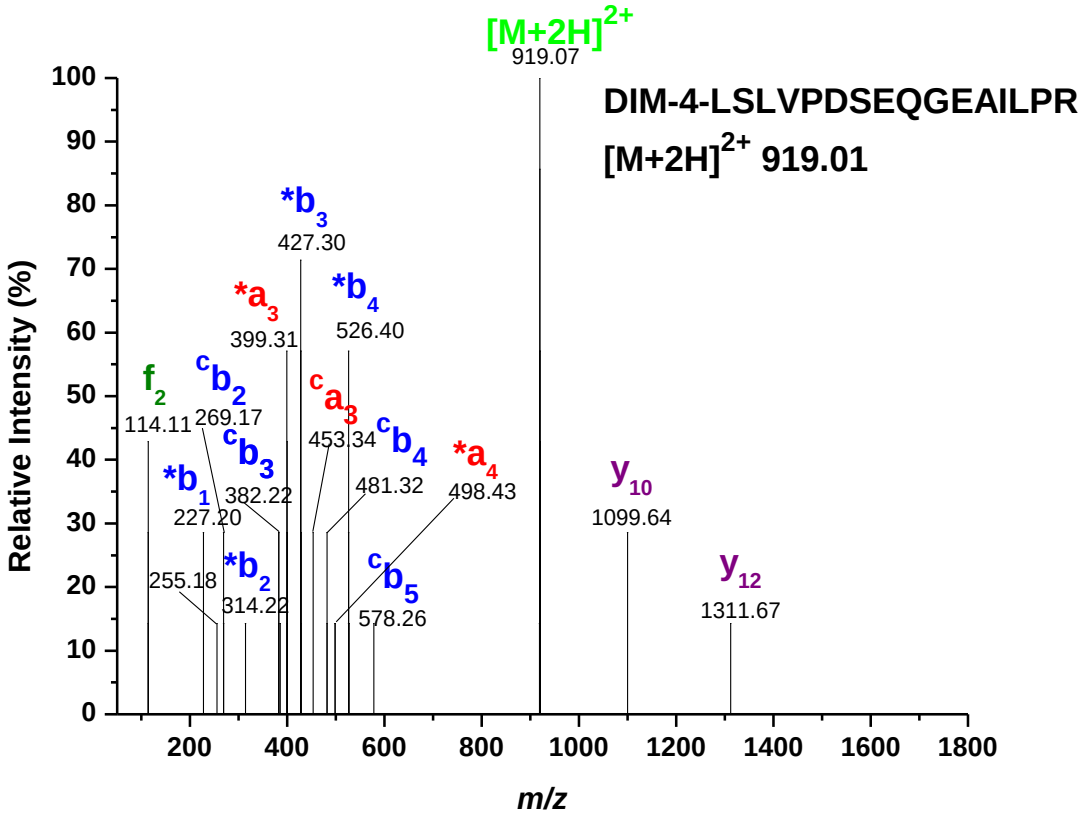

Figure A1.4c: Dim-4 derivatized LSLVPDSEQGEAILPR $[M+3H]^{3+}$ MS/MS spectrum.

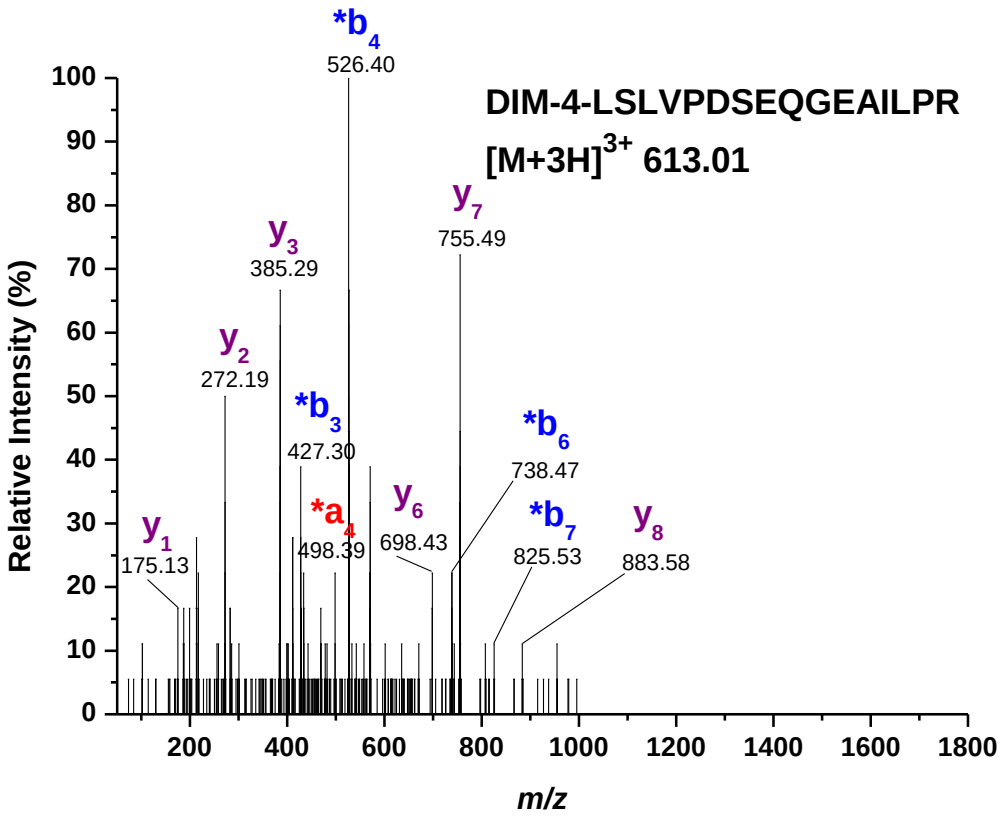

Figure A1.4d: Dim-4 derivatized LSEPAELTDAVK $[M+2H]^{2+}$ MS/MS spectrum.

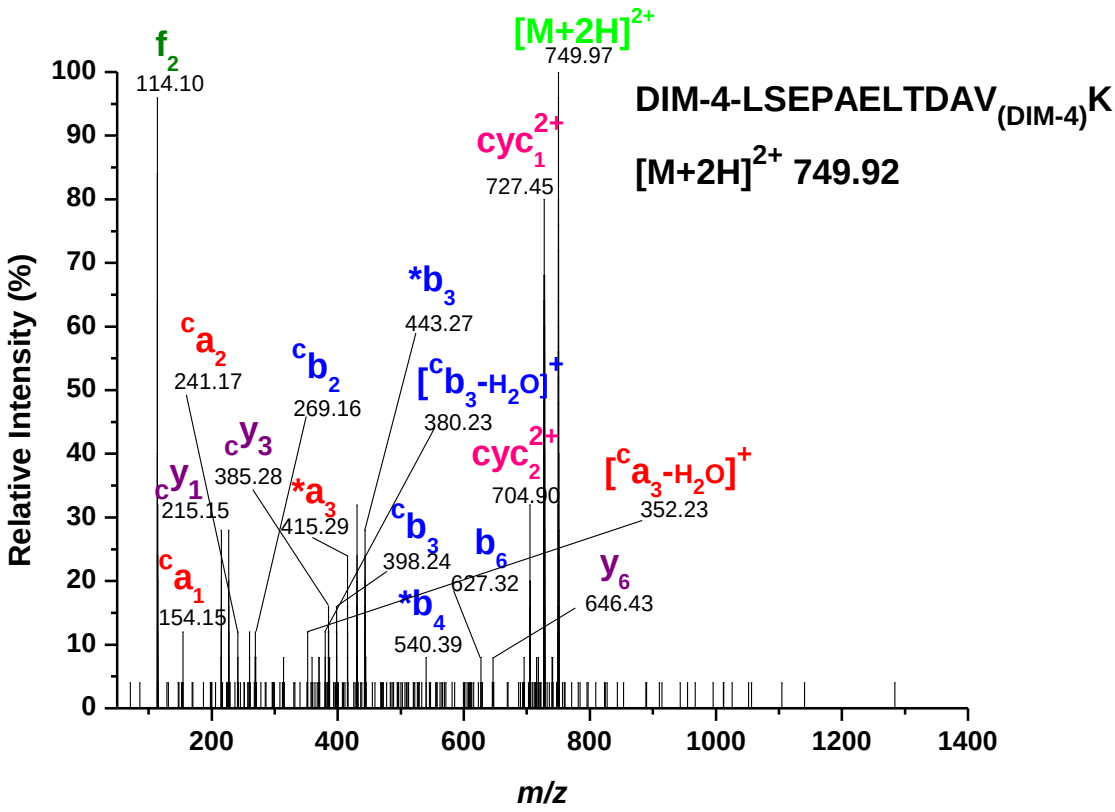

Figure A1.4e: Dim-4 derivatized SVILLGR $[M+2H]^{2+}$ MS/MS spectrum (y ions carrying an imido lactone on the lysine's side chain amine are denoted $_{c}y$).

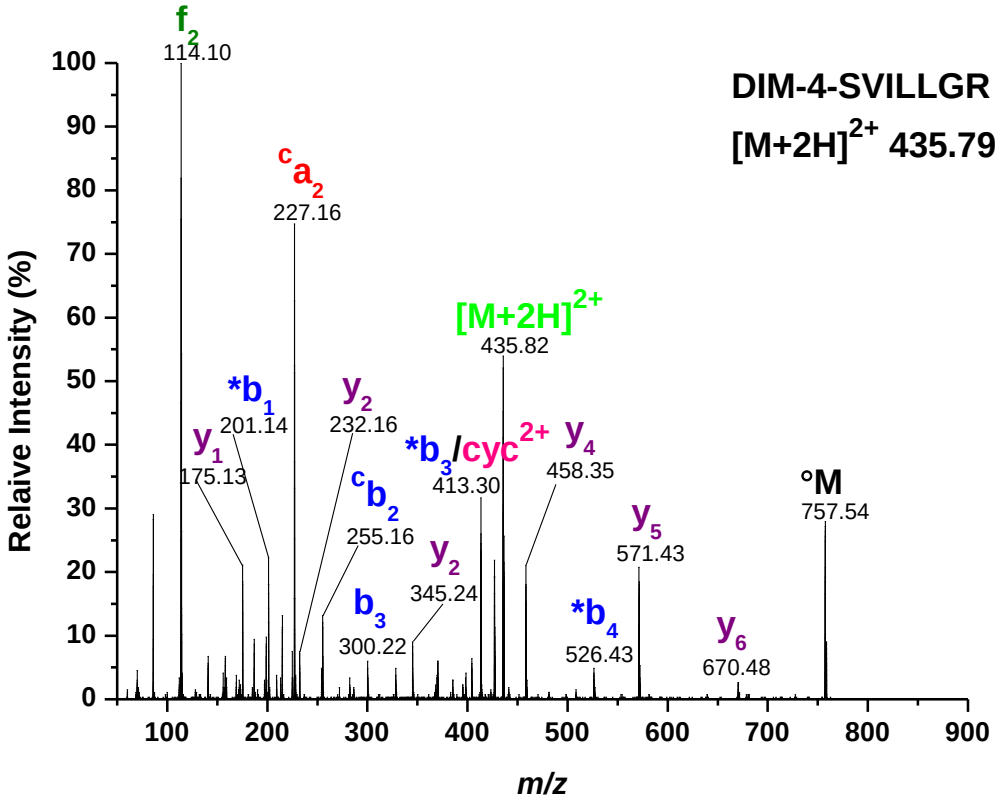

Figure A1.5a: Dim-5 derivatized NSILTETLHR $[M+2H]^{2+}$ MS/MS spectrum.

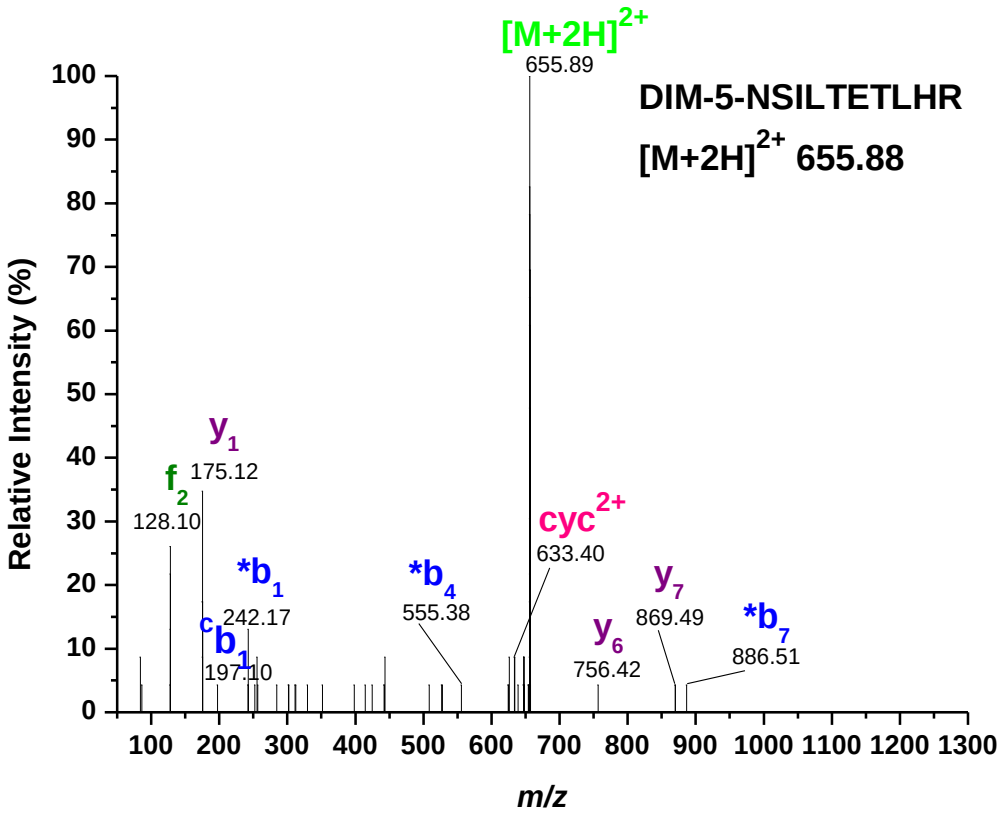

Figure A1.5b: Dim-5 derivatized NSILTETLHR $[M+3H]^{3+}$ MS/MS spectrum.

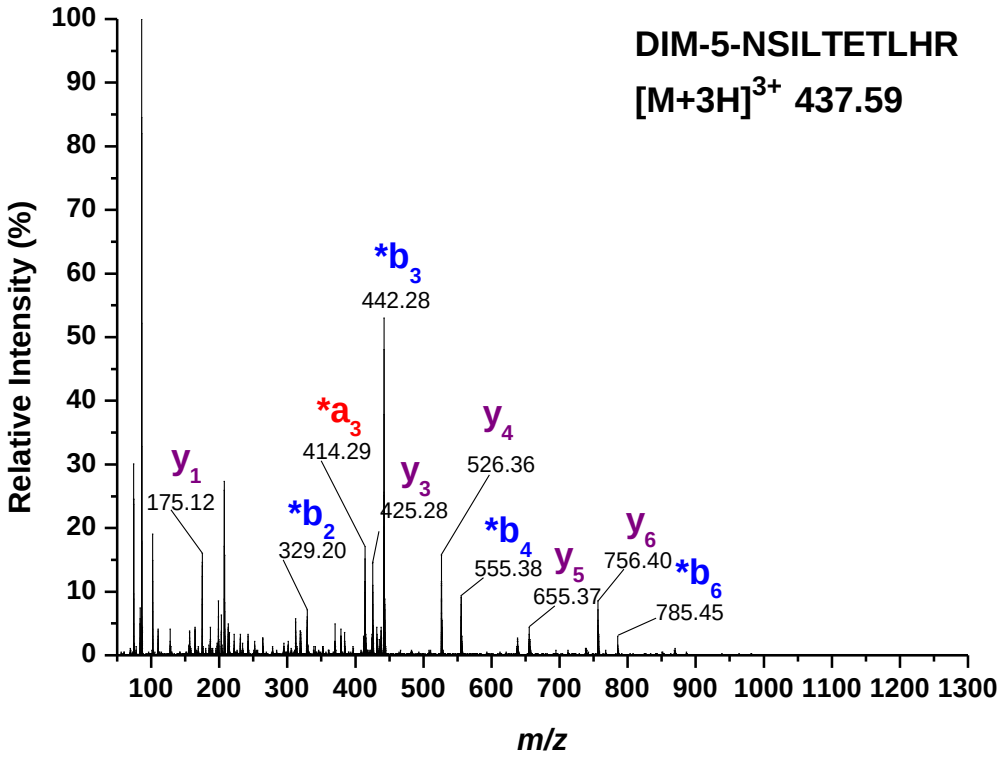

Figure A1.5c: Dim-5 derivatized LSLVPDSEQGEAILPR $[M+2H]^{2+}$ MS/MS spectrum.

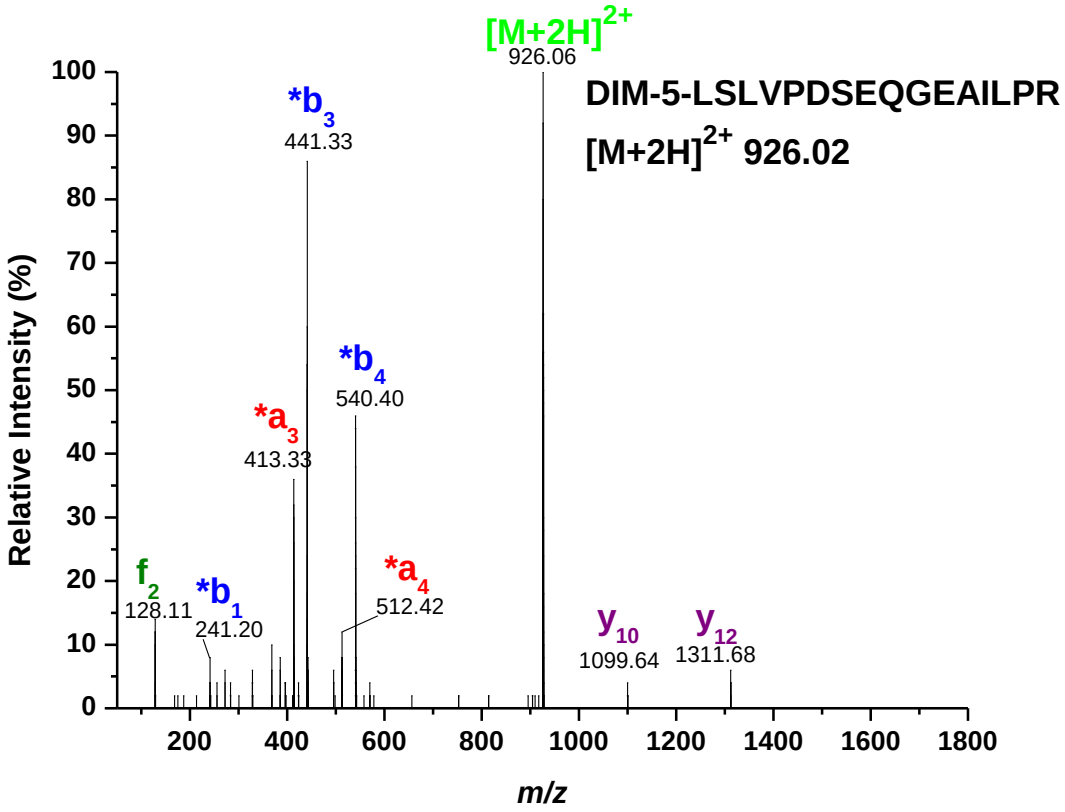

Figure A1.5d: Dim-5 derivatized LSLVPDSEQGEAILPR $[M+3H]^{3+}$ MS/MS spectrum.

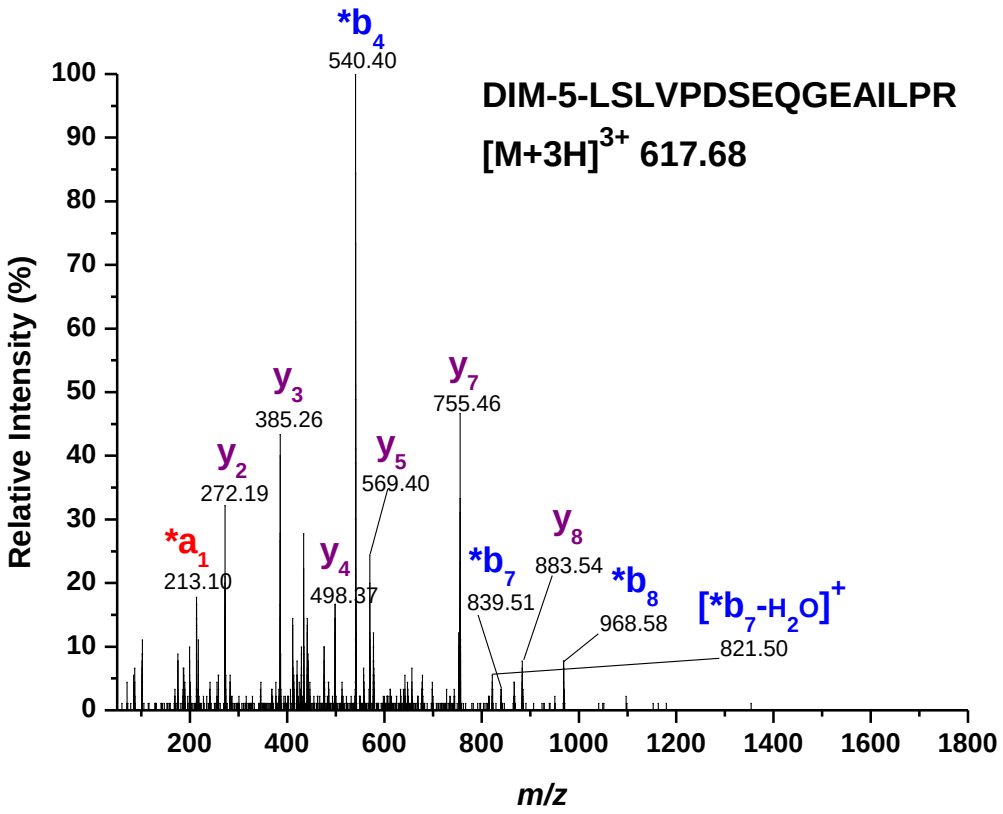

Figure A1.5e: Dim-5 derivatized LSEPAELTDAVK $[M+2H]^{2+}$ MS/MS spectrum (y ions carrying the derivatizing group, on the lysine's side chain amine, are denoted as *y).

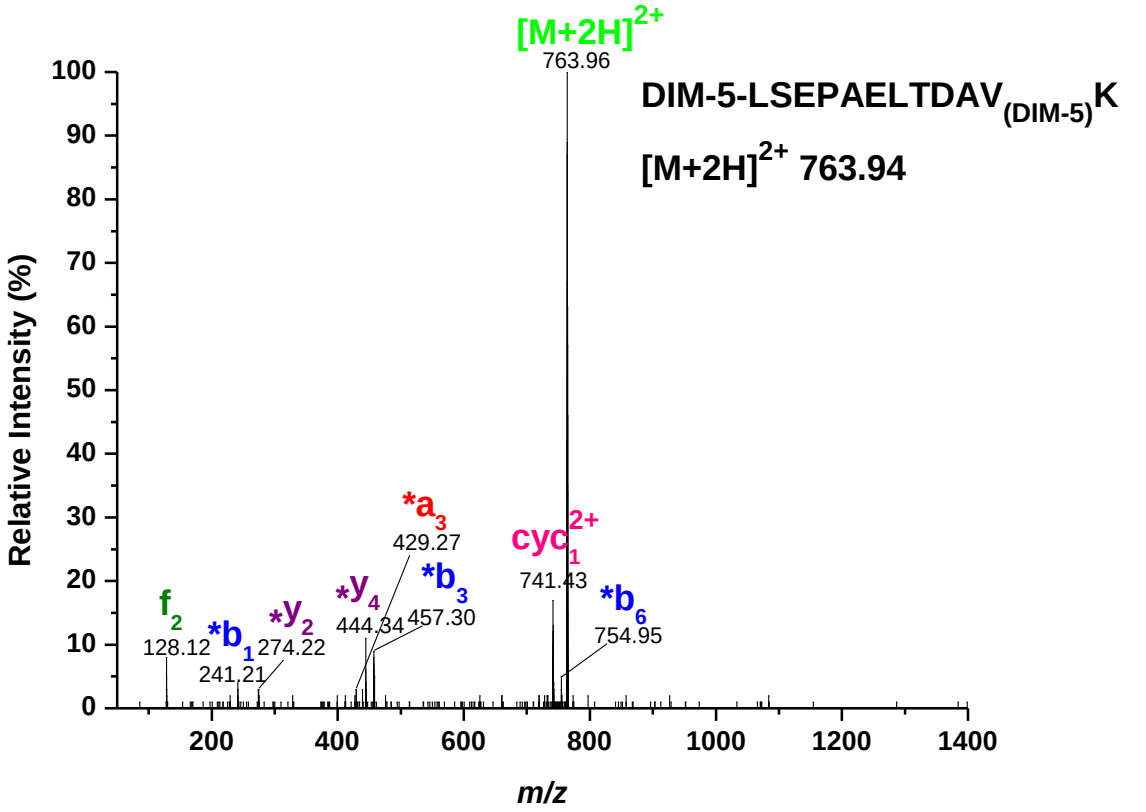

Figure A1.5f: Dim-5 derivatized SVILLGR $[M+2H]^{2+}$ MS/MS spectrum.

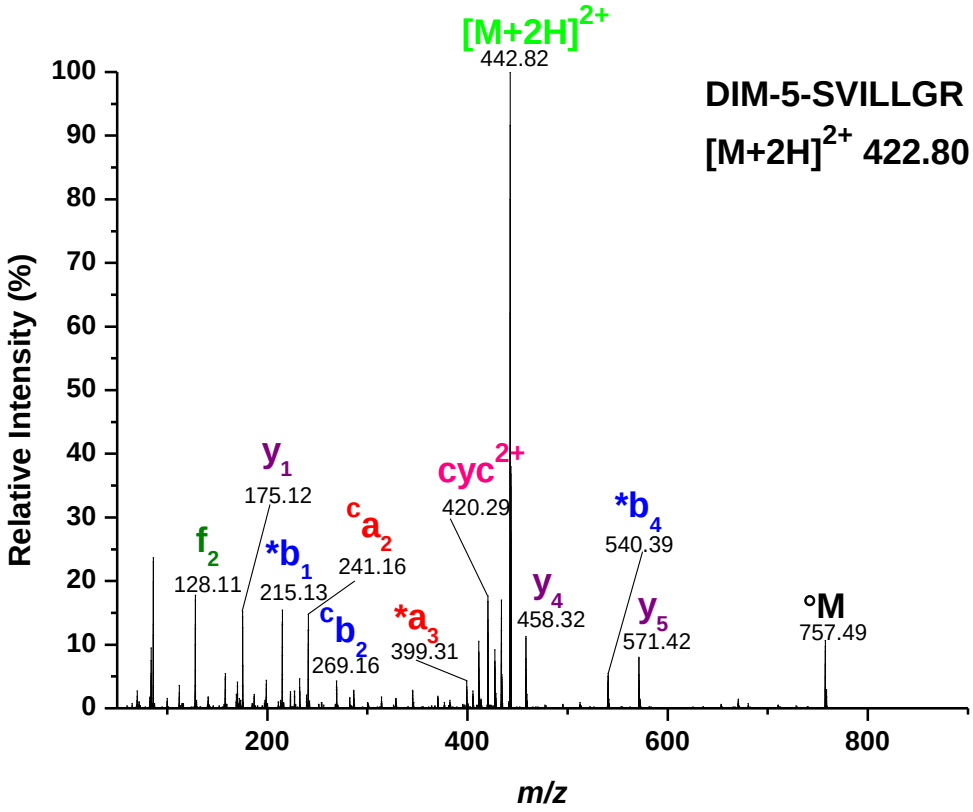

Figure A1.6a: Dim-6 derivatized NSILTETLHR $[M+2H]^{2+}$ MS/MS spectrum.

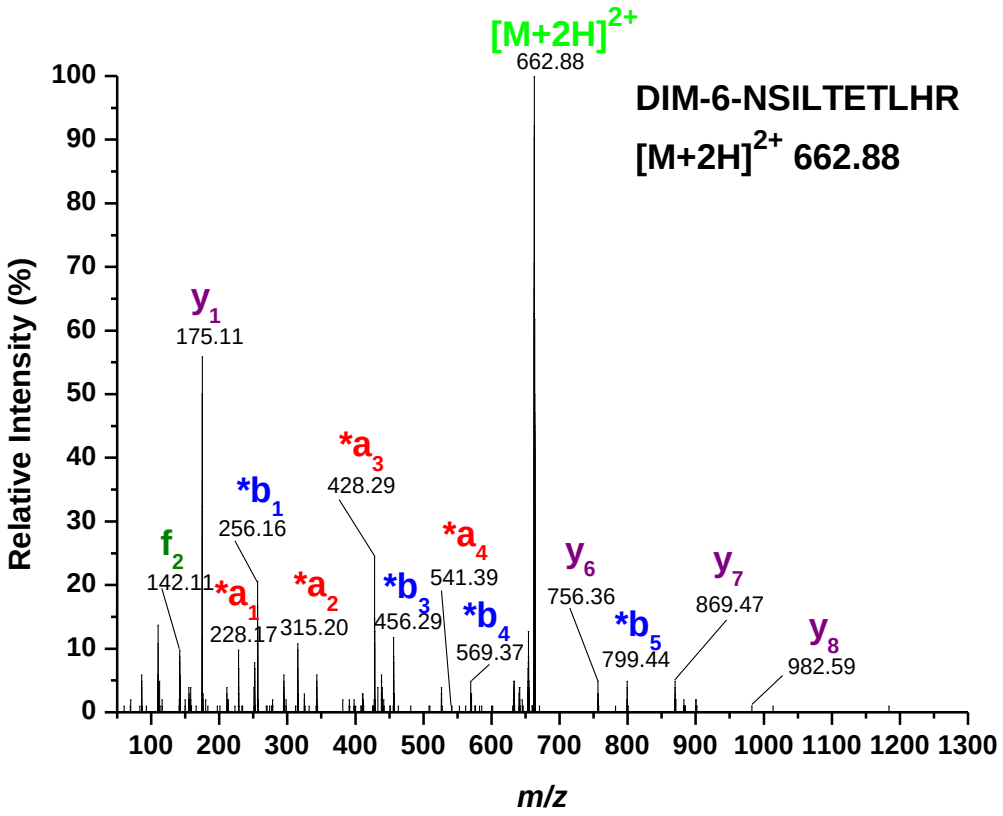

Figure A1.6b: Dim-6 derivatized NSILTETLHR $[M+3H]^{3+}$ MS/MS spectrum.

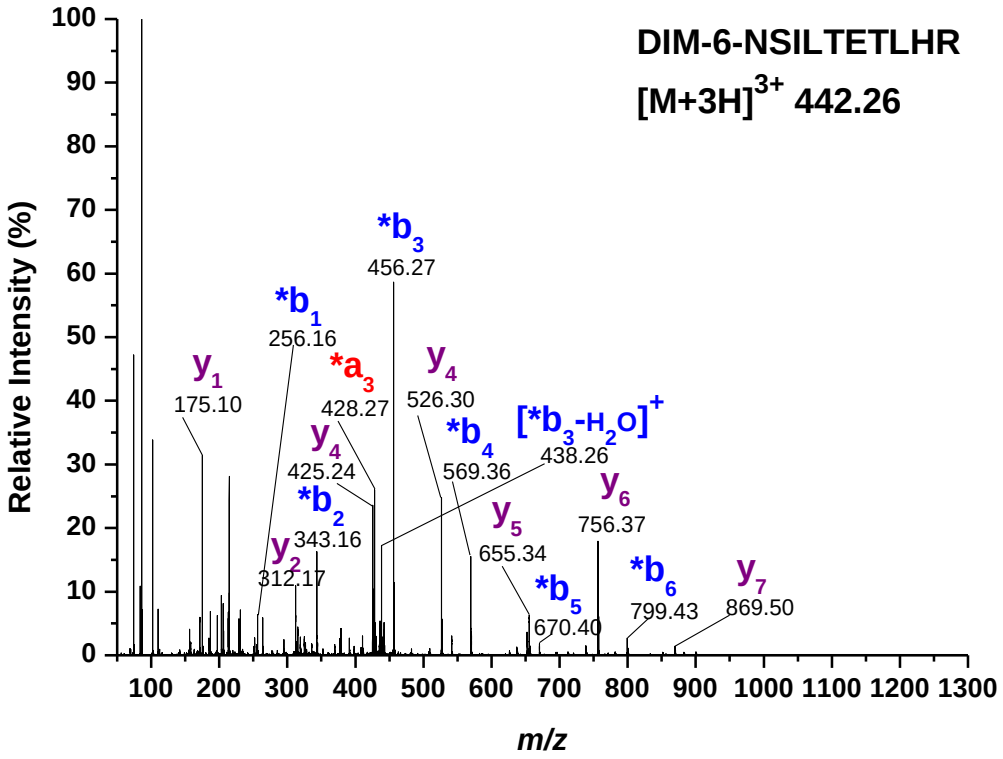

Figure A1.6c: Dim-6 derivatized LSLVPDSEQGEAILPR $[M+2H]^{2+}$ MS/MS spectrum.

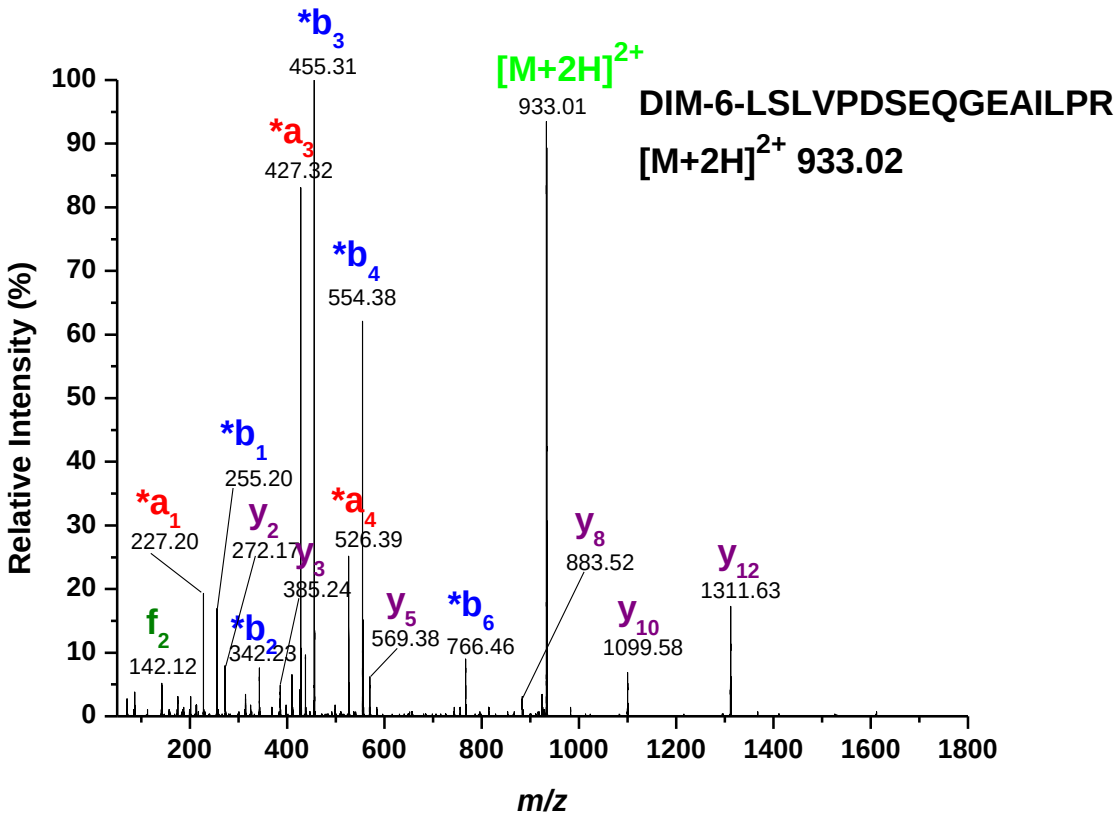

Figure A1.6d: Dim-6 derivatized LSLVPDSEQGEAILPR $[M+3H]^{3+}$ MS/MS spectrum.

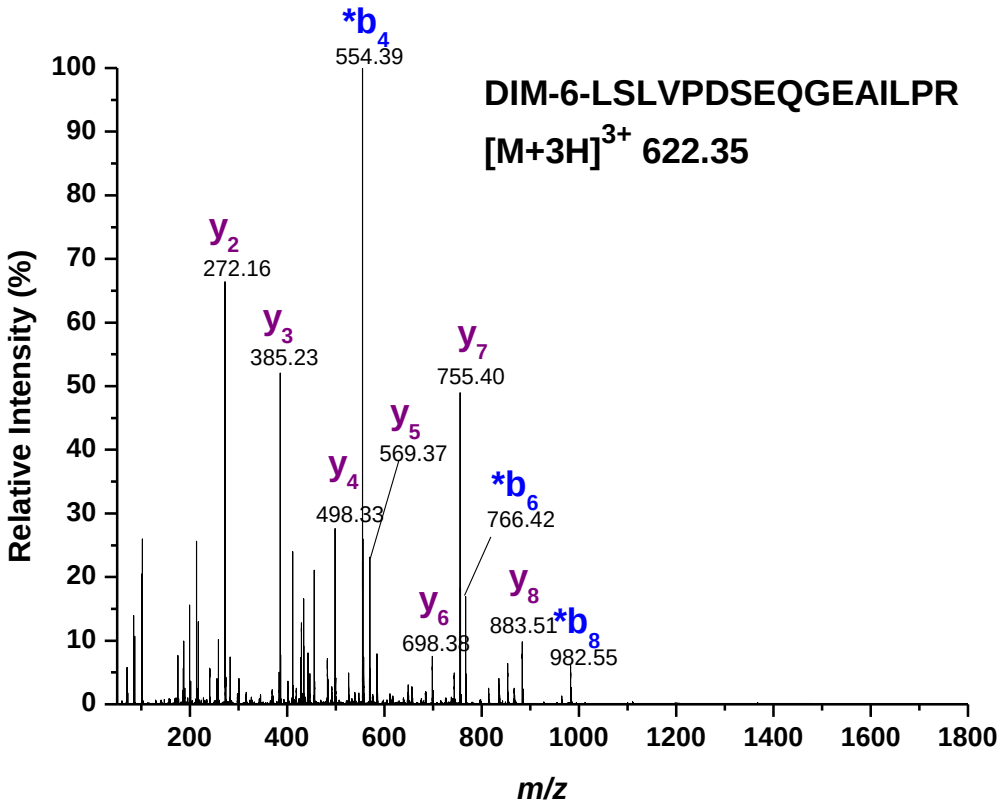

Figure A1.6e: Dim-6 derivatized LSEPAELTDAVK $[M+2H]^{2+}$ MS/MS spectrum (y ions carrying the derivatizing group, on the lysine's side chain amine, are denoted as *y).

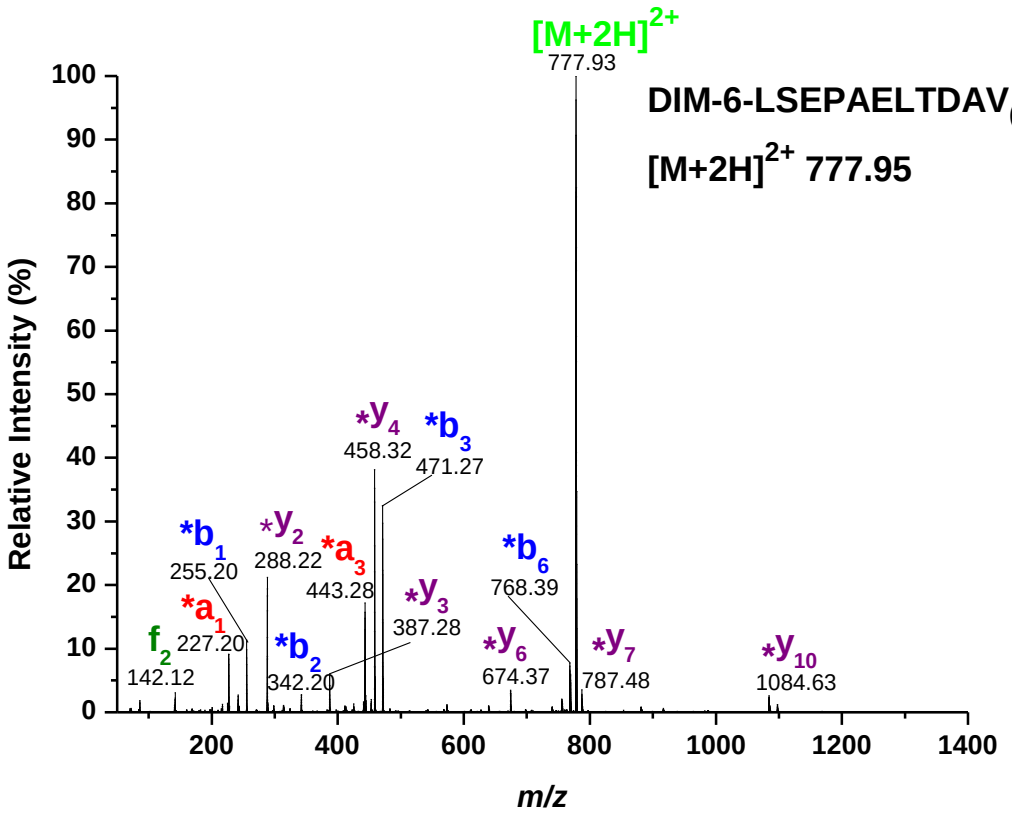

Figure A1.6f: Dim-6 derivatized SVILLGR $[M+2H]^{2+}$ MS/MS spectrum.

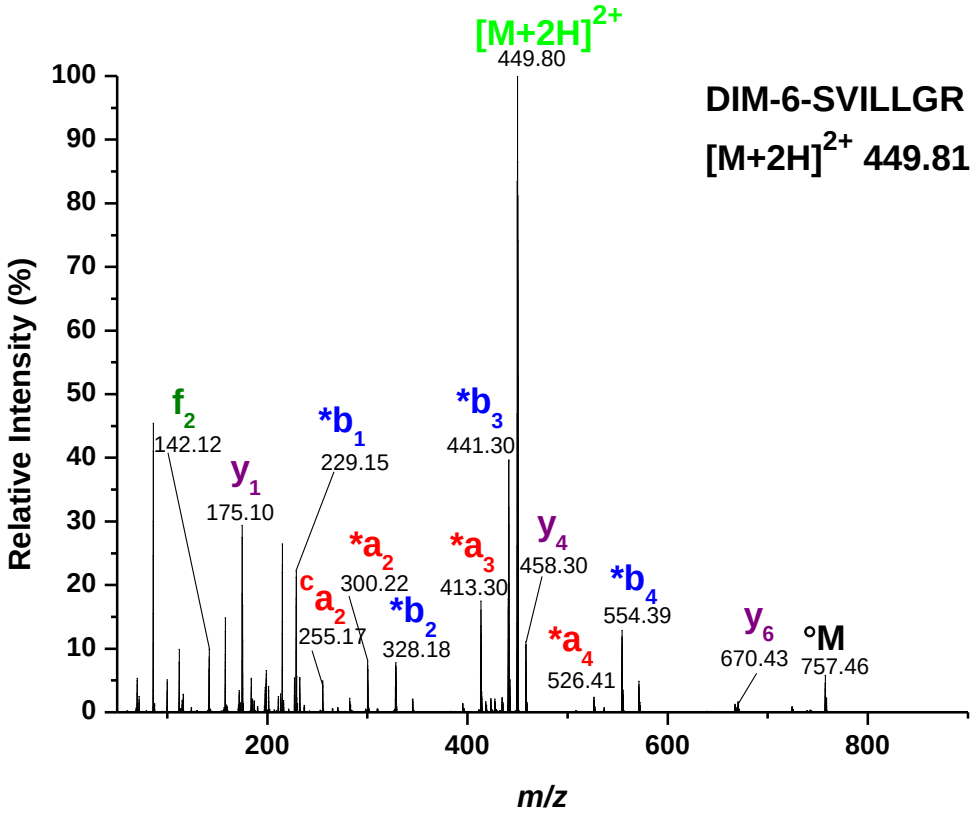

Figure A1.7a: Charge state shift of SVILLGR (top) and dim-2-SVILLGR (bottom).

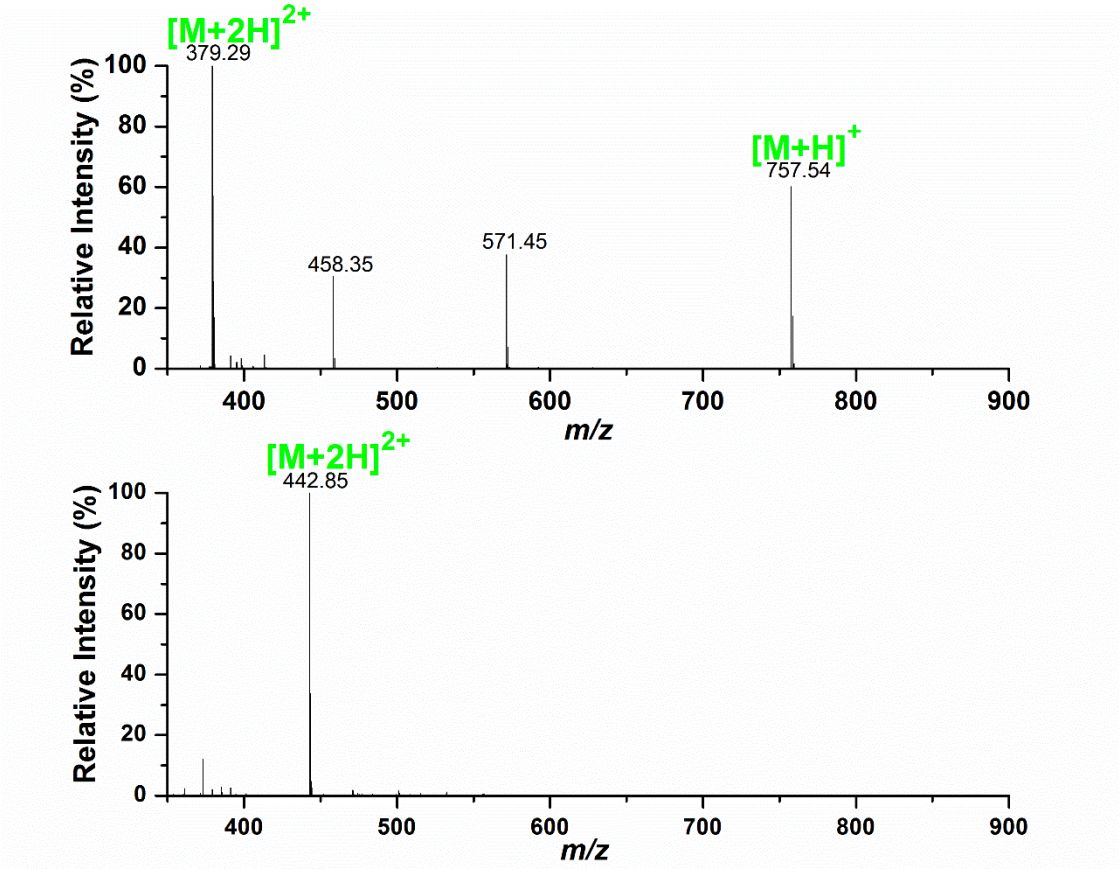

Figure A1.7b: Charge state shift of YGGFLR (top) and dim-2-YGGFLR (bottom).

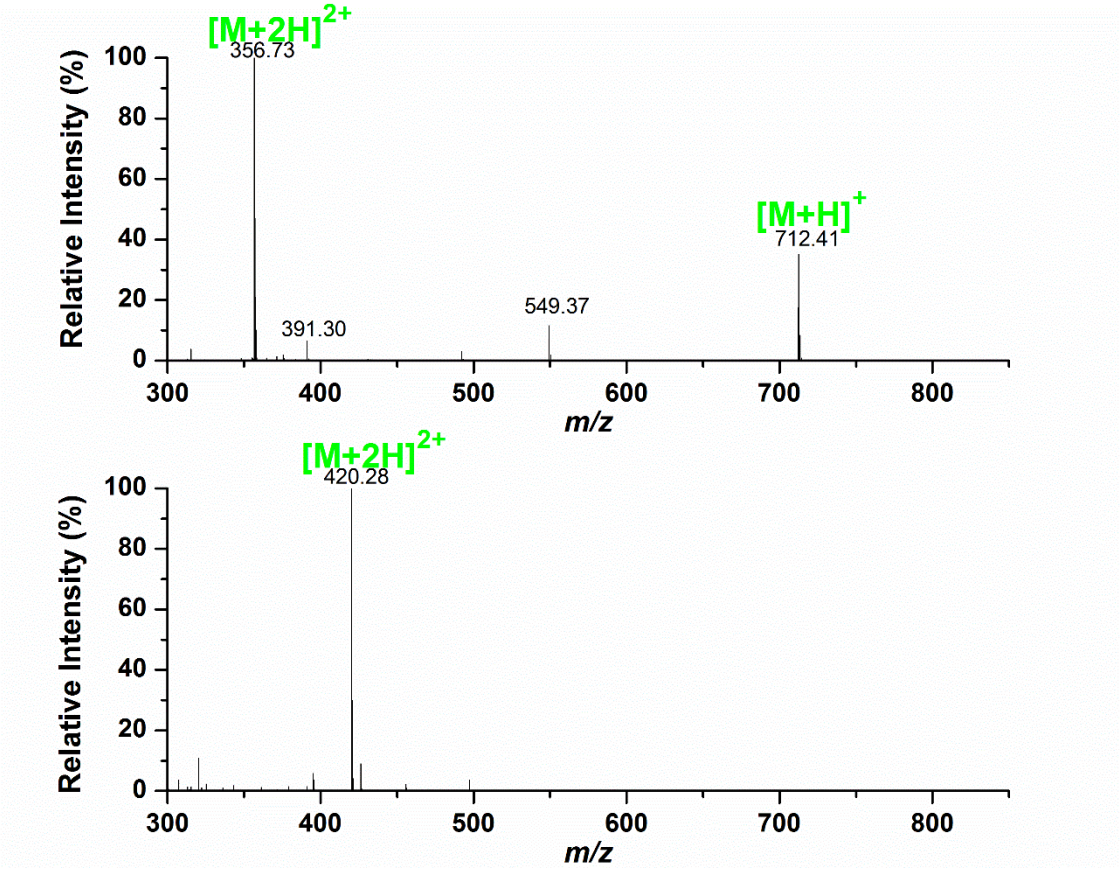

Figure A1.7c: Charge state shift of LSLVPDSEQGEAILPR (top) and dim-2-LSLVPDSEQGEAILPR (bottom).

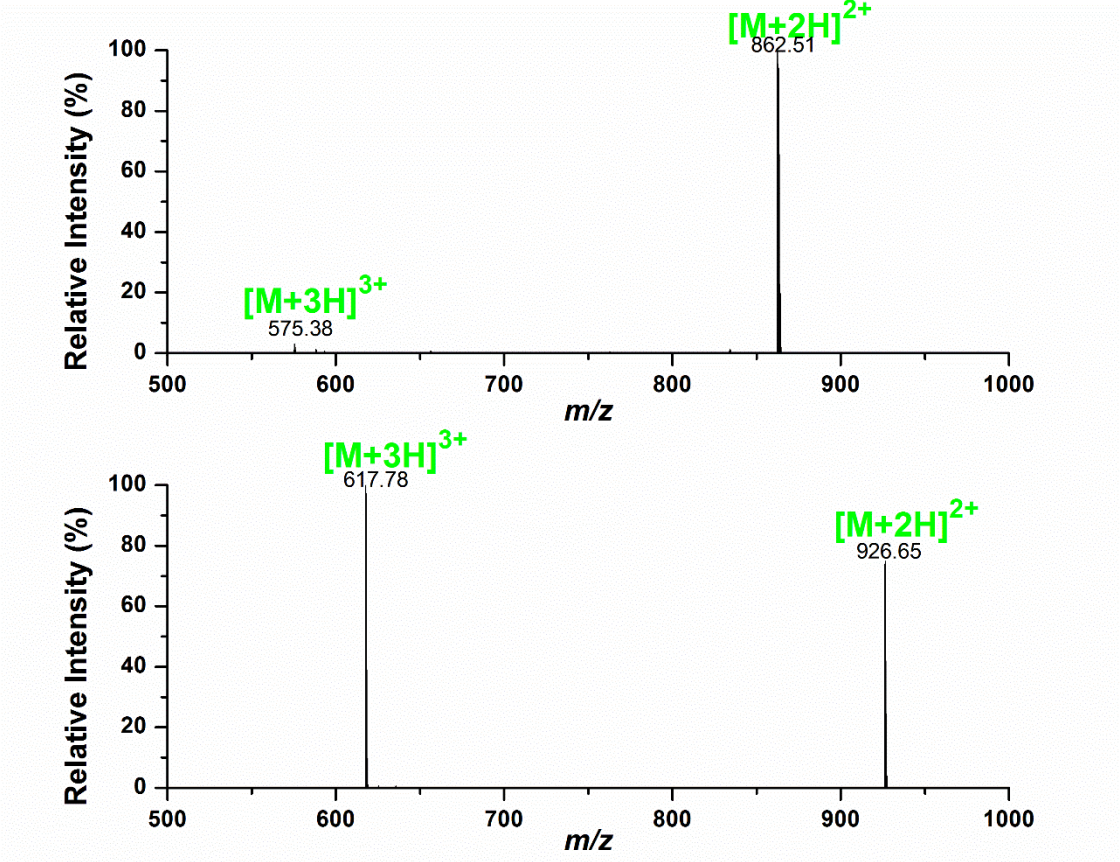

Figure A1.8: Sigmoidal dose-response fitted precursor survival curves of YGGFLR peptides (normalized).

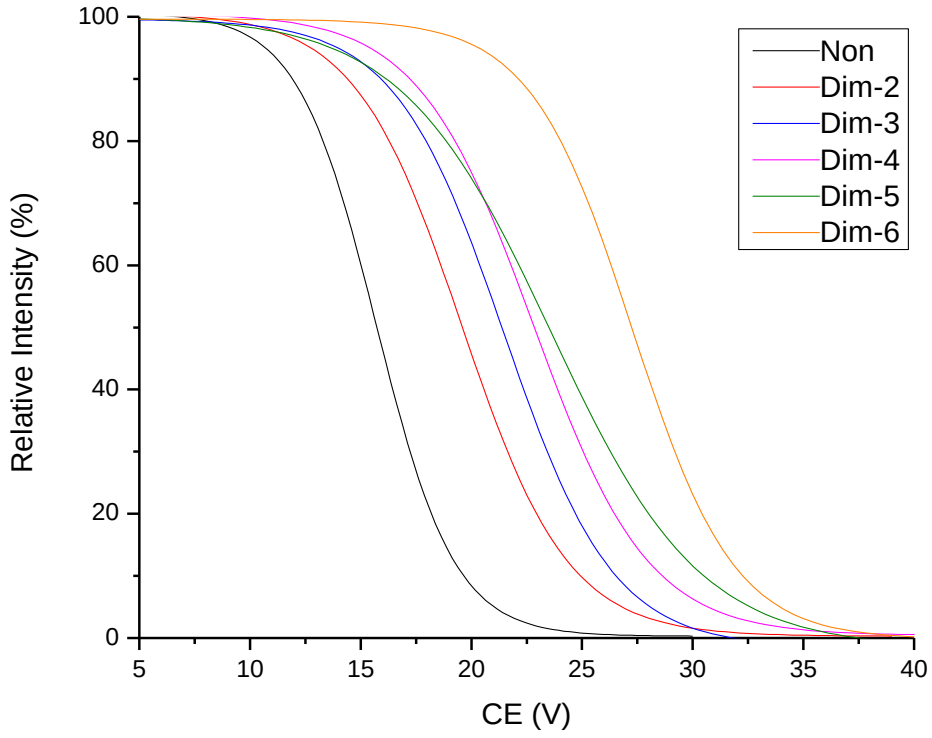

Equation A1.1: Percent of chemical conversion

After the reaction between the 5-peptide mix and the derivatizing dimethylated amino acid was quenched, an equal amount of isotopic SVIL[L-$^{13}C_6{}^{15}N$]GR was added. After desalting, LC-MS was performed. The following equation was then applied based on intensity to calculate the PCC.

$$PCC = \frac{Intensity\ of\ Isotopic\ SVILLGR - Intensity\ of\ SVILLGR}{Intensity\ of\ Isotopic\ SVILLGR} \times 100\%$$

Equation A1.2: Signal yield for mass spectrometry

After the reaction between the 5-peptide mix and the derivatizing dimethylated amino acid was quenched, an equal amount of isotopic SVIL[L-$^{13}C_6{}^{15}N$]GR was added. After desalting, LC-MS was performed. The following equation was then applied based on intensity to calculate the SYMS.

$$SYMS = \frac{Intensity\ of\ Derivatized\ SVILLGR}{Intensity\ of\ Isotopic\ SVILLGR} \times 100\%$$

Equation A1.3: Adjusted signal yield for mass spectrometry

To account for an inefficient reaction, the following equation was developed to predict SYMS if the reaction went to 100% completion.

$$Adjusted\ SYMS = \frac{SYMS}{PCC} \times 100\%$$

Table A1.1: Collisional energy optimization for non-derivatized peptides.

Non-Derivatized Peptide	**Multiplication Factor for CE**
NSILTETLHR $[M+2H]^{2+}$	1.15
NSILTETLHR $[M+3H]^{3+}$	1.1
LSLVPDSEQGEAILPR $[M+2H]^{2+}$	1.1
LSEPAELTDAVK $[M+2H]^{2+}$	1.1
SVILLGR $[M+2H]^{2+}$	1.1
YGGFLR $[M+2H]^{2+}$	1.25

Table A1.2: Collisional energy optimization for derivatized peptides.

Dimethylamino Derivatized Peptide	**Multiplication Factor for CE**
NSILTETLHR $[M+2H]^{2+}$	1.25
NSILTETLHR $[M+3H]^{3+}$	1.25
LSLVPDSEQGEAILPR $[M+2H]^{2+}$	1.1
LSLVPDSEQGEAILPR $[M+3H]^{3+}$	1.1
LSEPAELTDAVK $[M+2H]^{2+}$	1.15
SVILLGR $[M+2H]^{2+}$	1.4
YGGFLR $[M+2H]^{2+}$	1.5

Table A1.3: Properties of the peptide mix.

Peptide	Mass (Da)	Number of Amino Acids	Isoelectric Point
NSILTETLHR	1183.32	10	7.55
LSLVPDSEQGEAILPR	1723.93	16	3.93
YGGFLR	711.81	6	9.34
SVILLGR	756.94	7	10.55
LSEPAELTDAVK	1272.41	12	3.93

Table A1.4: Formulae and goodness of fit for the sigmoidal dose-response fitting of the survival curve for the dimethylamino peptides.

$$y = A1 + \frac{A2 - A1}{1 + 10^{log(x0 - x) \times p}}$$

Peptide	A1	A2	Logx0	p	Reduced χ^2	Adjusted R^2
Non-Derivatized	0.002328	0.999005	15.699651	-0.244595	0.001484	0.9916
Dim-2	0.021004	1.00113	20.392597	-0.190917	0.006084	0.9654
Dim-3	-0.014948	1.00080	21.466005	-0.176504	0.005218	0.9704
Dim-4	0.002769	0.995858	22.800792	-0.166370	0.008025	0.9574
Dim-5	-0.016008	0.996510	23.644762	-0.130546	0.01062	0.9408
Dim-6	-0.002919	0.999499	27.274779	-0.189113	0.001272	0.9916